

PFKFB3 as a potential therapeutic target in acute myeloid leukaemia



Zhuoma Suonan

School of Medicine

Cardiff University

Submitted in partial fulfilment of the requirements for the degree of

Master of Philosophy

December 2022

Abstract

NADPH oxidase 2 (NOX2) derived reactive oxygen species (ROS) play an important role in cancer cell signalling, proliferation, differentiation, and survival. Higher levels of extracellular derived ROS are known to be present in acute myeloid leukaemia (AML) patients' blasts compared to normal haematopoietic cells. In a human haematopoietic progenitor cell model, elevated ROS led to increased extracellular lactate production and glucose uptake, and proteins that critically regulate glycolytic enzymes 6-phosphofructo-2-kinase/fructose-2,6-bisphosphate enzyme 3 (PFKFB3). However, little is known regarding the expression levels or role of PFKFB family members in normal haematopoiesis and AML. My analysis from online transcriptome data (Bloodspot and TCGA databases) revealed that *PFKFB3* and *PFKFB4* mRNA significantly increased with differentiation. *PFKFB3* mRNA expression is significantly higher in AML with complex cytogenetics than in all *PFKFBs* in haematopoietic stem cell (HSC). *PFKFB3* mRNA expression level does not correlate with overall survival. *PFKFB3* mRNA expression level correlates with *Cytochrome b-245 beta chain (CYBB)* expression in AML patients. I found that NOMO-1 cells produced the highest ROS and *PFKFB3* in AML cell lines. By using Western blotting and Diogenes, I found a positive correlation between ROS and expressed *PFKFB3* in AML cell lines. However, single-cell *PFKFB3* flow cytometry detection failed because antibody may bind nuclear *PFKFB3* with less efficiency than cytosolic in some cell lines. In summary, this study supports the evidence that ROS-increased glycolysis and metabolic reprogramming are associated with *PFKFB3* in AML, but more experimental validation is needed.

Abbreviations

ADP	adenosine diphosphate
ALL	acute lymphocytic leukaemia
AML	acute myeloid leukaemia
AMP	adenosine monophosphate
AMPK	adenosine monophosphate kinase
APC	allophycocyanin
APL	acute promyelocytic leukaemia
ATCC	American Type Culture Collection (USA)
ATO	arsenic trioxide
ATP	adenosine triphosphate
ATRA	all-trans-retinoic acid
BM	bone marrow
BSA	bovine serum albumin
CBFB	core-binding factor subunit beta
CD	cluster of differentiation.
CITE	REAP-seq combined with total-seq
CLL	chronic lymphocytic leukaemia
CLO	clofibrilic acid
CLOCK	circadian motor export cyclin kaput
CLP	common lymphoid progenitor Cell
CML	chronic myeloid leukaemia
CML	chronic myeloid leukaemia
CMP	common myeloid progenitor
CSF	colony stimulating factor
CV	coefficient of variation
CYBB	Cytochrome b-245 beta chain
DFS	decreased disease-free survival
DMEM	dulbecco's modified eagle's medium
DMSO	dimethyl sulfoxide
DNA	deoxyribonucleic acid
DNR	daunorubicin
DPI	diphenyleneiodonium
DSMZ	German Collection of Microorganisms and Cell Cultures
DUOX	dual oxidases
ECACC	European Collection of Authenticated Cell Cultures
EDTA	ethylenediaminetetraacetic Acid
ELN	European Leukaemia Net

ETC	electron transport chain activity
FAB	French American and British
FBS	foetal bovine serum
FDA	U.S. Food and Drug Administration
FSC	forward scatter
GAPDH	glyceraldehyde-3-phosphate dehydrogenase
GFP	green fluorescent protein
GLUT	glucose transporter
GMCSF	granulocyte/macrophage colony stimulating Factor
GMP	granulocyte-monocyte progenitor Cell
GOX	glucose oxidase
GSEA	gene set enrichment analysis
GSH	glutathione
HDAC	histone deacetylase
HEPES	-(2-hydroxyethyl)-1-piperazineethanesulfonic acid
HIF	hypoxia-inducible factor-1
HK	hexokinase
HPC	haematopoietic progenitor cells
HRP	horseradish Peroxidase
HSC	haematopoietic stem cell
HSCT	HSC transplantation
HSPC	haematopoietic progenitor cells
IDH	isocitrate Dehydrogenase (NADP(+))
IHH	isolated hypogonadotropic-4
IMDM	Iscove Modified Dulbecco's Medium
KD	knock down
KI	knock in
LDH	lactate dehydrogenase
LMPP	lymphoid primed multipotential progenitors
LSC	leukaemia stem cells
LT - HSC	long-term haematopoietic stem cell
MAPK	mitogen activated protein kinase
MDP	monocyte-dendritic cell progenitor cell
MDS	myelodysplastic syndrome
MEM	minimum essential medium
MEP	megakaryocyte-erythroid progenitor
MEP	megakaryocytic-erythroid progenitor cell
MLL	mixed lineage leukaemia
MMP	multipotent progenitors
MPP	multipotent progenitor cells
NADH	nicotinamide adenine dinucleotide
NADPH	nicotinamide adenine dinucleotide phosphate

NEB	New England BioLabs
NK cell	natural killer cell
NO	nitric oxide radicals
NOX	NADPH oxidase
NS	not significantly
OS	overall survival
PBS	phosphate Buffer Saline
PCR	polymerase chain reaction
PDH	pyruvate dehydrogenase
PEP	phosphoenolpyruvic acid
PFK	phosphofructokinase
PFKFB	6-phosphofructo-2-kinase/fructose-2,6-bisphosphatase
PICALM	phosphatidylinositol binding clathrin assembly protein
PKC	protein kinase C
PMA	para-Methoxyamphetamine
PO	peroxisomes
PPP	pentose phosphate pathway
PVDF	polyvinylidene fluoride
QRT	real-time qRT-PCR
RLU	relative luminescent units
RNA	ribonucleic acid
RNS	reactive nitrogen species
ROS	reactive oxygen species
RPMI	Roswell Park Memorial Institute 1640 medium
RT-qPCR	quantitative reverse transcription PCR
RUNX1	runx-associated transcription factor 1
SOD	superoxide dismutase
SSC	side scatter
ST - HSC	short-term haematopoietic stem cell
TBS	tris-buffered Saline
TCGA	the cancer genome atlas
TEAB	tetraethylammonium bromide
TGF	transforming growth factor
TIGAR	TP53-induced glycolysis and apoptosis regulator
TPA	PMA
UC	universal container
UV	ultraviolet
WHO	World Health Organization
XO	xanthine oxidase

Acknowledgements

I would like to express my deepest gratitude to my supervisors Prof. Alex Tonks, Prof. Richard Darley, and Prof. Steven Knapper for their continuous support and guidance throughout my MPhil. Their knowledge, guidance, and inexhaustible patience, alongside their unswerving support and encouragement have been essential in completing this study.

I would like to thank Dr Andrew Robinson for his generous offer of MV4;11 PFKFB3 Knock-in cell line. I would also like to acknowledge the contribution of my senior colleagues for technical assistance.

I would also like to thank the PGR office team and my assessment panel team for their support.

I would also like to thank Welcome Trust to fund this project and my supervisors gave me this opportunity to join this project.

I would like to reiterate my gratitude to my supervisor Prof. Alex Tonks. I would not be able to complete the project without his support.

Thank you very much!

Table of contents

Abstract	I
Abbreviations	II
Acknowledgements	V
Table of contents.....	VI
List of figures.....	X
List of tables	XII
Chapter 1 Introduction.....	1
1.1 Normal haematopoiesis	1
1.1.1 Haematopoietic stem cells and bone marrow niche	4
1.2 Acute myeloid leukaemia	6
1.2.1 Overview.....	6
1.2.2 AML pathophysiology and Treatment.....	9
1.2.3 Leukaemia stem cells	16
1.3 Reactive oxygen species (ROS)	17
1.3.1 NOX2 derived ROS and electron transport chain (ETC)	19
1.3.2 ROS and cell signalling.....	22
1.3.3 ROS induced cell proliferation	25
1.3.4 ROS induced proliferation in haematopoietic cells	26
1.4 Glycolysis	28
1.4.1 Glycolysis pathway	28
1.4.2 PFK regulation.....	29
1.4.3 6-phosphofructo-2-kinase/fructose-2,6-biphosphatase (PFKFB) family	32

1.4.4	Metabolic rewiring in cancer and leukaemia	36
1.5	Aims and Objectives	40
Chapter 2	Materials and Methods	42
2.1	General materials.....	42
2.1.1	Antibodies.....	44
2.2	Cell culture	45
2.2.1	Culture of cell lines	45
2.2.2	Thawing and cryopreservation of cells	45
2.2.3	Cell counting.....	46
2.3	Diogenes assay to measure NOX2-derived reactive oxygen species	46
2.4	Western blotting	47
2.4.1	Total cell protein extraction.....	47
2.4.2	Cytosolic and nuclear protein extraction.....	50
2.4.3	Protein quantitation by Bradford assay.....	50
2.4.4	SDS Polyacrylamide electrophoresis and electroblotting.....	51
2.4.5	Immunodetection of proteins	52
2.5	Flow cytometry.....	53
2.5.1	Intracellular PFKFB3 expression	53
2.5.2	Data acquisition and gating strategy.....	55
2.6	Data analysis.....	57
2.6.1	Publicly available datasets.....	57
2.6.2	Statistical analysis	58
Chapter 3	<i>PFKFB3</i> mRNA is overexpressed in AML	59
3.1	Introduction	59
3.1.1	Aims and objectives.....	60

3.2	<i>PFKFB3</i> mRNA expression increases during normal human haematopoietic differentiation	61
3.2.1	<i>PFKFB1</i> mRNA expression does not change during normal haematopoietic differentiation	62
3.2.2	<i>PFKFB2</i> mRNA expression does not change during normal haematopoietic differentiation	62
3.2.3	<i>PFKFB3</i> mRNA expression increases along with differentiation in normal haematopoiesis	62
3.2.4	<i>PFKFB4</i> mRNA expression increases along with differentiation in normal haematopoiesis	63
3.3	<i>PFKFB3</i> mRNA expression is significantly higher in AML patient blasts compared to normal HSC	69
3.4	<i>PFKFB3</i> mRNA expression correlates with <i>CYBB</i> mRNA expression	75
3.5	<i>PFKFB3</i> expression does not correlate with overall survival in AML patients	75
3.6	High <i>PFKFB3</i> mRNA expression is linked to FAB groups M4, M5	76
3.7	Discussion	80
Chapter 4	<i>PFKFB3</i> protein expression is associated with NOX2 derived ROS in AML	87
4.1	Introduction	87
4.1.1	Aims and objectives	88
4.2	AML cell lines produce varying amounts of extracellular superoxide	89
4.3	<i>PFKFB3</i> expression in cell lines by western blot	90
4.4	<i>PFKFB3</i> protein expression correlates with ROS production in AML cell lines	98
4.5	Development of an assay to measure intracellular <i>PFKFB3</i> protein expression by flow cytometry	98
4.5.1	Development of a positive control for intracellular <i>PFKFB3</i> protein expression	98

4.5.2	Intracellular PFKFB3 protein expression in AML cell lines.....	99
4.5.3	PFKFB3 is mainly expressed in the nucleus in some cell lines which affected the result of intracellular staining assay.....	99
4.6	Discussion.....	105
Chapter 5	General Discussion	110
5.1	Future directions	114
5.2	Conclusion	116
References	117

List of figures

Figure 1-1 Hierarchical representation of human haematopoietic development.....	3
Figure 1-2 Bone marrow niche.....	7
Figure 1-3 Production of reactive oxygen species.....	21
Figure 1-4 Glucose metabolism.	30
Figure 1-5 Abnormal glucose metabolism pattern of tumour cells and PFKFB3.	31
Figure 2-2 Gating strategy for intracellular PFKFB3 protein expression by flow cytometry.....	Error! Bookmark not defined.
Figure 3-1 <i>PFKFB1/Pfkfb1</i> mRNA expression in normal haematopoiesis.....	65
Figure 3-2 <i>PFKFB2/Pfkfb2</i> mRNA expression in normal haematopoiesis.....	66
Figure 3-3 <i>PFKFB3/Pfkfb3</i> mRNA expression in <u>normal</u> haematopoiesis.....	67
Figure 3-4 <i>PFKFB4/Pfkfb4</i> mRNA expression in normal haematopoiesis.....	68
Figure 3-5 <i>PFKFB1</i> mRNA expression changed in AML compared to normal HSC	71
Figure 3-6 <i>PFKFB2</i> mRNA expression is not changed in AML compared to normal HSC.....	72
Figure 3-7 <i>PFKFB3</i> mRNA expression is higher in AML complex compared to normal HSC.....	73
Figure 3-8 <i>PFKFB4</i> mRNA expression is not changed in AML compared to HSC...	74
Figure 3-9 PFKFB3 mRNA expression level correlates with CYBB expression in AML patients.....	77
Figure 3-10 PFKFB3 mRNA expression level does not relate with overall survival..	78
Figure 3-11 High and low PFKFB3 mRNA expression in AML disease subtypes	79
Figure 4-1 Extracellular superoxide production in AML cell lines	92
Figure 4-2 Optimisation of the best beta-actin detecting dilution by western blot.....	93

Figure 4-3 Determination of optimal clone of antibody to detect PFKFB3 by western blot 94

Figure 4-4 Determination of optimal Abcam PFKFB3 antibody dilution in THP1 cells 95

Figure 4-5 Determination of optimal Abcam PFKFB3 antibody dilution in M4v;11 cells PFKFB3 Knock In cells over expressing PFKFB3 96

Figure 4-6 PFKFB3 expression in AML cell lines detected by Western Blot 97

Figure 4-7 PFKFB3 protein expression (Western Blot) correlation with ROS production in AML cell lines 100

Figure 4-8 Intracellular PFKFB3 expression detected by flow cytometry using MV4;11 in which PFKFB3 was ectopically expressed 101

Figure 4-9 Intracellular PFKFB3 expressions detected by flow cytometry..... 102

Figure 4-10 Intracellular PFKFB3 expression does not correlate with western blot total cell extraction PFKFB3 expression in AML cell lines..... 103

Figure 4-11 PFKFB3 expression in nucleus detected by western blot 104

List of tables

Table 1-1 FAB classification of AML.....	10
Table 1-2 WHO (2016) AML Classification.....	11
Table 1-3 Class and frequency of gene mutations involved in AML.....	12
Table 1-4 2022 ELN risk classification by genetics at initial diagnosis	13
Table 2-1 Summary of reagents and suppliers.....	42
Table 2-2 Summary of antibodies used in western blot and flow cytometry Assays	44
Table 2-3 Summary of cell lines characteristics and culture conditions.....	48
Table 2-4 Table outlining the instrument specifications of the Accuri™ C6 plus	54

Chapter 1 Introduction

1.1 Normal haematopoiesis

Blood has the capacity to regenerate and is one of the most active tissues in the human body, being able to produce about 1×10^{12} cells/day in a human adult, all derived from the haematopoietic stem cell (HSC) within the bone marrow (BM) niche (Keidar 2015; Weltmann and von Woedtke 2016). Haematopoiesis is the process through which cellular blood and plasma components are produced. Throughout all the stages of human haematopoietic development, haematopoietic cells are continuously produced and replaced.

The traditional view is that the haematopoietic system (Figure 1-1) is a hierarchy composed of three main types of haematopoietic cells: thrombocytes, erythrocytes, and leukocytes. HSC have "multipotent" and "self-renewal" capabilities (Renders et al. 2021) and can respond rapidly to the microenvironment while maintaining their identity (Balmer and Riley 2012). Multipotent allows limited HSC to differentiate into all mature blood cells in the body. HSC are mainly differentiated into two major groups: myeloid lineage and lymphoid lineage, both of which are involved in the formation of dendritic cells (Renders et al. 2021). Self-renewal means that most long-term (LT)-HSC exist in the BM in a resting state. When the marrow or HSC is stimulated, LT-HSC can be rapidly activated into short-term (ST)-HSC, and then to haematopoietic progenitor cells (HPC). More recently, niche inflammation and clonal haematopoiesis as a result of aging, expands the blood cell pool and maybe a precursor to haematologic lesions

(Konieczny and Arranz 2018). HSC can also under certain conditions migrate to other bodily sites (1.1.1).

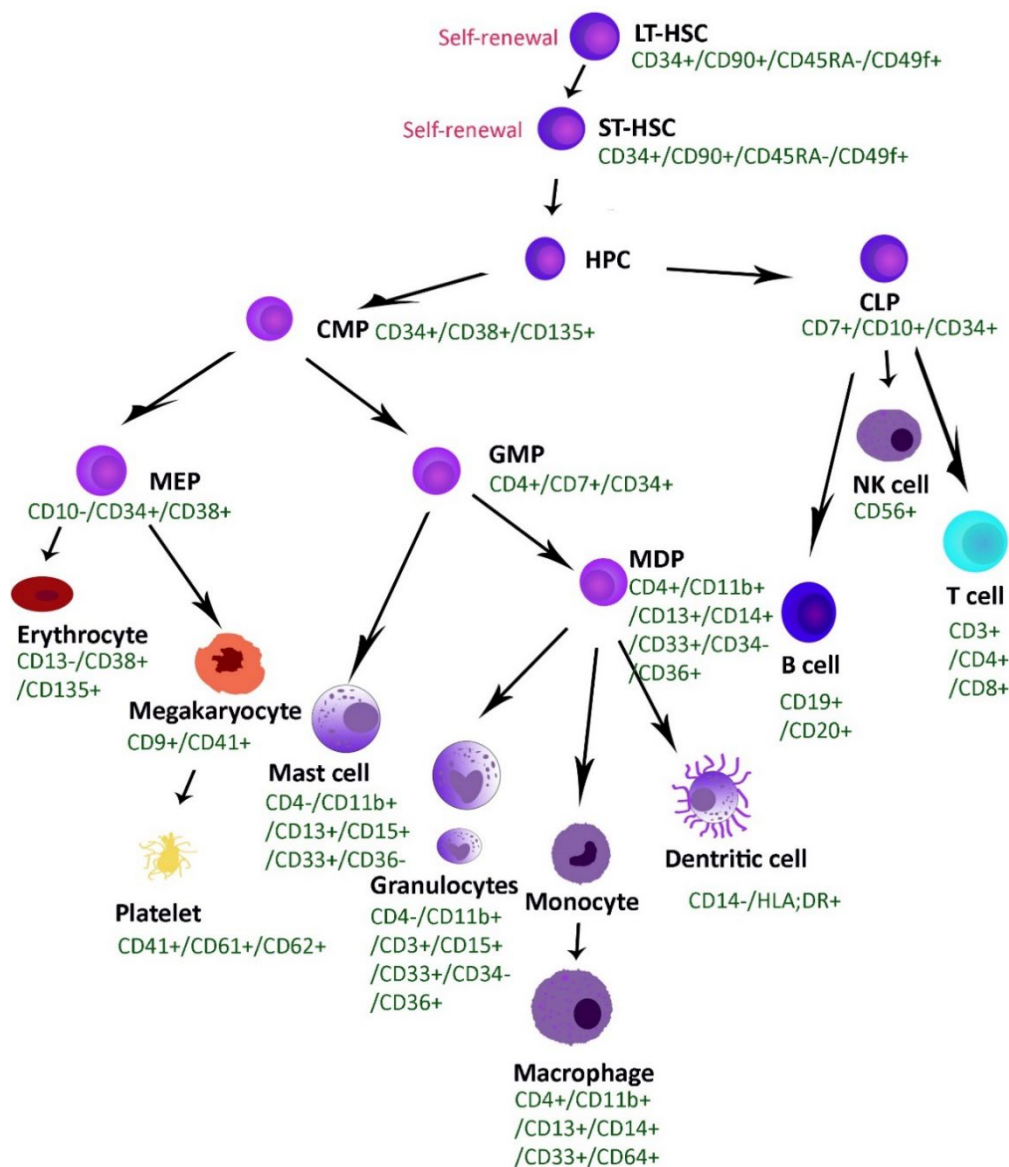


Figure 1-1 Hierarchical representation of human haematopoietic development

This figure shows the differentiation of self-renewing HSCs into mature progeny and the lineage markers (CDs) of the corresponding stages. Modified from (Keidar 2015; Weltmann and von Woedtke 2016).

LT-HSC – long term Haematopoietic Stem Cell; **ST-HSC** – short term Haematopoietic Stem Cell; **MPP** – Multipotent Progenitor Cell; **HPC** – Hematopoietic Progenitor Cell; **MEP** – Megakaryocytic-Erythroid Progenitor Cell; **GMP** – Granulocyte-Monocyte Progenitor Cell; **MDP** – Monocyte-Dendritic cell Progenitor Cell; **CLP** – Common Lymphoid Progenitor Cell; **NK cell** – Natural Killer Cell; **CD** – Cluster of Differentiation.

The functions of haematopoietic cells are variable and depends on the specific haematopoietic cell type. For example erythrocytes carry nutrients and oxygen (O₂) as they circulate the body until they reach tissues where they transport away carbon dioxide (CO₂) and other metabolic waste produced by the tissues (Hamidi and Tajerzadeh 2003). Leukocytes provide immunity (McEver 2015) and thrombocytes control bleeding and coagulation (Brandes 2014). Blood as a tissue can also regulate body temperature and osmotic pressure and balances the pH of the internal environment. The main function of plasma is to transport nutrients and lipids, form osmotic pressure, participate in immunity, coagulation and anticoagulation, and buffer the internal environment reaction (Keidar 2015; Weltmann and von Woedtke 2016).

1.1.1 Haematopoietic stem cells and bone marrow niche

HSC develop from the mesoderm and then establish themselves and further develop within the BM. Recent advances in bioinformatics coupled with single cell analyses have provided powerful tools to analyse haematopoiesis (Renders et al. 2021) . HSC in the BM are dormant while ensuring the body is composed of sufficiently mature haematopoietic cells, which protects the HSCs from being perturbed by cancer mutation factors. HSC start to differentiate into multipotent progenitor cells (MPP) and subsequent mature blood cells. Cytokines and growth factor stimulation, infection, inflammatory factors (1.3.2) are examples of activation signals for haematopoiesis. Single-cell studies of haematopoietic cells have shown that specific cell surface receptors may act as a type of switches to promote self-renewal and multipotent ability. For example: Neogenin-1 is identified as a key surface receptor for self-renewal. Dormant HSCs carry a large amount of the receptor Neogenin-1 on the surface (Renders et al. 2021). HSC in Neogenin-1-knockdown-mice are no longer dormant and become tired prematurely until they lose self-renewal ability. Conversely, when

the amount of Neogenin-1 (the binding and activator of the Neogenin-1 receptor) is increased, HSC remain in a deeper state of dormancy (Renders et al. 2021).

HSC ageing is the process through which HSC gradually lose their self-renewal and multipotency with age. HSC ageing greatly increases the incidence of cellular derailment. Whether the senescence of HSC is caused by intrinsic or extrinsic mechanisms is highly controversial. Regarding the intrinsic mechanism of HSC senescence, there are several factors identified such as: genetic damage (Alter et al. 2012), infinite hibernation (Baker et al. 2016), polarity changes due to asymmetric distribution of proteins such as Cdc42 (Florian et al. 2012), impaired autophagy and mitochondrial activity (Mohrin et al. 2015; Ho et al. 2017), epigenetic reprogramming (Kamminga et al. 2006; Klauke et al. 2013; Steensma et al. 2015). There is also a study that quantified the Cluster of Differentiation changes of HSC using clonal assays. This study showed that the mature progeny regenerated from old HSC were reduced, the proliferative response was delayed, and the BM homing efficiency was reduced by two times in the same stromal cell culture (Rossi et al. 2005) marked in Figure 1-1). On the other hand, there are some transplant experiments that compared the differentiation of young HSC transplanted into the BM niche of old mice and old HSCs transplanted into the BM niche of young mice. The latter showed better preservation of the differentiation and self-renewal capacity of HSC after transplantation (Van Zant et al. 1990; Gardner et al. 1998; Rossi et al. 2005). Even young HSC transplanted into the BM niche of old mice fared worse (Rossi et al. 2005). This indicates an extrinsic mechanism showing that the BM niche is one of the important effects of HSC aging. The BM microenvironment comprises of the vascular BM niche and the endosteal BM niche (Figure 1-2). The BM microenvironment is used to characterise the activity of cell types, structural proteins and signalling molecules which affects HSC. For example, megakaryocytes differentiated from HSC have a feedback loop that promotes HSC quiescence through direct mechanisms (CXCL4 and TGF- β).

independent of stromal niche cells. Macrophages can also indirectly regulate HSC-retaining T cells through niche cells. Neutrophils influence macrophages and stromal cells to promote HSC regulation (Li et al. 2003; Scadden et al. 2003; Visnjic et al. 2004). Structural proteins and signalling molecules also promote HSC quiescence. Interestingly, the survival niche of leukaemia stem cells (LSCs; 1.2.3) is similar to that of HSC (Huntly and Gilliland 2005). However, malignant cells may alter normal niches or create their own to proliferate. The following sections will describe in detail the various changes in acute myeloid leukaemia (AML) compared to normal haematopoiesis.

1.2 Acute myeloid leukaemia

1.2.1 Overview

Leukaemia is a term for a group of haematological malignancy resulting from the accumulation of genetic and epigenetic aberrations in haematopoietic progenitor cells. Leukaemia can be classified through four main types based on the cell it affects and how rapid or long term the onset of disease was: chronic lymphocytic leukaemia (CLL), chronic myeloid leukaemia (CML), acute lymphocytic leukaemia (ALL) and acute myeloid leukaemia (AML). Acute refers to a rapid increase in the expansion of immature cells, and chronic refers to the slow accumulation of abnormal cells under abnormal conditions. The median age at diagnosis of AML is 65 years (Deschler and Lübbert 2006; Shysh et al. 2017), and there are more male patients than female patients (Sinisa 2018).

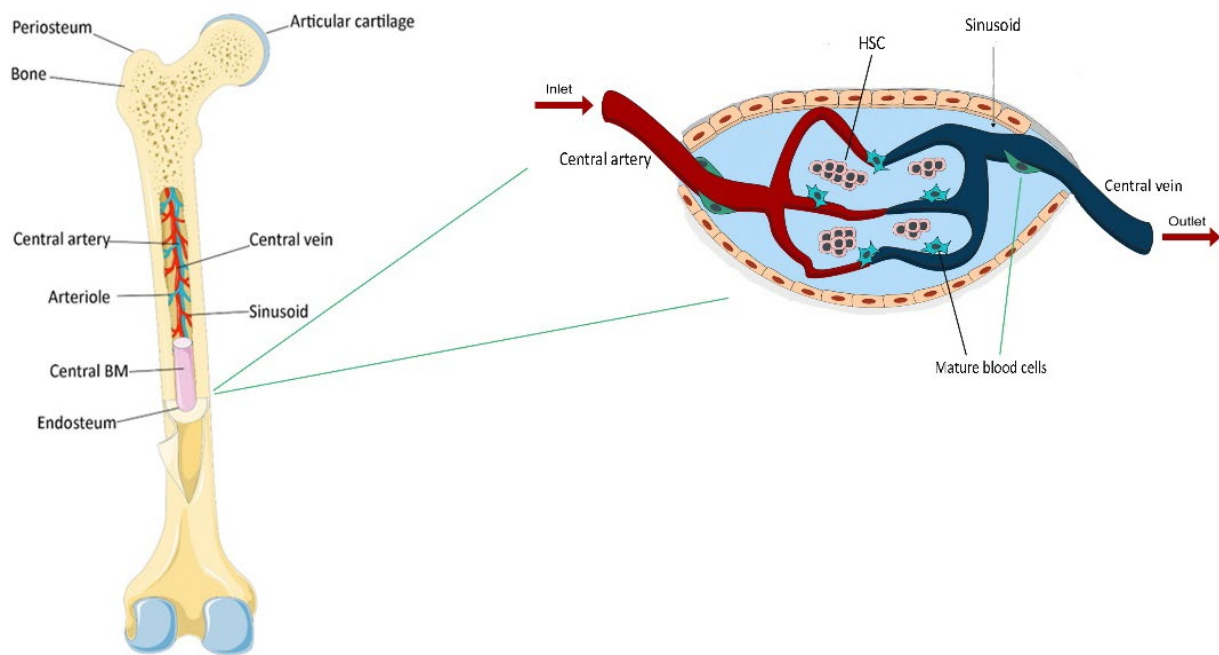


Figure 1-2 Bone marrow niche

A longitudinal section view of a femoral head is shown. The outer surface of the bone is filled by the periosteal layer, and the endosteal layer is the interface between the bone and the BM. Branching arteries and veins are distributed close to the intima along the long axis of the BM lumen. Femur background material from Wikipedia free creative commons source and from (Bessy et al. 2021). HSC differentiate stepwise into mature blood cells in sinusoids.

HSC –Haematopoietic Stem Cell

AML is a complex and heterogeneous haematological malignancy caused by genetic mutations and a block in myeloid differentiation coupled with enhanced proliferation. Different AML subtypes respond differently to treatment and their long-term outcomes are very different is association with different chromosomal and molecular aberrations (Wojcicki et al. 2020). For example, balanced translocations t(8;21) and inv(16) can disrupt the formation of the runx-associated transcription factor 1 (RUNX1), core-binding factor subunit beta transcription factor complex required for normal haematopoiesis (De Kouchkovsky and Abdul-Hay 2016; Edmonson et al. 2019). The French American-British (FAB) classification was devised based only on cellular morphology and cytochemistry, classifying AML into M0 (undifferentiated acute myeloblastic leukaemia) to M7 (acute megakaryoblast leukaemia) subtypes in the 1970s (Table 1-1). Two main classification systems have been used to stratify AML into different subtypes, the FAB system and more recent WHO classification system (Table 1-2). Some patients with special type of mutation tend to be associated with good clinical response and some with less good responses, but poor, intermediate and favourable risk groups have different relative overall survival (OS) durations. In another words, the phenotype of AML is caused by a combination of oncogenic mutations, epigenetic modifications, and metabolic disturbances (Wojcicki et al. 2020).

Previously, a highly consensual '2-hit' model suggested that haematological malignancies require at least two genetic mutations. In this model, mutations in signalling pathways associated with cell proliferation and survival (Class I mutations) must occur together with mutations in transcription factors (Class II mutations) that regulate cell differentiation and self-renewal (Conway O'Brien et al. 2014; Kihara et al. 2014; Takeshima et al. 2014). However, more recently, AML has been defined by including epigenetic regulators as Class III mutations (Sun et al. 2018) (Table 1-3). As an example, 30% of AML have FLT3 mutations (Table 1-3), which are mainly associated with poor prognosis (Ju et al. 2017). Interestingly, studies have shown that

the FLT3-ITD mutation promotes dependence on aerobic glycolysis by upregulating mitochondrial hexokinase (Ju et al. 2017). Another example includes AML with mutated RUNX1 which is known to have a poor prognosis (Gaidzik et al. 2016; Stengel et al. 2018)(1.4.4). However, most RUNX1 mutations are single sub benign, usually frame-shifted or missense, without any hotspots (Schnittger et al. 2011). Later, grouping AML patients on risk have been developed by the European Leukaemia Net (ELN) (Döhner et al. 2017). This divided patients into three groups based on different mutations and its prognostic performance: Favourable, Intermediate and Adverse. OS was 35-45% associated with risk grouping (Short et al. 2020). Allogeneic HSC transplantation (HSCT) generally improves the outcome of favourable and intermediate AML patients (Short et al. 2018), which also responses better to standard chemotherapy (Koreth et al. 2009; Stelljes et al. 2012). Recently, ELN updated a newer guideline with more new genomic diagnostics and molecular markers of disease in 2022 (Table 1-4).

1.2.2 AML pathophysiology and Treatment

AML is associated with a number of risk factors including age (Shysh et al. 2017), exposure to ionizing radiation (Boddu et al. 2017), cigarette smoking, inherited Down syndrome and Li-Fraumeni syndrome (Deschler and Lübbert 2006), after receiving chemotherapy and radiation therapy, or from progressed myelodysplastic syndrome (MDS) (Boddu et al. 2017), although the majority of newly diagnosed cases will have none of these risk factors (Boddu et al. 2017). Relapsed AML or secondary AML transformed from other diseases are more difficult to treat and associated with adverse poor clinical outcomes. AML patients usually present with dyspnoea, fatigue, anaemia, dizziness, and inappropriate bleeding or bruising.

The initial assessment is based on patient characteristics including age, performance status, and complications. In this step, patients can potentially receive more specific

Table 1-1 FAB classification of AML

FAB Classification	Description
M0	Undifferentiated AML
M1	Acute myeloblastic leukaemia with maturation
M2	Acute promyelocytic leukaemia (APL)
M3	Acute myelomonocytic leukaemia
M4	Acute myelomonocyte leukaemia with eosinophilia
M5	Acute monocyte leukaemia
M6	Acute erythroid leukaemia
M7	Acute megakaryoblast leukaemia

This table outlines the FAB classification of AML based on morphological and cytological analysis (Bennett et al. 1976).

Table 1-2 WHO (2016) AML Classification

	Cytogenetic and Molecular Characteristics
AML with recurrent Genetic Abnormalities	AML with t(8;21)(q22:22.1);RUNX1::RUNX1T1 AML with inv(16)(p13.1q22) or t(16;16)(p13.1;q22);CBFB::MYH11 APL with PML::RARA AML with t(9;11)(q23.1q26.2);MLLT3::BCR2A AML with t(6;9)(p23;q34.1);DEK::NUP214 AML with inv(3)(q21.3q26.2) or t(3;3)(p13.3;q13.3);RBM15::MKL AML with biallelic mutations of CEBPA
AML with Myelodysplasia-related changes; Therapy-Related Myeloid Neoplasms ; AML, not otherwise specified	Alkylating -agent or radiation-related type Topoisomerase-II-inhibitor related type Others AML with minimal differentiation AML without maturation AML with maturation Acute myelomonocytic leukaemia Pure erythroid leukaemia Acute megakaryoblastic leukaemia Acute monoblastic/monocytic leukaemia Acute basophilic leukaemia Acute panmyelosis with myelofibrosis
Myeloid Sarcoma; Myeloid Proliferations related to Down Syndrome	Transient abnormal myelopoiesis Myeloid leukaemia associated with Down Syndrome

This table outlines the WHO classification system for AML with its cytogenetic and molecular aberrations which are associated with the disease sub-types (Arber et al. 2016; Medinger and Passweg 2017).

Table 1-3 Class and frequency of gene mutations involved in AML

Group	Gene	Mutational Frequency
Class 1 (Signal Transduction)	FLT-3	25-45%
	c-KIT	6-10%
	PTPNII	2-5%
	RAS	15-30%
	CBL	2-3%
	JAK	2-3%
Class 2 (Transcription Factors)	RUNX1	6-11%
	C/EBP α	4-9%
	NPM1	25-35%
	GATA2	3-5%
	RUNX1::ETO	10-15%
	CBF β	3-8%
	PML::RARA	5-10%
	MLL	5-9%
Class 3 (Epigenetic Regulators)	TET2	8-27%
	IDH1	6-9%
	IDH2	9-12%
	DNMT3A	18-23%
	TP53	7-12%
	WT1	10-13%
	ASXL1	3-11%
	BCOR	5%
	BCOR1	6%

This table outlines the Class and frequency of gene mutations involved in AML (Naoe and Kiyoi 2013)

Table 1-4 2022 European LeukemiaNet (ELN) risk classification by genetics at initial diagnosis

Risk category	Genetic abnormality
Favourable	t(8;21)(q22;q22.1)/RUNX1::RUNX1T1 inv(16)(p13.1q22) or t(16;16)(p13.1;q22)/CBFB::MYH11 Mutated NPM1 without FLT3-ITD bZIP in-frame mutated CEBPA
Intermediate	Mutated NPM1 with FLT3-ITD Wild-type NPM1 with FLT3-ITD t(9;11)(p21.3;q23.3)/MLLT3::KMT2A Cytogenetic and/or molecular abnormalities not classified as favorable or adverse
Adverse	t(6;9)(p23;q34.1)/DEK::NUP214 t(v;11q23.3)/KMT2A-rearranged t(9;22)(q34.1;q11.2)/BCR::ABL1 t(8;16)(p11;p13)/KAT6A::CREBBP inv(3)(q21.3q26.2) or t(3;3)(q21.3;q26.2)/GATA2, MECOM(EVI1) t(3q26.2;v)/MECOM(EVI1)-rearranged -5 or del(5q); -7; -17/abn(17p) Complex karyotype, monosomal karyotype Mutated ASXL1, BCOR, EZH2, RUNX1, SF3B1, SRSF2, STAG2, U2AF1, or ZRSR2 Mutated TP53

This table outlines the AML classification system based on the ELN stratification ((Döhner et al.)2022).

therapy due to our increased understanding of AML malignant macromolecules disorders. Treatment strategies for AML are generally divided into induction, consolidation, and maintenance therapy. Induction chemotherapy is to reduce the tumour burden and achieve complete remission, which is defined as <5% blasts in BM, neutrophil counts >1,000/ μ L, doesn't have Auer rods and extramedullary leukaemia (Döhner et al. 2017). For young or 'fit' patients, induction therapy usually uses variations on '3+7' strategy. This comprises three days of anthracycline (usually daunorubicin (DNR) at 60mg/m²/day), accompanied by 7 days of cytarabine (Ara-C; 100mg/m²/day) (Ferrara and Schiffer 2013).

The mechanism of DNR is mainly through the inhibition of topoisomerase II to cause uncontrolled DNA double bond breakage to cause cytotoxicity (Lima and Mondragón 1994), or DNR undergoes a redox reaction in cells to generate ROS to damage cells (Doroshov 2019). Ara-C cooperates with cytarabine triphosphate to inhibit DNA synthesis to prevent cell cycle progression (Li et al. 2017).

The response to induction therapy was relatively successful in younger patients less than 60 years old (Burnett et al. 2009; Ferrara and Schiffer 2013). However, there are additional complications that can occur after induction therapy for patients who are over 65 years old. Complete remission rates vary between 45%-55% and survival rates of <6 months in elder group (Burnett et al. 2009; Ferrara and Schiffer 2013). A follow-up study reported that the patient age and treatment strategy are the most effective factors to OS (Čolović et al. 2019). In this experiment, patients had median white blood cell count 1.9×10^9 /L, platelets 47.2×10^9 /L and haemoglobin 85.9 g/L. Nineteen patients were treated with standard 3 + 7 protocol (daunorubicin 45 mg/m² 1, 3, 5 days, cytosine-arabioside 100 mg/m²/12 h for 7 days), 5 patients with HDAC protocol and, 3 patients with low dose cytosine-arabioside and in 6 patients only supportive therapy was applied. The median OS of patients receiving low-dose

cytosine-arabioside was 6 months, the median age of the patients was 58.9 years (19-88 years), and the patients were 33, 21 men and 21 women. 12 cases (Čolović et al. 2019).

There is a need to develop low toxicity therapies for patients with AML. The advent of genetic sequencing and the identification of specific gene segments has made targeted therapy for AML possible. The most successful targeted therapy for AML to date has been the treatment based on all-trans-retinoic acid (ATRA) and arsenic trioxide (ATO) for acute promyelocytic leukaemia (APL) patients. APL is characterised by the reciprocal translocation of chromosome 15 and 17 (t(15;17) (q22;q21) ,which was previously considered as a poor prognosis disease. With the addition of ATRA to induction chemotherapy, long-term survival stands at around 90% (Sanz et al. 2019).

The US Food and Drug Administration approved eight new targeted therapies for AML, including inhibitors of mutant FLT3, IDH1 and IDH2, KRAS and NRAS, KIT and TP53 (Pandor et al. 2018). Patients with mutations at these genetic loci received more precise and less toxic treatments (Reviewed in (Short et al. 2020)). Inhibitors targeting specific abnormalities are continually being developed. For example, inhibitors of FLT3: the first generation is Midostaurin, which has broad activity against non-FLT3 targets; while the second generation is Gilteritinib reduces the probability of off-target activity because of its higher specific targeting (Short et al. 2020). The excellent performance of targeted therapy in prognosis has been reflected in the overall survival data (Paschka et al. 2018). Targeted therapy can help induction therapy to be more effective.

Other examples include the use of Venetolax. Chemotherapy resistance can be circumvented by targeting the intrinsic apoptosis pathway: such targets include BCL-2, MCL1 and MDM2 (Short et al. 2020). In 2018, the FDA also approved the combination of the selective BCL-2 inhibitor Venetoclax to be used in AML patients

who were unsuccessful with generic therapy and elder group (Wei et al. 2018; DiNardo et al. 2019).

1.2.3 Leukaemia stem cells

Leukaemia stem cells (LSCs) are the structural apex in initiating and maintaining disease relapse (Thomas and Majeti 2017). LSCs exhibit properties of self-renewal (Ito and Suda 2014), cell cycle quiescence (Kunisaki et al. 2013; Takubo et al. 2013), and chemoresistance (Zhao 2016). Because AML is often not diagnosed at an ultra-early asymptomatic stage, the nature of LSCs lesions origin and the sequence of LSCs subsequent mutations remain poorly understood. In fact, the evolution of leukaemia, whether spontaneously or influenced by external forces, is a very complex phenomenon. Targeted therapy based on monoclonal antibodies relies on specific inhibitors of various molecular abnormalities. This therapy often faces relapse precisely because of the target change (Madaci et al. 2021). Trajectory analysis to identify distinct tumour subpopulations by single-cell analysis would be of great benefit to this (Papaemmanuil et al. 2016). Clonal heterogeneity and evolution are precisely defined by novel approaches through single-cell analysis and next-generation sequencing, enabling characterized and time-variable adaptation of therapy. FLT3, IDH1/IDH2 and BCL-2 are all available targets identified by this strategy (Madaci et al. 2021).

There are 84 genes in LSCs (with CD34⁺CD38⁺) was tested by single-cell culture techniques. It found 27 genes with decreased expressions involved in cell activation pathways. Particularly those genes who associated with tumour growth factors, such as Wnt, FGF, Hh, Notch, IL6ST (Interleukin 6 Signalling Sensor) and the leukaemia inhibitory factor receptor superfamily (Won et al. 2015). The quiescent phenomenon of LSCs exhibited here may be due to a reduction in mitochondrial DNA copy number, which is not protected by histones and is closer to ROS generation sites and may be

more prone to mutation (Won et al. 2015). Proliferative and self-renewal functions are separate in LSCs and HSCs (Zhu et al. 2018). Other characteristics of LSC include DNAMT3A^{MUT} in HSC which have emerged in the early evolution of AML (Shlush et al. 2014b); this showed multilineage repopulation advantages over normal HSCs. There are also several surface markers which are unregulated in LSCs compared to HSC such as CD44 (Dick et al. 2006), CD123 (Jin et al. 2009) and CD47 (Jaiswal et al. 2009).

Drug resistance is a cause of poor treatment outcomes and recurrence (Saha and Lukong 2022). A study showed that ATP binding cassette transporters in cancer stem cells support chemoresistance (Begicevic and Falasca 2017). In general, preleukaemic HSC are undetectable, and mutations are found only in the blast phase of leukaemia (Corces et al. 2016). Sometimes a single mutation provides a decisive selection advantage for cells associated with multiple mutations, for example: when 10 HSC clones with different basic driver mutations were transplanted into mice, 9 produced dominant mutant NPM1 clones. However, the study found that NPM1 mutations can only be powerful driver mutations when they occur in cells with increased self-renewal capacity acquired through DNMT3A or TET2 mutations (Potter et al. 2019).

1.3 Reactive oxygen species (ROS)

ROS refers to free radicals and other reactive oxygen molecules (such as hydrogen peroxide, H₂O₂) (1.2.3). ROS play an important role in many diseases, such as atherosclerosis, rheumatoid arthritis, and many cancers (1.3.3). There are several sources of ROS production, such as hydroxyl radical, hydroxide ion, triplet oxygen, superoxide anion, peroxide ion, hydrogen peroxide, and nitric oxide. The amount of intracellular ROS is maintained at non-destructive levels by enzymatic and non-

enzymatic antioxidant activities, but under special conditions, ROS production increases rapidly and exceeds the ability of antioxidants to scavenge oxidative bursts that affect biomolecules and interfere with cellular redox homeostasis (Juan et al. 2021; Sachdev et al. 2021; Cheung and Vousden 2022). The majority of ROS are produced either as a by-product of electron transport chain activity (ETC) (Nolfi-Donagan et al. 2020) during oxidative phosphorylation in mitochondria, or from nicotinamide adenine dinucleotide phosphate (NADPH) oxidase family of enzymes (NOX) (Hole et al. 2011). ROS have several functions including in innate immunity, helping proteins fold on the endoplasmic reticulum, signalling for cell proliferation and, differentiation, and modulating gene expression. ROS have also been shown to regulate signal transduction and gene expression through redox-sensitive kinases, phosphatases, and transcription factors to sustain the cell in a nonequilibrium steady-state supporting several normal cellular functions including cell proliferation (Hitchler and Domann 2012) (1.3.3).

The detection of ROS is also evolving, ranging from UV–visible spectrometry (Liu et al. 2019), chromatography (Hanaoka et al. 2001), spectrophotometry (Beyer and Fridovich 1987; Bartosz 2006), luminometry ((Eltzschig et al. 2006)) to nanotechnology (Zhao et al. 2020), biomimetic engineering *ex vivo* (Feizabadi et al. 2019), three-dimensional culture methods in *vitro* detection (Lyu et al. 2019), and implanted sensors in *vivo* detection (Zhang et al. 2020b), which combined action of light, oxygen and photosensitizers. Chemiluminescence is the emission of light resulting from a chemical reaction. The activity is the excitation of the photosensitizer by chemiluminescent, and the light emission does not necessarily correspond to the absorption maximum of the photosensitizer. Light and photosensitizers are harmless to cells, and when combined with oxygen, ROS will be generated, so the laser response value reflects the amount of ROS (Bancirova and Lasovský 2011). Here we used luminometry to quantify ROS; extracellular superoxide was detected by luminol,

enhanced by Diogenes (Figure 1-3) (Eltzschig et al. 2006). The specificity of the Diogenes™ probe for superoxide has previously been validated (Hole et al. 2010).

1.3.1 NOX2 derived ROS and electron transport chain (ETC)

The NADPH oxidase (NOX) family is composed of NOX1, 2, 3, 4, and 5 and dual oxidases (DUOX) 1 & 2. They are transmembrane proteins that convert electrons from NADPH to molecular oxygen to help generate ROS (Figure 1-3). The NOX family is highly expressed in specific tissues: NOX1 - colon tissue; NOX2 - phagocytic cells; NOX3 - inner ear; NOX4 - kidney and blood vessels; NOX5 - lymphoid tissue and testis; DUOX1, 2 - thyroid. In osteoclasts, B cells and HSCs have moderately expressed NOX2, and NOX4 is also expressed (Augsburger et al. 2019). It has been shown that ROS which is generated by NOX enzymes, and nontoxic doses of exogenous H₂O₂, activate growth factor mediated MAPK/ERK mitogenic signalling and promote the self-renewal of murine pluripotent stem cells (Kang et al. 2016).

The catalytic core structure of NOX2 is cytochrome b558, which is mainly composed of six subunits: gp91phox (NOX2) and p22phox, and p40phox, p47phox, p67phox and RAS-related C3 botulinum toxin substrate 2 (Rac2). NOX2 is a protein encoded by the NOX2 gene (also known as the *CYBB* gene) that forms an enzyme complex called NADPH oxidase, which plays a vital role in the immune system (Kang et al. 2016).

The chemical process of ROS production is shown in Figure 1-3. There are three production pathways following the monovalent reduction of molecular oxygen to produce superoxide (O₂^{•-}) (Bienert et al. 2006). The first pathway is to produce H₂O₂ through enzyme superoxide dismutase (SOD) or spontaneous reaction (Sies 1993). Alternatively, reactive nitrogen species (oxidative nitrate, etc.) are formed from superoxide and nitric oxide. The third pathway is the formation of hydroxyl radicals (OH[•]) by superoxide and hypochlorous acid (HOCl). H₂O₂ forms hydroxyl radicals and

OH^- under the catalysis of Fe^{2+} or Cu^{2+} , and the generated Fe^{3+} is reduced by superoxide to produce O_2 and Fe^{2+} (Rae et al. 1999). The process of this chemical reaction is achieved through the cellular level of free iron/copper, which is tightly controlled by transferrin. Free iron in haematopoietic cells ratio is 0.2-1.5:1000 (Epsztejn et al. 1997). Transferrin prevents Fe^{2+} from reacting with H_2O_2 to produce highly destructive OH^\bullet (Ponka 1999). Patients with β -thalassemia often have more excess free iron that results in a large amount of ROS production, which causes them to develop high levels of oxidative stress (Sengsuk et al. 2014). Its symptoms are primarily DNA damage, proteins and lipids are oxidized and enzymes are inhibited (reviewed in (Valko et al. 2007)). Thus, the level of ROS is tightly regulated by normal cells although it is required for many normal biological functions.

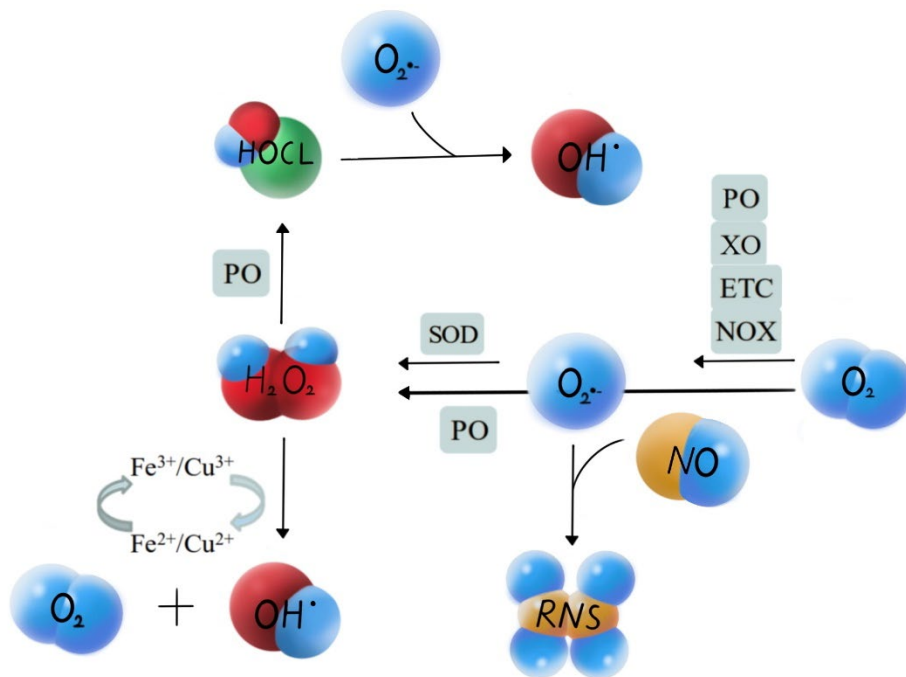


Figure 1-3 Production of reactive oxygen species

The reaction between peroxisomes (PO) and xanthine oxidase (XO) reacts with the electron transport chain (ETC) or NADPH oxidase (NOX) produces superoxide ($O_2^{\bullet-}$) by univalently reducing diatomic oxygen (O_2). H_2O_2 can be produced through the reduction on O_2 by PO. The enzymatic action of superoxide dismutase (SOD) or spontaneous reactions can also cause $O_2^{\bullet-}$ to dismutate to H_2O_2 . Subsequently, H_2O_2 can produce Hydroxyl radicals (OH^{\bullet}) by generating hypochlorous radicals ($HOCl$) in the PO or through Fenton chemistry. Nitric oxide radicals (NO) can also react with $O_2^{\bullet-}$ to produce Reactive Nitrogen species (RNS).

Whilst not a focus of this thesis it is important to appreciate another major source of ROS. ROS is also produced by the activity of electron transport chain (ETC) composed of four complexes produced in the inner mitochondrial membrane, which are Complex I (nicotinamide adenine dinucleotide (NAD)H: ubiquinone oxidoreductase or NADH dehydrogenase), Complex II (succinate dehydrogenase or succinate co-enzyme Q10 (CoQ) reductase), Complex III (cytochrome bc₁ complex) and Complex IV (cytochrome c oxidase). The resulting series of redox reactions allow protons to appear in the intermembrane space of the electrochemical gradient, resulting in oxidative phosphorylation. When oxidative phosphorylation occurs, complexes I, II, and IV establish a proton gradient across the membrane for proton return, and adenosine diphosphate is catalysed by complex V to generate ATP (Nolfi-Donagan et al. 2020). Complex I does not affect ROS production, but instead flavin-dependent dehydrogenases utilize the NADH/NAD pool and operate at a similar redox potential to complex I to generate large amounts of ROS; complex II is not generally considered the main source of ROS Source, contribution remains unknown; ROS are produced at a lower rate at complex III; oxygen limitation of complex IV leads to increased electron accumulation and reduction of complexes I-III, extramitochondrial cytokines may regulate ETC ROS during cellular hypoxia Production, phosphorylation can regulate the activity of cellular kinases that regulate ETC activity (Nolfi-Donagan et al. 2020).

1.3.2 ROS and cell signalling

The role that ROS play will also vary based on their physiological ROS levels. Damage caused by higher levels of oxidative distress can impair the function of all classes of macromolecules (Sies 1986). Oxidative distress damage has been identified in mutagenesis and cancer development (Jackson and Bartek 2009). However, lower levels of ROS can act in cell signalling. The key redox signalling agents generated belong to two species, H₂O₂ and O₂^{•-} (1.3.1). H₂O₂ is the major agent signalling through

specific protein targets at low physiological levels in the nanomolar range (Reczek and Chandel 2014). The intracellular concentration of H_2O_2 is maintained in the low nanomolar range (approximately 1 – 100nM) and held under tight control (Parvez et al. 2018). H_2O_2 occurs physiologically at a low steady state level in normally respiring eukaryotic cells and is generated through stimulus by metabolic cues and/or various stressors, while being able to be removed by efficient reducing systems (Parvez et al. 2018).

Redox signalling can occur through oxidation of sulphur (thiolate groups) in target proteins or reversible methionine oxidation (Kaya et al. 2015), through sialoproteins (Brigelius-Flohe and Flohe 2017), oxidation of protein metal centres and oxidized lipids (Poli et al. 2004). Redox signalling through oxidation of sulphur shows rates of reaction with H_2O_2 several orders of magnitude higher than those of other protein thiols (Zeida et al. 2019). Redox relays, which are carriers of oxidant messages are used to identify physiological targets of oxidant signals by analysing the specificity of signalling by directed and confined interactions (Sobotta et al. 2015). These targets play a key role as molecular redox switches in signal transduction and act at various levels of cell regulation (Ristow and Schmeisser 2014). The key cellular hubs of redox signalling are the plasma membrane when signal transduction occurs, the nucleus when redox signalling occurs and ROS in mitochondria. Given the extensive nature of the interactions between oxidants and cellular processes they are involved in several organs in terms of their physiology and in dysregulated disease processes.

Redox signalling affects protein function, leading to changes in signalling outputs, enzyme activity, gene transcription and membrane and genome integrity amongst others (Marinho et al. 2014). Protein kinases mediate a wide range of distinct cellular processes that cover proliferation (1.3.3) and differentiation to decisions on survival or cell death/apoptosis by protein phosphorylation. Direct redox based regulation of

protein-tyrosine kinases impacts protein-tyrosine phosphorylation (Dustin et al. 2020). Protein tyrosine kinases such as epidermal growth factor receptors and Src kinases are activated by H_2O_2 (Truong and Carroll 2013). It has been shown that ROS which is generated by NOX enzymes, and nontoxic doses of exogenous H_2O_2 , activate growth factor mediated MAPK/ERK mitogenic signalling and promote the self-renewal of murine pluripotent stem cells (PSCs) (Kang et al. 2016).

While the list of redox signalling targets is very extensive, I have provided examples below that are closely related to my research which include hypoxia inducible factor (HIF), glyceraldehyde phosphate dehydrogenase and metabolic adaptation (GADPH), uncoupling proteins (UCPs) and protein-tyrosine phosphorylation and dephosphorylation.

HIF is a transcription factor that functions as the master regulator of transcriptional responses where there are lowered levels of oxygen (Kaelin and Ratcliffe 2008). Hypoxia has been associated with an increase in $O_2^{\bullet-}$ (and subsequent H_2O_2) generation through inhibiting mitochondrial ETC (Hernansanz-Agustín et al. 2017). During hypoxia, oxidants serve to stabilise HIF by mounting a hypoxic response (Waypa et al. 2016). Oxidant generation also interferes with HIF mediated transcription in normoxia thus affecting HIF pathways under non-hypoxic conditions leading to a stress adaptive response (Pouyssegur and Mechta-Grigoriou 2006). GADPH, a central glycolytic enzyme (1.4), can acquire non-glycolytic functions on oxidation thus making it a ROS target. H_2O_2 can inhibit GADPH through reactions with a conserved catalytic cysteine that catalyses sensitivity towards its glycolytic substrate, glyceraldehyde 3-phosphate (Sirover 2018). $O_2^{\bullet-}$ promotes uncoupling activity in UCPs causing mild mitochondrial uncoupling. The uncouple limits activity in the mitochondrial ETC which downregulates mitochondrial oxidant production.

Conversely, slight increases in mitochondrial oxidant production leads to deglutathionylation that activates the UCPs (Mailloux and Harper 2011).

Nitric oxide, hydrogen sulphide and oxidised lipids are other ROS molecules that are involved in redox signalling. Methodological advances have enabled the discovery of the interactions between specific ROS molecules with targets in redox signalling pathways resulting in advances in understanding their role in physiology and disease including cancer. Nitric oxide, hydrogen sulphide and oxidised lipids are other ROS molecules that are involved in redox signalling (Forrester et al. 2018) but beyond the scope of this current study. The next section will introduce ROS and how they can influence proliferation.

1.3.3 ROS induced cell proliferation

If ongoing aerobic glycolysis produces high levels of ROS and is followed by pyruvate oxidation in mitochondria (also known as the Warburg effect (1.2)) , this leads to an increase in receptor and oncogene activity, and the stimulation of growth factor-dependent pathways or oxidizing enzymes (Finkel 2001). ROS can control cell proliferation and apoptosis by impacting several cell signalling pathways through interactions with proteins. The role of ROS in the regulation of cell proliferation is well documented (reviewed in (Burch and Heintz) 2022) .

Signalling events of the cell cycle that are dependent on ROS can be classified into those involved in promoting the mitogenic signal transduction from the cell membrane to the nucleus and those, that are involved in stimulating the progression of the proliferative phases of the cycle and ensuring the phases occur sequentially (Burhans and Heintz 2009). The signalling events that promote the mitogenic signal transduction from the cell membrane to the nucleus include the canonical mitogenic pathways

MAPK/ERK and PI3K/Akt that are stimulated by ligand-dependent activation of tyrosine kinase receptors.

It has been shown that cell proliferation is promoted by the generation of ROS by NOX by stimulating the activation of corresponding transmembrane receptors in response to EGF, FGF, PDGF, insulin, and other growth factors ((Burch and Heintz), 2022). The cell cycle dependent increase of intracellular ROS levels was necessary to promote cellular proliferation through the activation of ROS-dependent signalling cascades. It has also been shown that that cytoplasmic NOX-produced ROS play a role in the regulation of hESC proliferation (Ivanova et al. 2021). ROS production which is mediated by the targeted activation of intracellular receptors also leads to the stimulation of murine PSCs proliferation through the activation of p38 MAPK and Wnt/ β -catenin pathways (Jeong et al. 2009). ROS can also play a vital role in the proliferation of cancer cells by activating other kinases such as the protein kinase C (PKC), after inducing the activities causing the release of calcium from cellular stores (Gopalakrishna and Jaken 2000).

1.3.4 ROS induced proliferation in haematopoietic cells

Low levels of ROS allow HSCs to maintain their normal functions, including proliferation and differentiation (Kinder et al. 2010). It has been shown that moderate elevation of ROS in HSCs by incubation of cell with low doses of the glutathione depleting agent, L-Buthionine-sulfonimine, increased their clonogenicity (Juntilla et al. 2010). Similarly, it has also been shown that ROS-dependent proliferation of HSCs also plays an important role in the nascent stages of haematopoietic reconstitution after HSC transplantation (Lewandowski et al. 2010). Higher levels of ROS can have a negative effect on HSCs. It has been shown that incubation of mouse BM HSCs with high concentrations of L-Buthionine-sulfonimine resulted in drastically lower HSC clonogenicity (Rodriguez et al. 2011). mTOR is a serine/threonine kinase belonging to

the PI3K-related kinase family that interacts with several proteins to form two distinct multiprotein complexes: mTOR complex 1 (mTORC1) and mTOR complex 2 (mTORC2). mTORC1 plays a vital role in regulating cell metabolism, growth, proliferation, autophagy, and other functions. Several upstream signalling pathways can regulate the activity of mTORC1 including the PI3K–Akt pathway. It was shown that deletion of phosphatase and tensin homologue (Pten) (a negative regulator of the PI3K–Akt pathway), resulted in HSC depletion and leukemic transformation by promoting HSC proliferation (Yilmaz et al. 2006). However, it was later proven that overactivation of mTORC1 stimulates HSC proliferation, impairs HSC renewal eventually causing HSC exhaustion in association with an increased production of ROS (Chen et al. 2008).

Activated Ras also promoted both the survival and the growth factor–independent proliferation of CD34⁺ cells (Hole et al. 2010). Moreover, overproduction of NOX-derived ROS promotes proliferation of AML blasts and inhibition of p38MAPK helps cancer cells resist normal mechanisms of proliferation inhibition, conferring a competitive advantage on leukemic clones. From the data. More than 60% of primary AML blasts produce high levels of ROS, which drive AML proliferation. Robinson *et al.* found that ROS promotes glucose uptake in HSPC model, mouse bone marrow model through PFKFB3 upregulate (Robinson et al. 2020) (1.4.3.3). Over expression of ROS also associated with the glucose upregulate in AML primary blasts (Robinson et al. 2020).

Dependent regulation of PFKFB expression is regulated by several molecular pathways, including those closely related to oncogenic signaling is described in 1.4.2.

1.4 Glycolysis

1.4.1 Glycolysis pathway

Glycolysis is the metabolic pathway that converts glucose to pyruvate, releasing adenosine triphosphate (ATP) and NADH in the process. Glycolysis begins with the transport of glucose by GLUT to intracellular phosphorylation and involves 10 enzymatic reaction steps. Glycolysis consists of two parts that require energy (conversion of glucose to triose phosphate) and energy production (conversion of glyceraldehyde-3-phosphate to pyruvate) (Figure 1-4). ATP stores and transmits chemical energy for the cell. Adenosine monophosphate (AMP) is formed in the body after ATP hydrolyses a pyrophosphate group and releases energy. It can also undergo a phosphoryl group transfer reaction with ATP to produce 2 adenosine diphosphate (ADP) molecules, and further bind ATP. Glycolysis, the conversion of pyruvate to lactate under anaerobic conditions, provides conditions for hypoxic high-speed glycolytic activity in malignancies (Belambri et al. 2018). Glycolysis is the largest contributor to cytoplasmic NADPH, and NADPH production is significantly increased by enhancing the flux of glucose into the oxidative branch of the Pentose phosphate pathway (PPP) in various cancers. Cytoplasmic NADPH is mainly produced by the PPP pathway (Belambri et al. 2018; Ju et al. 2020). With the help of four additional types of enzymatic reactions, the gluconeogenesis pathway completes the opposite effect of the glycolysis pathway from the process of synthesizing sugar from pyruvate, ensuring that the body's blood sugar is at a normal level. The main precursors of gluconeogenesis are lactic acid, pyruvate, amino acids and glycerol (Hatting et al. 2018).

1.4.2 PFK regulation

Phosphofructokinase (PFK) is a major regulatory glycolytic enzyme and is considered to be the regulator of glycolysis (Sola-Penna et al. 2010). This enzyme is regulated by a variety of metabolites and intracellular proteins, and its morphology is transferred between monomeric, dimeric, tetrameric and more complex oligomeric structures (Li et al. 1999; Sola - Penna et al. 2010). The transition between PFK dimers and tetramers is directly related to enzyme regulation, with dimers having very low catalytic activity, while tetramers are fully active(Luther et al. 1986; Li et al. 1999). In cellular metabolism, metabolites that regulate PFK activity in turn regulate the enzyme oligomeric conformation. Inhibition of PFK by high ATP levels is a clear signal to the cell that the rate of glycolysis should be reduced, avoiding unnecessary ATP synthesis (Costa Leite et al. 2007). The elevated rate of oxidative glycolysis produces lactate and the accumulation of this metabolite results in direct inhibition of PFK (Costa Leite et al. 2007). Elevated ADP and AMP due to high ATP utilization counteract the inhibitory effect of lactate accumulation on PFK, signaling the need for ATP synthesis to cells (Hers and Van Schaftingen 1982). The regulatory mechanism of PFK exhibits a balance of PFK inhibitors and activators by driving the enzyme activity toward an active or inactive conformation by a single mechanism (Hers and Van Schaftingen 1982). Phosphorylation of PFK increases the affinity of the structure, thereby regulating the proportion of enzymes associated with the ultrastructure of the cell (Kotowski et al. 2021).

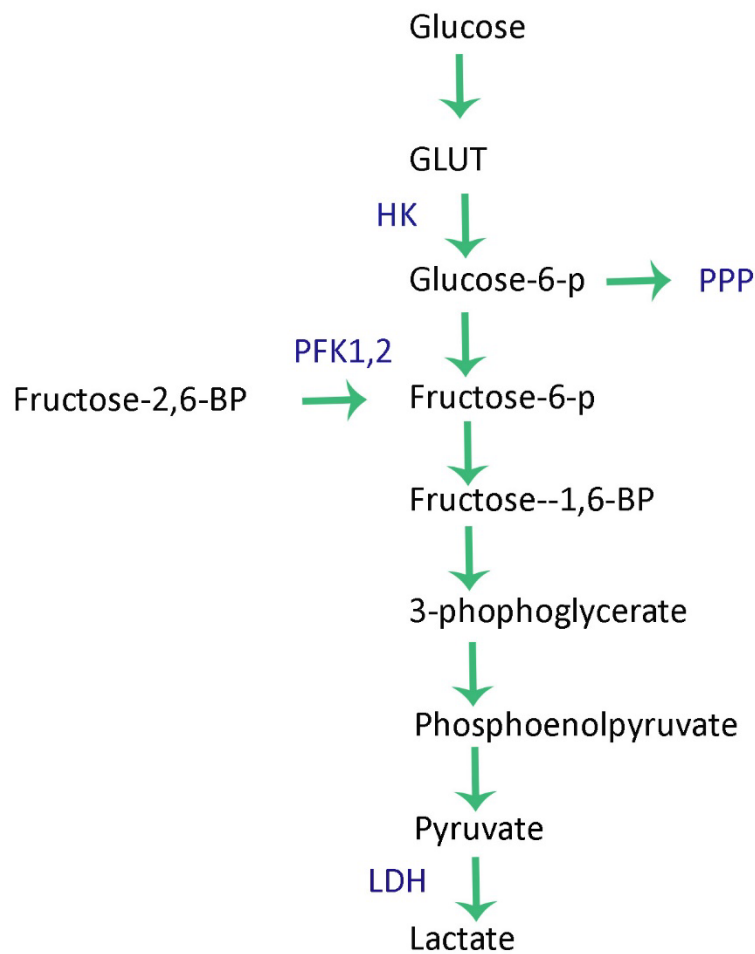


Figure 1-4 Glucose metabolism

This is a schematic diagram of a glycolysis reaction. Glycolytic intermediate, and the pentose phosphate pathway (PPP) catalyzed by glucose-6-phosphate dehydrogenase, gluconolactonase. Glucose is transported across cell membranes by the glucose transporter (GLUT) and then catalyzed by hexokinase (HK) to glucose-6-phosphate. Additional irreversible steps in glycolysis are catalyzed by phosphofruktokinase (PFK) and pyruvate kinase (PM), as indicated by the arrows. Pyruvate can be converted to lactate by lactate dehydrogenase (LDH) or to acetyl-CoA by pyruvate dehydrogenase (PDH).

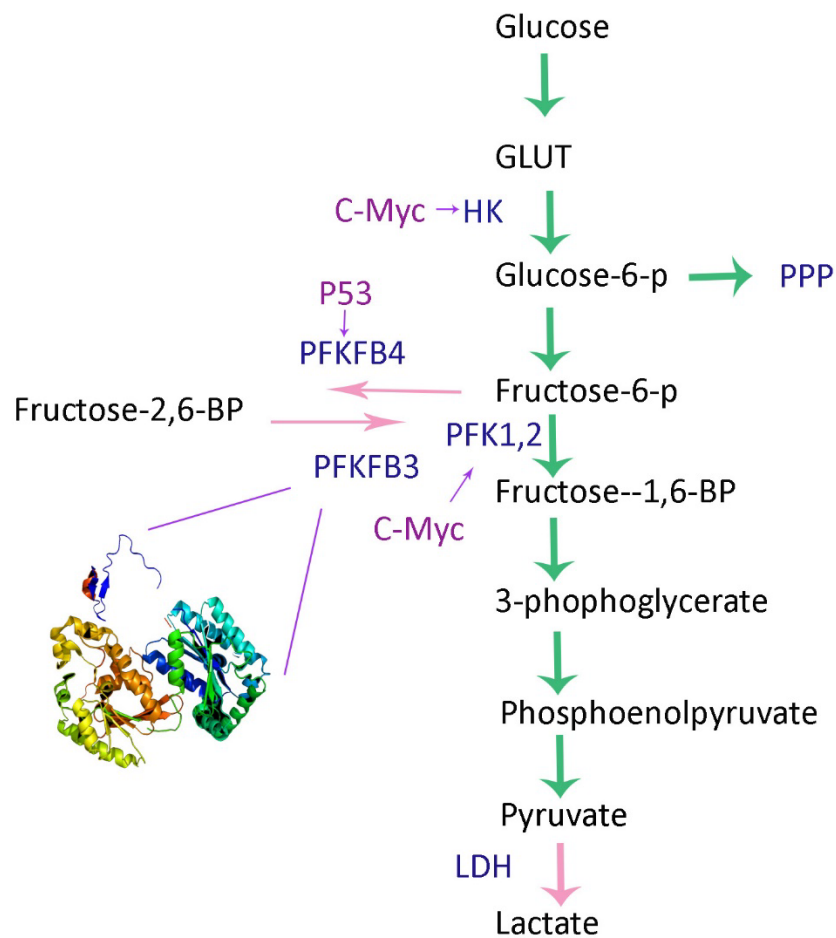


Figure 1-5 Abnormal glucose metabolism pattern of tumour cells and PFKFB3

The cancer cells maintain high-throughput glycolytic flux through variable mechanisms. Intracellular concentrations of F2, 6BP, and activated PFK-1 increase because of increased glucose transporter and hexokinase activities. PFK-1 is not inhibited by rising ATP but activated by F2, 6BP. PFKFB3 (enlarged view of protein structure is on the left) has strong kinase activity and promotes the synthesis of F2, 6BP, which subsequently activates PFK-1 and upregulates glycolytic flux. There are also some cancer-related genes, such as MYC and P53, which are involved in the formation of abnormal metabolic patterns of cancer cells (Lu et al. 2017). PFKFB3 structure is come from Wikipedia free creative commons source.

G6P- glucose-6-phosphate, **F6P**- fructose-6-phosphate, **F1, 6BP**- fructose-1, 6-bisphosphate; **F2, 6BP**- fructose-2, 6-bisphosphate; **PFK-1**- phosphofructokinase-1; **PEP**- phosphoenolpyruvic acid; **PC**- pyruvate kinase.

Therefore, PFK fraction can be stimulated with other linked enzymes. This association was described by PFKFBs to activate PFK and glycolysis. In the context of high glycolytic flux rates as a core metabolic hallmark of tumors, the level of the most potent regulator fructose-2,6-bisphosphate (F-2,6-BP) in PFK is significantly correlated with fructose-6-phosphate-2-kinase/fructose-2,6-bisphosphatase activity (PFK-2/FBPase-2, PFKFB) are closely related (Kotowski et al. 2021).

1.4.3 6-phosphofructo-2-kinase/fructose-2,6-bisphosphatase (PFKFB) family

1.4.3.1 PFKFB1

Fructose-2,6-bisphosphatase (PFKFB1), a homodimer with independent catalytic domains, is an activator of the glycolytic pathway and an inhibitor of the gluconeogenesis pathway. PFKFB1 encodes isoenzymes identified in fetal tissue and liver (Yi et al. 2019). The *PFKFB1* gene has a total of 17 exons that form three distinct isoforms, mainly in liver, muscle, and foetal tissue (Li et al. 2003). It has the function of enabling PFK2 kinase activity, ATP binding. It plays an important role in animal organ regeneration and gluconeogenesis, glycolysis, positive regulation of glucokinase activity, regulation of glucocorticoids and glucagon (Li et al. 2003). Higher level of *PFKFB1* was found to be significantly associated with the prognosis of bladder cancer patients in The Cancer Genome Atlas (TCGA) (Zhang et al. 2020a). Higher level of PFKFB1 was also found to be closely associated with siderophore leuconid in a study investigating TP53 in head and neck squamous cell carcinoma (Chandel et al. 2021). Two breakpoints found in the sporadic haemophilia pedigree which including an upstream breakpoint on the X chromosome *PFKFB1* had been identified as a cause of haemophiliacs (Xin et al. 2017). However, the role of PFKFB1 in cancer and haematological malignancies including AML is not well described in blood cancers.

1.4.3.2 PFKFB2

Fructose-2,6 -Diphosphate is a regulatory molecule that controls glycolysis. 6-phosphofructo-2-kinase/fructose-2,6-biphosphatase2 (PFKFB2) is a homodimer involved in the synthesis and degradation of fructose-2,6-bisphosphate. PFKFB2 encodes a protein mainly expressed in heart and kidney (Yi et al. 2019). It can activate PFK1 in the heart, enable ATP binding, and make fructose-2,6-bisphosphate 2-phosphatase active in the liver (Li et al. 2003). PFKFB2 was found to associate with LINC00092 to upregulate glycolysis and maintain local support functions in cancer-associated fibroblasts to promote metastasis in ovarian cancer (Zhao et al. 2017). PFKFB2 cytoplasmic expression is required for steady-state F2, 6BP levels, glycolytic activity and proliferation in pancreatic cancer cells (Ozcan et al. 2020). In the JB6 model of skin cell transformation, it was found that uncoupling protein 2 and PFKFB2 are positively correlated through the AKT signalling pathway (Sreedhar et al. 2017). Overexpression of PFKFB2 increases proliferation, migration, glucose uptake, lactate levels and ATP levels in lung cancer cells (Sha et al. 2021). Direct targeting of miR-1297 to the 3'UTR reduces the expression of PFKFB2 resulting in decreased oxygen glycolysis, and thus miR-1297 acts as a tumour suppressor in osteosarcoma (Pan et al. 2020). However, similar to PFKFB1, role of PFKFB2 in haematological cancers has not been highlighted.

1.4.3.3 PFKFB3

6-phosphofructo-2-kinase/fructose-2,6-biphosphatase 3 (PFKFB3) gene consists of 19 exons, 15 of which are regularly expressed and contain multiple binding sites. PFKFB3 protein is an enzyme that can activate PFK1 and stimulate glycolysis. It is a regulator of cyclin-dependent kinase 1 (Yi et al. 2019). *PFKFB3* mRNA is widely expressed in adipose tissue, brain, and frequently in cancer in cancer tissues to provide nutrients and signals in conjunction with other disordered molecules (Yi et al.

2019). In PFKFBs, PFKFB1 is found expressed in cytoplasm(KB 2020); PFKFB2 is found overexpressed in nucleus in pancreatic adenocarcinoma(Ozcan et al. 2020); PFKFB3 is found express in nucleus in HeLa, HCT116, and MDA-MB-231 cells; PFKFB4 is found localized to the cytoplasm in HeLa, HCT116, and MDA-MB-231 cells (Yalcin et al. 2009). In sepsis, *PFKFB3* mRNA expression and stability are manipulated by LncRNAs, supporting the activation of inflammatory cytokines by enhancing glycolysis (Liu et al. 2022). *PFKFB3* mRNA was significantly elevated in MEP and GMP during HSC differentiation(Figure 3-3), which may provide a potential basis for the enhancement of glycolytic power for the activation of inflammatory factors in disordered tissues (Ran et al. 2022). Robinson found PFKFB3 promoted AML proliferation (Robinson et al. 2020) (1.3.4).

ROS producing relaying on NADPH (1.4) (Figure 1-5). IDHs and MEs contribute to NADPH stocks in the cytoplasmic matrix and mitochondria by catalysing the oxidative decarboxylation of isocitrate by α -KG and malate by pyruvate, respectively, silencing ME1 significantly reduces NADPH and increases ROS levels, ultimately inducing apoptosis under oxidative stress in neutrophils (Belambri et al. 2018; Augsburger et al. 2019; Ju et al. 2020). One-carbon metabolism contributes to the NADPH in the cytoplasmic matrix and mitochondria in neutrophils (Belambri et al. 2018). Since the inner mitochondrial membrane is impermeable to NADPH, NADPH communication between the cytoplasmic matrix and mitochondria occurs via the isocitrate-a-KG shuttle transporter SLC25 in mouse and human Cell Lines (Palmieri 2004). The cytosolic enzyme IDH1 catalyses the oxidative decarboxylation of isocitrate, alpha-keto glutaric acid and produce NADPH (Ciccarese and Ciminale 2017). These are the up/downstream signals potentially affecting ROS production, PFKFB3 expression in cancer cells (exclude AML). Paying attention to the dynamics of these regulators might help explain future modelling studies of the linkage of PFKFB3.

1.4.3.4 PFKFB4

6-phosphofructo-2-kinase/fructose-2,6-biphosphatase 4 (PFKFB4) gene contains approximately 14 exons, and different splice variants of *PFKFB4* mRNA are found in various tissues, each PFKFB4 variant having the same catalytic domain (Minchenko et al. 2003). PFKFB4 is almost exclusively expressed in testis and significantly expressed in tumour cells (Yi et al. 2019). The PFKFB4 protein is a bifunctional enzyme that increases cellular F-2,6-BP levels (thereby generating glycolytic flux) or decreases F-2,6-BP concentrations, resulting in glucose-6-phosphate (G- 6-P) to ribose-5-phosphate (R5P) and nicotinamide adenine dinucleotide phosphate (NADPH) synthesis in PPP (Yi et al. 2019). Increased PFKFB4 expression found to be a marker of increased prostate cancer (Li et al. 2020b). Moreover, knockdown of PFKFB4 inhibited the proliferation and invasiveness of IHH-4 thyroid cancer cells. There is an inverse correlation between the expression of PFKFB4 and the histone acetyltransferase GCN5 in thyroid cancer (Lu et al. 2020).

In summary, the phosphatase kinase (k/p) activity of each isoform is critical in determining its metabolic role, whereas PFKFB1 (liver) is 1.2, PFKFB2 is 1.8, PFKFB4 is 0.9, and PFKFB3 has a k/p of 740 (Marsin et al. 2002). Importantly, PFKFB3 activity produced F-2,6-BP, which is a powerful allosteric activator of PFK as a rate limiting step in glycolysis (Pilkis et al. 1981). A survey of reports on the proportion of *PFKFB3* and *PFKFB4* mRNA in IDH glioblastoma marked by high levels of aerobic glycolysis showed that wild type was lower than mutant type (Kessler et al. 2019). IDH wild-type primary glioblastoma patients had a higher *PFKFB3* to *PFKFB4* mRNA ratio than an average of 7.7:1, and their OS (14 months) was significantly longer than patients with a lower ratio (9 months)(Kessler et al. 2019). PFKFB3 was again highlighted as a potential target for inhibiting cancer cells.

1.4.4 Metabolic rewiring in cancer and leukaemia

Metabolic rewiring plasticity modulates crosstalk between metabolic and transcriptional programs to maintain the energy and anabolic demands of cancer cells (Bonanomi et al. 2021). Metabolic rewiring is therefore a hallmark of cancer by allowing cells to change their metabolism and meet the requirements needed to maintain survival, quiescence, differentiation or proliferation (Hanahan and Weinberg 2011). This knowledge has been used clinically for prognosis, diagnosis and treatment (Koglin et al. 2011). Scientists are now exploring the unique characteristics of different types of cancers due to metabolism derived nutrient availability, oncogenic activation, proliferative state or microenvironment changes (Gentric et al. 2017; Wolpaw and Dang 2018).

Glucose metabolism, mitochondrial metabolism, and fatty acid metabolism all embody metabolic rewiring in Leukaemia (Locasale 2012). Although the Krebs cycle and mitochondrial oxidative phosphorylation activity are essential for nearly all cells in the human body, they are associated with and support different processes in each cell type. There is a strong link between increased glycolytic flux and cancer development. For example, HSCs tend to be glycolysis-dependent when in a dormant state, have lower levels of mitochondrial oxidative phosphorylation activity, and undergo metabolic rewiring to be more oxidative upon differentiation (Ito and Ito 2018; Filippi and Ghaffari 2019). HSCs rely on the anaerobic glycolytic pathway to meet their energy requirements for intact survival in the hypoxic BM niche environment (Simsek et al. 2010). In contrast, LSCs have been reported to mainly depend on mitochondrial oxidative phosphorylation (Simsek et al. 2010).

Glycolytic flux increases due to cancer genes(P53,c-Myc Figure 1-5) (Koczula et al. 2016), methotrexate interferes with folate synthesis and carbon metabolism (Cheng et al. 2011; Chaneton et al. 2012). For example, breast cancer cells promote cancer

proliferation through enhanced glycolysis and increased NADH/NAD(+) ratio, rewiring glucose metabolism through aerobic glycolysis, providing cancer cells with rapid production of pyruvate, ATP and NADH, whereas the oxidation of pyruvate to lactate ensures fueling of oxidized NAD(+) to maintain glycolysis. NADH has a critical role in controlling oncogene-dependent crosstalk between metabolism and epigenetic-mediated transcriptional programs (Bonanomi et al. 2021).

Chemical resistance in hypoxic tumors is caused by hypoxia-induced glycolysis and metabolic rewiring of mitochondria by cooperating with factors such as increased ATP and decreased apoptosis, EMT activation, increased DNA repair, altered drug metabolism, and changes in drug targets. Specific metabolic modifiers can reverse the metabolic phenotype of hypoxic tumors to those typical of chemo sensitive cells, which is benefiting targeted chemotherapy (Belisario et al. 2020). Although the metabolic rewiring of different cancers is different, membrane transporters of specific amino acids act as participants in the metabolic rewiring of cancers to ensure the uptake and transport of amino acids between tissues, and some transporters are more commonly used than others (Scalise et al. 2020). Understanding these could help with a new perspective on cancer treatment (Scalise et al. 2020).

Hyperactivation of the mammalian target of rapamycin (mTOR) is frequently observed in many cancers (Fruman and Rommel 2014). This leads to cell proliferation and down-regulation of autophagy (Tian et al. 2019), and up-regulation of PFKFB3 expression in AML (Feng and Wu 2017). PFKFB expression is also steroid-dependently regulated (Imbert-Fernandez et al. 2014; Trenti et al. 2017), such as: activation of estrogen receptor signaling (Imbert-Fernandez et al. 2014; O'Neal et al. 2016), overexpression of human epidermal growth factor receptor 2 (Zawacka-Pankau et al. 2011), and loss of p53 and PTEN all stimulate glycolysis through PFK-2 (Cordero-Espinoza and Hagen 2013).

Unlike its expression in blood cancers, PFKFB4 plays a key regulatory role in other cancers. The cervical cancer prognostic risk scoring model also identified the high expression levels of 6 mRNAs including *PFKFB4* in cervical cancer tissues as indicators of poor OS (Cai et al. 2020). The proliferation and migration of thyroid cancer cells are negatively affected by the signalling negative regulation of *PFKFB4* mRNA on GCN5 expression and PI3K/AKT phosphorylation (Lu et al. 2020). *PFKFB4* promotes breast cancer metastasis by inducing HAS2 expression and mediated by hyaluronic acid (Gao et al. 2018). Similarly, *PFKFB4* mRNA expression was higher in metastatic prostate cancer than in primary tumours (Ros et al. 2012). PFKFB4 increases the activity of the oncogenic transcription factor steroid receptor coactivator through its phosphorylation, which leads to the redirection of glucose metabolism to PPP and initiates purine synthesis, which helps breast cancer cells to proliferate and metastasize (Dasgupta et al. 2018).

1.4.4.1 Targeting glycolysis and PFKFB3 to treat cancer

Cancer cells with high proliferative activity have increased energy requirements and increased glycolytic flux. PFKFB3 is a key factor in tumour transformation because the regulatory function of PFKFB3 in catalytic activity is related to the metabolic changes of cells (1.4.2). Therefore, the role of PFKFB3 in regulating tumour cell proliferation and metabolism is attractive.

Decreased PFKFB3 in gastric cancer cells using PFK15 (a small molecule inhibitor of PFKFB3) leads to cell cycle arrest; Downregulation of PFKFB3 in HeLa cells by using the cyclin-dependent kinase inhibitor p27 leads to cell cycle arrest; Jurkat cells (human T lymphocytes G2/M phase arrest was induced by the PFKFB3 inhibitor 3PO in the immortalized line of. PFKFB3 promotes the survival of AML cells by reprogramming its metabolism to meet its increased energy demands (Robinson et al. 2020). The up-regulation of PFKFB3 expression is regulated by HIF1, while the glucose transporter

1 (GLUT1) is regulated by ROS, and NOX2-derived ROS can have a more positive effect on glucose uptake in AML cells as described in 1.3.1. PFKFB3 is involved in the glucose metabolism pathway (include glycolysis and pentose phosphate pathway) (Shi et al. 2017), but it activates fructose-6-phosphate-1-kinase (PFK1), in glycolysis by producing fructose-2,6-bisphosphate (F2,6P2) from fructose-6-phosphate (F6P), which allowing PFK1 to limit the rate of glycolysis. 1-kinase (PFK1) is an allosteric enzyme that limit the rate of glycolysis (Shi et al. 2017). *PFKFB3* gene activate HIF-1 by HIF-1 promoter on its binding site (Bolaños 2013); mitogen-activated protein kinase and activate protein kinase 2 activate *PFKFB3* gene promoter region (Cordero-Espinoza and Hagen 2013), phosphatase and tensing Homologs increase *PFKFB3* transcription (Van Schaftingen et al. 1980). Interestingly, simultaneous knockdown of P53-induced glycolysis and apoptosis regulator makes AML cells heavily dependent on glycolysis for proliferation and up-regulation of *PFKFB3*, which also provides new potential for targeted therapy (Qian et al. 2016).

Upstream regulators of *PFKFB3* were also found to have the potential to be included in *PFKFB3*-targeted therapeutics, such as several oncogenic transcription factors are also involved in enhancing the transcriptional expression of *PFKFB3* mRNA (Navarro-Sabaté et al. 2001). Some studies have found that the DNA sequence of the promoter region of the 5' flanking promoter region of the *PFKFB3* gene can bind to progesterone receptor (PgR) (Hamilton et al. 1997; Novellademunt et al. 2012), nucleus factor 1 (NF1) and contains regulatory motifs of the E-box (Chen et al. 2016). Transcription of *PFKFB3* is also regulated by hormones. Progesterone can recruit PgR in the promoter region and oestrogen can recruit estragon to upregulate *PFKFB3* transcription in breast cancer (Hamilton et al. 1997; Novellademunt et al. 2012). According to reports, there is a reactive element that can directly bind to progesterone in 3490 base pairs upstream of the promoter, and after 1 hour of treatment with oestradiol, the assay results in a 4-fold recruitment of $E\alpha$ (Imbert-Fernandez et al. 2014). CLOCK (circadian

motor export cyclin kaput) activates PFKFB3 transcription through promoter binding in tongue cancer cells (Chen et al. 2016).

Further, there are therapeutic regimens for hepatocellular carcinoma using inhibition of PFKFB3 in combination with sildenafil (Liu et al. 2021). There are 8 metabolic gene signatures (including *PFKFB3* mRNA) which were incorporated into the reference index in the hepatobiliary cancer prognosis prediction model (Ran et al. 2022). In addition, through lncRNA/mRNA profiling of oral squamous cell carcinoma patients, it was found that siRNA knockdown of *lncRNA H19* inhibited the MAPK signalling pathway, *PFKFB3* mRNA and *miR-675-5p* (Yang et al. 2021). After knocking out *miR-192-5p* in liver cancer stem cells, which up-regulates PFKFB3, it was found that liver cancer stem cells tended to be normal stem cells. Subsequently, glycolysis was activated with the upregulation of key glycolytic genes including *PFKFB3* (Yang et al. 2021). In summary, PFKFB3-targeted therapy is gradually proven to be an effective treatment.

1.5 Aims and Objectives

The main aim of this thesis is to investigate the mRNA expression of the *PFKFB* family (*PFKFB1*, 2, 3 and 4) in normal haematopoiesis and AML. Determining the relationship between the expression of *PFKFB1*, 2, 3 and 4 in different subtypes of AML (and with disease demographic features) with clinical outcome data may provide compelling evidence for further studies that will establish the role of these isoforms in AML. Given that preliminary data (1.4.3.3) suggests PFKFB3 expression is modulated by ROS in AML, I will also determine the relationship between extracellular ROS production and PFKFB protein expression in AML cell lines. To achieve this goal, this thesis has the following objectives:

- **Determine the mRNA expression levels of *PFKFB/ Pfkfb* 1, 2, 3 and 4 during normal human and mouse haematopoiesis and compare to AML**

To understand whether the expression of *PFKFB/ Pfkfb* family members differ between haematopoietic stem cells, differentiated lineages and AML. The TCGA dataset will be used to analyse mouse/human mRNA (Ley 2013). This will potentially explain how *PFKFB* family mRNA expression associates with stem cell differentiation in normal human and mouse haematopoiesis.

- **Determine whether *PFKFB* expression is associated with ROS**

To understand whether increased *PFKFB* expression is associated with increased ROS production. To investigate the relationship between *PFKFB3* protein expression and ROS in AML cell lines, I will measure extracellular ROS (superoxide) production using the chemiluminescent probe Diogenes in 10 AML cell lines. *PFKFB* protein expression will be analysed by western blot.

- **Develop a flow cytometry assay to detect intracellular *PFKFB* expression**

Developing a flow cytometry assay to detect *PFKFB* protein expression at the single cell level can overcome the challenge of insufficient primary AML cells and/or heterogenous cell populations in AML patient samples which can be a limitation for western blot testing. Ectopically expression of *PFKFB* was used as a positive control to test whether the intracellular staining protocol was successful. Optimal conditions were used to detect *PFKFB* expression by flow cytometry in 10 AML cell lines.

Chapter 2 Materials and Methods

2.1 General materials

Common reagents used in this study are detailed in Table 2-1. Antibodies used are listed in Table 2-2.

Table 2-1 Summary of reagents and suppliers

Reagent	Supplier
Human Granulocyte Colony-Stimulating Factor (G-CSF)	Invitrogen, Paisley, UK
paraformaldehyde	Sigma-Aldrich, Poole, UK
α -Minimum Essential Medium Eagle (MEM)	Merck Life Science, Gillingham, UK
sodium phosphate (Na ₂ HPO ₄)	Sigma-Aldrich, Poole, UK
Amersham™ ECL™ Prime	Cytiva, Little Chalfont, UK
Calcium chloride (CaCl ₂)	Sigma-Aldrich, Poole, UK
Magnesium chloride (MgCl ₂)	Sigma-Aldrich, Poole, UK
Biovision Nuclear/Cytosol Fractionation Kit	Cambridge Bio., Cambridge, UK
Bovine Serum Albumin (BSA)	Biosera Europe, Nuaille, France
Deoxyribonuclease (DNase) I from Bovine Pancreas	Merck Life Science, Gillingham, UK
Dimethyl Sulfoxide (DMSO)	Merck Life Science, Gillingham, UK
Diphenyliodonium (DPI)	Sigma-Aldrich, Poole, UK
Diogenes	National Diagnostics, Hessle, UK
Ethanol	Merck Life Science, Gillingham, UK
Ethylenediaminetetraacetic Acid (EDTA, 0.5 M)	Merck Life Science, Gillingham, UK
Foetal Bovine Serum (FBS)	Biosera Europe, Nuaille, France
Ponceau S solution	Sigma-Aldrich, Poole, U.K.
Gentamycin (50 mg/mL)	Fisher Scientific, Loughborough, UK
Glucose	Sigma-Aldrich, US
Iscove's Modified Dulbecco's Medium (IMDM)	Fisher Scientific, Loughborough, UK
L-Glutamine (200 mM)	Fisher Scientific, Loughborough, UK
MagicMark™ XP Western Protein Standard	Fisher Scientific, Loughborough, UK
PVDF membrane	Fisher Scientific, Loughborough, UK
Methanol	Merck Life Science, Gillingham, UK
Nuclear/Cytosol Fractionation Kit	Cambridge Bioscience, Cambridge, UK
NuPAGE™ Antioxidant	Fisher Scientific, Loughborough, UK
NuPAGE™ LDS Sample Buffer (4X)	Fisher Scientific, Loughborough, UK
NuPAGE™ MOPS SDS Running Buffer (20X)	Fisher Scientific, Loughborough, UK
NuPAGE™ Sample Reducing Agent (10X)	Fisher Scientific, Loughborough, UK
NuPAGE™ Transfer Buffer (20X)	Fisher Scientific, Loughborough, UK
Phosphate-buffered Saline (PBS, 10X)	Sigma-Aldrich, US
Plasticware	Nunc, DK; Fisher Scientific, Loughborough, UK
Roswell Park Memorial Institute (RPMI) 1640	Fisher Scientific, Loughborough, UK
Sodium azide	Sigma-Aldrich, US
Sterile water	Sigma-Aldrich, US
Sodium Bicarbonate 7.5% Solution	Fisher Scientific, Loughborough, UK
Sodium Chloride (NaCl)	Merck Life Science, Gillingham, UK
Sodium Dodecyl Sulfate (SDS)	Merck Life Science, Gillingham, UK
Sodium Orthovanadate	Merck Life Science, Gillingham, UK
Tris Hydrochloride (HCl)	Merck Life Science, Gillingham, UK
Triethylammonium Bicarbonate Buffer (TEAB, 1 M)	Merck Life Science, Gillingham, UK
TWEEN® 20	Merck Life Science, Gillingham, UK
UltraPure™ Agarose	Fisher Scientific, Loughborough, UK
Tris-Buffered Saline	Sigma-Aldrich, Poole, UK
phorbol 12-myristate-13-acetate (PMA, also known as TPA)	Cayman Chemical

2.1.1 Antibodies

Antibodies used in flow cytometry (2.5) and western blotting (2.4) procedures are alphabetically listed below.

Table 2-2 Summary of antibodies used in western blot and flow cytometry Assays

Use	Antibody name	Clone	Concentration	Supplier
Western blot	Beta actin	Monoclonal antibody 5-15739-D680	1 mg/mL (1/10,000)	Invitrogen, Paisley, UK
	6-phosphofructokinase/fructose-2,6-biphosphatase 3 (PFKFB3)	(D7H4Q) Rabbit Monoclonal antibody	(1/000 for)	Cell Signalling Technology, Leiden, Netherlands
	6-phosphofructokinase/fructose-2,6-biphosphatase 3 (PFKFB3)	Monoclonal antibody 5-35419 Recombinant Rabbit	1.04mg/mL (1/1000 for)	Invitrogen, Paisley, UK
	6-phosphofructokinase/fructose-2,6-biphosphatase 3 (PFKFB3)	Ab181861 Rabbit Monoclonal antibody	0.583mg/mL (1/1000, 1/2000)	Abcam, Cambridge, UK
Flow cytometry	Purified Rabbit Polyclonal Isotype Ctrl Antibody	Rabbit Polyclonal Antibody 29108	1 mg/mL (1/50)	BioLegend, London, UK
	6phosphofructokinase/fructose-2,6-biphosphatase 3 (PFKFB3)	Ab181861 Rabbit Monoclonal antibody	0.583mg/mL (1/30)	Abcam, Cambridge, UK
	Goat Anti- Rabbit Alexa Fluor IgG CS4414	AffiniPure Fab Fragment Goat Anti-Rabbit IgG (H+L)	(1/1000)	Jackson ImmunoResearch, Europe

2.2 Cell culture

2.2.1 Culture of cell lines

All cell lines were grown and passaged according to supplier and laboratory guidelines. Incubation conditions were 37°C, 5% CO₂ in air. All cell culture was performed in Class II biosafety cabinet and the waste disinfected with bleach and/or autoclaved. The specific culture conditions are detailed in Table 2-3. Cells were maintained in logarithmic growth at an approximate density of 1 - 2 x10⁵ cells/mL in the appropriate medium. All media contained 10% (v/v) heat-inactivated foetal bovine serum (FBS, Biosera Europe, Nuaille, France), 1% (v/v) L-glutamine (Invitrogen, California, USA) and 20 µg/mL Gentamycin (Life Technologies, California, USA), individual changes will be specially noted in the table.

2.2.2 Thawing and cryopreservation of cells

AML cell lines cryopreserved in liquid nitrogen were thawed at 37°C in a water bath for 2 minutes followed by washing in 5mL of pre-warmed culture medium, added dropwise. Cells were centrifuged for 5 min at 270 x g, the supernatant was removed. Subsequently, cells were resuspended in the volume of culture medium recommended in Table 2-4 and transferred to T25 flask and placed in a 37°C, 5% CO₂ incubator.

For cryopreservation, cell suspensions were transferred to a UC and centrifuged at 270 x g for 10 min. Supernatant was replaced with fresh culture medium (refer to Table 2-3 for volume) and an equal volume of freezing solution (Iscove Modified Dulbecco's Medium (IMDM, Gibco) supplemented with 30% (v/v) FBS and 20% (v/v) Dimethyl Sulfoxide (DMSO; Sigma-Aldrich)). The cells were placed in 1mL in a 1.8 mL cryovial and slowly cooled in Cool Cell™ Cell Freezing Container (BioCision, California, USA)

in a -80°C freezer. Cells were then transferred to liquid nitrogen for long-term storage after 24 hours.

2.2.3 Cell counting

Cell counts in this study were performed in a Neubauer chamber (Hawksley, Brighton, UK). There were 9 large squares in the counting plate with a volume of 0.1 μ L (1mm (length) x 1mm (width) x 0.1mm (height)). If a large square had the number of cells X, then the cell number of 1mL of the solution Y was calculated by the following formula:

$$X \text{ cells} \times 1000 = Y \text{ cells}/1 \text{ mL}$$

2.3 Diogenes assay to measure NOX2-derived reactive oxygen species

Superoxide measurement of AML cell lines was performed using Diogenes (National Diagnostics, Hesse, U.K.) and a luminometer (Chameleon HIDEX, UK). Diogenes was stored in vapour liquid nitrogen in cryovials in 525 μ L aliquots. This stock was made from Diogenes powder (National Diagnostics, Hesse, U.K.) mixed with 10 mL TC water, and Diogenes enhancer.

An appropriate number of cells (normally 50,000 cells/well) were plated into 96-well plates according to the experimental design and divided into three groups according to the reaction conditions with: PBS (vehicle control), DPI (100nM; NOX2 inhibitor oxidase inhibitor), TPA (a potent NOX2 agonist) was prepared from a 100 μ M master stock by diluting 1/10 in PBS to generate a 10 μ M working stock. Cells were centrifuged and resuspended in PBS twice (settings: 5 min, 1200 rpm). The pellet was resuspended in standard buffer (KH₂PO₄ (4.58mM), Na₂HPO₄ (8.03mM), NaCl (130mM), KCl (4.43mM), glucose (5.55mM), MgCl₂ (0.5mM), CaCl₂ (0.45mM), BSA

(0.1% v/v) all purchased from Sigma). Each well had 135 μ L of the cell suspension, 50 μ L of Diogenes, 15 μ L of 1 μ M DPI to the wells, 15 μ L of PBS to control wells, 15 μ L of TPA to stimulated wells (positive control). Luminescence was measured over 3h at 37 °C. Chemiluminescent traces were plotted and initial reaction rate, measured as relative light units (RLU/min). The luminescence value of DPI-treated sample was then subtracted to obtain a bar graph of the net value of superoxide production (Figure 4-1A). Each assay incorporated a 'NOMO-standard' , which acted as a positive control and was used to standardise the assay, this reference data is come from Figure 4-1A, please refer to chapter 4 for the details.

2.4 Western blotting

2.4.1 Total cell protein extraction

An appropriate number (typically 1×10^6) cells were centrifuged 270xg for 5 min followed by washing in 10mL tris-buffered saline and centrifugation (10min, 270xg.). Supernatant was removed and cell lysis performed by 3- freeze/thaw cycles using liquid nitrogen. Finally, 1 μ L of DNase (1 mg/mL) was added to the sample for 5 minutes, and 50 μ L of homogenisation buffer (of 0.25 M sucrose, 10 mM HEPES, 1 mM magnesium acetate, 0.5 mM EDTA, 0.5 mM EGTA, 10 mM β ME, 200 mM sodium orthovanadate, protease inhibitor cocktail, 1% v/v Triton-X100) was added followed by incubation for 30 minutes on ice during which the samples were vortexed every 10 minutes. After incubation, the cell suspension was transferred to Eppendorf tubes and centrifuged (settings: 5 min; 10,000xg; 4°C.) to remove any remaining insoluble material. The supernatant was aspirated and the final volume are recorded. Protein quantification was carried out by Bradford assay.

Table 2-3 Summary of cell lines characteristics and culture conditions

Name	Media	Primary density (cells/mL)	division cycle(hour)	Description	Molecular characteristics	Source
NOMO	RPMI 1640	5x10 ⁵	35	AML	t(9;11)(p22;q23) – KMT2A-MLLT3	DSMZ
THP-1	RPMI 1640	2x10 ⁵ - 4x10 ⁵	40-50	Acute Monocytic Leukaemia	(9;11)(p21;q23) leading to KMT2A-MLLT3 (MLL-MLLT3; MLL-AF9)	ECACC
MV4;11	IMDM	1x10 ⁵ - 1x10 ⁶	50	Myelomonocytic Leukaemia	t(4;11)(q21;q23) – KMT2A-AFF1	ATCC
OCI-AML5	αMEM; 20% v/v FBS; 10 ng/mL GM-CSF	5x10 ⁵ - 1.5x10 ⁶	30-40	AML	t(1;19)(p13;p13)	DSMZ
OCI-AML2	αMEM; 20% v/v FBS	7x10 ⁵ - 1x10 ⁶	40-50	AML	DNMT3A mutation (R635W)	DSMZ
U937	RPMI 1640	1x10 ⁵ - 2x10 ⁶	30-40	Histiocytic Lymphoma	t(10;11)(p12;q14) – MLLT10-PICALM	ATCC
PLB985	RPMI 1640	5x10 ⁵ – 1.5x10 ⁶	40	APL	t(5;17)(p11;q11)	ATCC
Kasumi	RPMI 1640; 20% v/v FBS	3x10 ⁵	48-72	AML	t(8;21) (q22;q22) – RUNX1-ETO	DSMZ
Hel	RPMI 1640	1x10 ⁵ - 1x10 ⁶	36	ErythroLeukaemia	JAK2 mutation (V617F)	ECACC
TF1	RPMI 1640	5x10 ⁵ – 1x10 ⁶	70	ErythroLeukaemia	-	ATCC

Chapter 2

SKNO 1	RPMI 1640; 10 ng/mL GMCSF	2×10^5 - 2×10^6	35-50	AML	t(8;21) (q22;q22) – RUNX1-ETO	DSMZ
-----------	------------------------------	--------------------------------------	-------	-----	-------------------------------	------

RPMI - Roswell Park Memorial Institute-1640 Medium; **FAB** -FAB classification of AML; **α MEM** - Minimum Essential Medium Eagle-Alpha Modification; **APL** – Acute Promyelocytic Leukaemia; **ATCC** – American Type Culture Collection (USA); CML – Chronic Myeloid Leukaemia; **DMEM** - Dulbecco's Modified Eagle's Medium; **DSMZ** - German Collection of Microorganisms and Cell Cultures (Germany); **ECACC** - European Collection of Authenticated Cell Cultures (UK); **FBS** – Heat-Inactivated Foetal Bovine Serum (Labtech, East Sussex, UK); **Gent** – Gentamycin (Gibco, ThermoFisher Scientific); **IMDM** - Iscove Modified Dulbecco's Medium; **L-Glu** – L-Glutamine (Gibco, ThermoFisher Scientific).

2.4.2 Cytosolic and nuclear protein extraction

Extraction was performed using Biovision Nuclear/Cytosol fractionation Kit according to manufacturer's instructions and as previously described (Robinson et al. 2020). Briefly, an appropriate number (typically $2-3 \times 10^6$) of cells were centrifuged (as 2.4.1). 20mL tris-buffered saline was added to the cell pellet to wash the cells. The cells were centrifuged for 10min at $270 \times g$. The cell pellet was lysed by freeze thawing 3 to 5 times (as 2.4.1). 100 μ L/million cells of extraction buffer A was added (containing protease inhibitor cocktail (2 μ L) and dithiothreitol (1 μ L)), vortexed 15 seconds and incubated for 10 min in Eppendorf tubes on ice, then 5.5 μ L/million cells of extraction buffer B were added. After 5min, the lysed cell suspension was centrifuged to pellet the released nuclei (settings: 3 min, $12,000 \times g$, 4°C). Finally, the supernatant containing the cytosolic extract was stored at -80°C .

The nuclear pellet was washed with 500 μ L of PBS supplemented with 5 mM MgCl_2 and centrifuged ($10,000 \times g$, 3 min). The pellet was retained and underwent 3 freeze/thaw cycles in liquid nitrogen to rupture the nuclear membrane. 2 μ L/million cells of benzonase (25 U/ μ L; Merck Millipore, USA) was added, and cells were incubated on ice for 30 min, subjected to occasional vortexing. After incubation, the disrupted nuclei were centrifuged (10 min; $10,000 \times g$; 4°C) and the supernatant collected to a fresh tube. Protein quantification was carried out by Bradford assay.

2.4.3 Protein quantitation by Bradford assay

Protein quantification was measured by spectrophotometry (ASYS Hitech, GmbH, Eugendorf, Austria) in combination with Bradfords assay. Cell lysate samples and BSA protein standards (0-10 $\mu\text{g}/\text{mL}$) were compared on the same 96 well plate resulting in a linear standard curve ($y = mx + c$: **y** is the dependent variable, **x** is the independent

variable, **m** is the gradient of the line, **c** is the y-intercept. Bradford's reagent (Sigma) was diluted with H₂O 1:1 to make a Bradford working solution. 190 µL Bradford working solution was added to 10 µL of cell lysate/standard per well in duplicate. Samples were incubated 5 to 45 minutes. The absorbance maximum is close to 595 nm. This wavelength was used to measure sample absorbance. Protein concentration was interpolated from the standard curve.

2.4.4 SDS Polyacrylamide electrophoresis and electroblotting

Electrophoresis experiments were performed according to the instructions provided by the manufacturer (Invitrogen). The experiment was carried out in 3 parts: SDS-PAGE, electroblotting and immunostaining. Initially, electrophoresis was used to separate proteins according to size. Samples were prepared in NuPAGE™ 4x Lithium Dodecyl Sulphate Sample Buffer (LDS), NuPAGE™ 10x Sample Reducing Agent and water. Samples were denatured at 70°C in a water bath for 10 minutes.

Protein gel electrophoresis was performed by using a NuPAGE™ XCell SureLock™ Mini-cell and XCell II blot module system. Each sample containing 10 – 20 µg of protein was loaded into NuPAGE™ 4-12% Bis-Tris gel with 12 or 17 wells run in NuPAGE™ MOPS SDS Running Buffer (made with 950 mL dH₂O and 50 mL 20x NuPAGE™ MOPS SDS Running Buffer stock). The outer chamber of the gel tank was filled with approximately 600 mL of 1 x MOPS buffer. Magic Marker XP protein ladder (1/10 dilution in 4x LDS sample buffer and dH₂O) was also loaded into the gel as a reference for the molecular mass of the protein samples. Electrophoresis was performed using 200V for 50min.

Following electrophoresis, electroblotting was performed. PVDF membranes were soaked in methanol prior to electroblotting for 10 minutes. After electrophoresis, the gel was removed from the plastic casing, a membrane sandwich was assembled. The tank cavity was filled with 1x NuPAGE™ Transfer buffer supplemented with 1 mL

NuPAGE™ Antioxidant and 10% v/v methanol (20% v/v if blotting two gels), the outer cavity was filled with dH₂O which serves to dissipate heat produced during the run. Eletroblotting performed at 30v for 60min.

Finally, following protein transfer, the membranes were washed twice with TBS-T (TBS supplemented with 0.1% (v/v) Tween-20 (Sigma-Aldrich)) on a shaker (setting: 1 revolution/sec, 5 min). Then, membranes were soaked in Ponceau S solution (Sigma-Aldrich) for 30 s for assessment of equal loading, identifying any bubbles and protein extract quality. The Ponceau S stain was removed by brief washing in water. 10 mL of blocking solution (2.5% powdered milk diluted in TBS-T) was added to the membrane and incubated on a shaker (setting: 1 revolution/sec, 45 min). After washing membranes twice on a shaker (setting: 1 revolution/sec, 5 min), the immunodetection of proteins was started as described below.

2.4.5 Immunodetection of proteins

Following blocking, immunodetection was performed. The membrane was washed with wash solution (TBS-T), 15min x 1, 5min x3 times followed by incubation with 10 mL of primary antibody solution (1% powdered milk diluted in TBS-T with the chosen primary antibody, in Table 2-2) overnight in a shaker at 4°C. The following day, the membrane was washed as before and incubated with a HRP conjugated anti-rabbit secondary antibody prepared in 10 mL of 1% w/v milk powder for 1 hour in a shaker at room temperature. Following another wash, the membrane was soaked in 2ml Chemiluminescence detection solution (combining reagent A and B at 1:1 ratio, Amersham™ ECL™ Prime from GE HealthCare Life Sciences). The reaction was developed over 5 minutes at RT and protected from light. The chemiluminescence reaction of the membrane was captured at between 1-30 minutes depending on signal strength using the LAS-3000 Imaging System (Fujifilm, Bedford, UK) to capture digital images.

Equal protein loading was further assessed using a fluorescent beta-actin antibody for total/cytosolic protein extracts (Table 2-2). Fluorescent beta-actin was imaged by Odyssey[®] FC Imaging System (LI-COR Biosciences, Nebraska, USA) for 30s.

Densitometry was performed using ImageJ v1.8 software (<https://imagej.nih.gov/ij/>) by plotting a histogram of peak intensity for each band. The peak area equal to arbitrary intensity value to estimate the differences in protein expression.

2.5 Flow cytometry

Samples for flow cytometry were analysed using Accuri[™] C6 plus flow cytometer (Becton Dickinson, US). Flow cytometer technical specifications are outlined in Table 2-4. All flow cytometry data was analysed using FCS Express[®] v7 (De Novo Software, Pasadena, USA).

2.5.1 Intracellular PFKFB3 expression

Cells were counted and washed prior to staining for intracellular PFKFB3 protein expression. 4×10^5 cells were fixed with 4% (w/v) paraformaldehyde and incubated for 10 minutes at room temperature. Fixed cells were centrifuged (270 x g), washed with 200 μ L PBS, aliquoted into labelled 1mL mini-tubes, and centrifuged as above. The supernatant was discarded, and cells placed on ice for 1 min. 200 μ L of ice-cold methanol was added to each mini tube, incubated on ice for 10 minutes, washed twice by centrifugation with the addition of 100 μ L of staining buffer (PBS+0.5% BSA + 0.02% sodium azide). Cells were incubated with 25 μ L of primary antibody solution (Recombinant Anti-PFKFB3 (Abcam, ab181861, Table 2-2) at room temperature for 30 minutes. A primary rabbit IgG (910801) antibody was used as a background control.

Table 2-4 Table outlining the instrument specifications of the Accuri™ C6 plus

	Laser Excitation	Emission Detection	Flow rates
Accuri™ C6 Plus	488nm 640nm	FL1 533/30nm (FITC/GFP) FL2 585/40nm (PE/PI) FL3 >670nm (PerCP-Cy™5.5) FL4 675/25 nm (APC)	10 – 100 µL/min

After incubation, cells were centrifuged (settings: 5 min; 270 x g.), supernatant discarded and 200 μ L of staining buffer was added to each mini tube followed by centrifugation (settings: 5 min; 270 x g.). Subsequently, 25 μ L of the secondary antibody incubation solution was added to each mini-tube (goat anti-rabbit IgG labelled with Alexa 647 cs4414) diluted at a ratio of 1:1000, Table 2-2) and incubated in the dark (settings: room temperature, 20 minutes). After incubation, cells were centrifuged (settings: 5 min; 270 x g.), and after discarding the supernatant 200 μ L staining buffer was added to each mini-tube, and centrifuged (settings: 5 min; 270 x g.). Finally, the pellet was resuspended in 100 μ L of staining buffer and analysed by flow cytometry. 30k events were collected using the Accuri™ C6 plus flow cytometer.

2.5.2 Data acquisition and gating strategy

For data processing, FCS Express v7 (De Novo Software, Pasadena, CA, USA) was used. Initially cell debris was excluded based on forward and side scatter (FSC/SSC) events (Figure 2-1A). Flow cytometric histograms were used to analyse PFKFB3 protein expression using the FL4 (APC channel). IgG-APC was used to set background fluorescence (Figure 2-1B). The ratio of PFKFB3/IgG for each cell line was calculated.

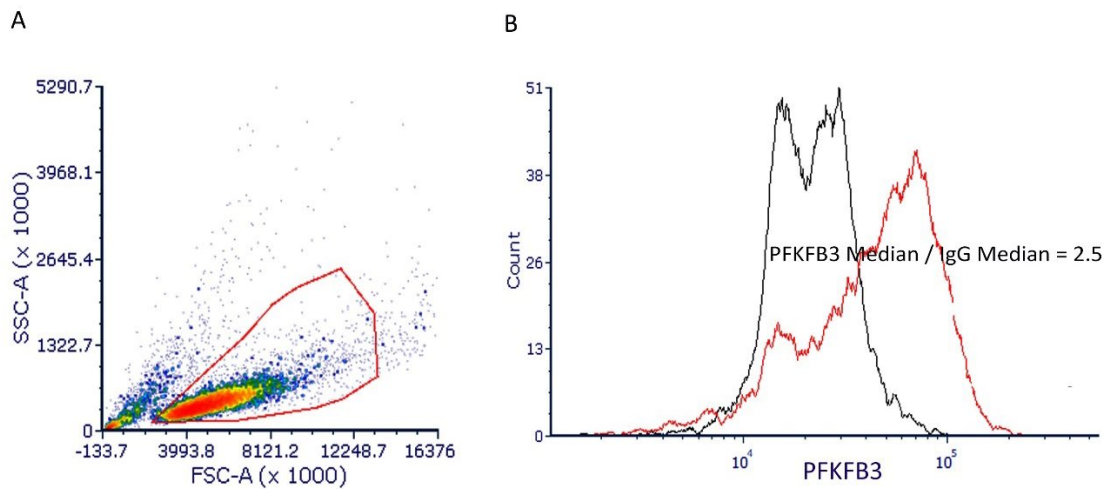


Figure 2-1 Gating strategy for intracellular PFKFB3 protein expression by flow cytometry

Example flow cytometric data for KG1 AML cell line.

- A. A density plot showing exclusion of cell debris based on forward scatter (FSC) and side scatter (SSC).
- B. Non-debris events were gated on FSC/SSC as in (A). The black histogram represents IgG-APC background staining. Red histogram represents cells stained with anti-PFKFB3-APC. PFKFB3 is 2.5-fold of IgG. The data is from the median of the histogram.

2.6 Data analysis

2.6.1 Publicly available datasets

2.6.1.1 Bloodspot

The data regarding PFKFBs mRNA expression in normal and AML haemopoiesis was assessed through publicly available databases such Bloodspot (Bagger et al. 2016), (<http://servers.binf.ku.dk/bloodspot/>). PFKFBs mRNA expression during normal haematopoiesis was derived from the 'Normal haematopoiesis with AML" dataset GSE42519; (Rapin et al. 2014). mRNA expression data during murine haematopoiesis was derived from GSE14833 and GSE6506 (Rapin et al. 2014).

Analysis of human *PFKFB1* and murine *Pfkfb1* was achieved using probeset 207537_at and 1417213_at respectively. Human *PFKFB2* and murine *Pfkfb2* was analysed with 238450_at and 1422090_at probesets respectively. For *PFKFB3* & *Pfkfb3*, I used human probeset 202464_s_at and 1416432_at probeset data in normal mouse haemopoiesis. Lastly human *PFKFB4* and murine *Pfkfb4* used the respective probesets 206246_at and 1456888_at.

2.6.1.2 cBioPortal

PFKFB3 and *CYBB* mRNA expression in AML patient samples was obtained from cBioPortal TCGA, NEJM 2013 dataset (Ley 2013) (<https://www.cbioportal.org/>). This dataset is comprised of mRNA sequencing of 163 adults complete *de novo* AML samples data. Patient data were stratified according to high PFKFB3 expressing patients (above the median) and low PFKFB3 (below median expression of *PFKFB3*). Clinical attributes associated with high and low PFKFB3 expression, including FAB classification of disease and OS was analysed using cBioPortal. All mRNA expression

data within cBioPortal is represented as accurate transcript quantification from RNA-Seq data with or without a reference genome.

2.6.2 Statistical analysis

Statistical significance in Bloodspot database was determined using a Log-Rank Test. The p-value for Bloodspot data were calculated by the website itself. The statistical tests used are outlined in the figure legends where appropriate. The statistical significant to very significant. is denoted by *: $p < 0.05$; ** $p < 0.01$; *** $p < 0.001$. Correlation analysis between *CYBB* & *PFKFB3*, *PFKFB3* & ROS were performed in Microsoft Excel (Microsoft Office 365). The Pearson value x , when $|x| > 0.5$, high correlation; when 0.5-0.1, medium correlation; when $|x| < 0.1$, low correlation. Positive numbers are positive correlations, negative numbers are negative correlations (Cohen 1988).

Chapter 3 *PFKFB3* mRNA is overexpressed in AML

3.1 Introduction

As introduced in section 1.3.4 malignant proliferation of AML blasts was previously shown to be associated with extracellular ROS production (Hole et al. 2010). Further, previous analysis of the AML blast metabolome demonstrated increased glucose metabolism in blast cells producing high levels of ROS (Robinson et al. 2020). In addition, Hopkins *et al.*, previously showed that when normal CD34⁺ haematopoietic progenitor cells (HSPC) were exposed to exogenous ROS, a change in glycolytic function was observed (Hopkins et al. 2014). Taken together, these studies suggest that the enzymes involved in carbohydrate metabolism may play an important role in ROS mediated AML proliferation.

Most solid tumour cells rely on glycolysis to generate energy to adapt to their heterogeneous microenvironment, which is also considered a hallmark of cancer (reviewed in (Abdel-Wahab et al. 2019)). Altering glycolysis not only provides energy to cancer cells, but also produces metabolic intermediates necessary for malignant cell proliferation, which are achieved by promoting macromolecular synthesis during metabolism. Clinical studies have shown that the combination of targeting glycolysis and chemotherapy can have enhanced therapeutic effects (reviewed in (Abdel-Wahab et al. 2019)). In addition to AML, glycolytic enzymes are also dysregulated in many solid tumours compared to healthy tissue (El Hassouni et al. 2020; Alharbi et al. 2021; Curcio et al. 2021). Interestingly, a study showed that increases in glycolysis were associated with poorer prognosis in lung cancers, as represented by decreased overall

survival (OS) and decreased disease-free survival (DFS)(Giatromanolaki et al. 2017). In haematopoietic studies, differential glycolytic and oxidative metabolism in leukocytes and platelets have been identified as a biomarker for studying them (reviewed in (Kramer et al. 2014)). Recently, Robinson *et al.*, showed that changes in expression of PFKFB3 was associated with ROS production in a human HSPC model (Robinson et al. 2020). However, little is known regarding the expression of other PFKFB family members in haematopoietic development, or their association with AML development. My research will further investigate the role of the *PFKFB* family (*PFKFB1*, 2, 3 and 4) in glycolysis dysregulation and relationship of the PFKFB family to ROS production in AML cell lines.

3.1.1 Aims and objectives

The main aim of this chapter is to investigate the role of the *PFKFB* family (*PFKFB1*, 2, 3 and 4) in normal haematopoiesis and to determine the relationship between the expression of *PFKFB1*, 2, 3 and 4 in different subtypes of AML (and with disease demographic features) from clinical data. To achieve this goal, this chapter has the following objectives:

- **Determine the mRNA expression levels of *PFKFB/Pfkfb* 1, 2, 3 and 4 during normal human and mouse haematopoiesis**

To understand whether the expression of *PFKFB/Pfkfb* family members differ between haematopoietic stem cells and differentiated lineages. The TCGA dataset will be used to analyse mouse/human mRNA (Ley 2013). This will potentially explain how *PFKFB* family mRNA expression associates with stem cell differentiation in normal human and mouse haematopoiesis.

- **Determine the expression levels of *PFKFB1*, *2*, *3* and *4* (*PFKFB* family) in AML**

To understand whether the expression of *PFKFB* family members differs between normal HSC and different AML subtypes using the TCGA dataset (Ley 2013). This will explain the relationship between expression of the *PFKFB* family involved in glycolysis and AML subtypes. The data will help me identify which *PFKFB* members may play an important role in AML.

- **Determine whether the *PFKFB* expression change is associated with ROS and overall survival**

To understand whether increased *PFKFB* expression is associated with increased ROS production and patient OS and DFS. This will be achieved using cBioPortal (Cerami et al. 2012; Gao et al. 2013). This may explain the relationship with ROS and *PFKFB* from the clinical perspective.

3.2 *PFKFB3* mRNA expression increases during normal human haematopoietic differentiation

Previous preliminary studies in AML suggest that NOX-2 derived ROS may regulate carbohydrate metabolism via changes in *PFKFB3* expression (Robinson et al. 2020). However, the roles of this protein and of other *PFKFB* family members in normal haematopoiesis and AML remain unclear. To understand how changes in *PFKFB* expression may contribute to AML development and survival, it is important to understand how *PFKFB1-4* are expressed during normal haematopoietic development and whether there are differences in expression between normal blood cells and AML. The following analyses of *PFKFB 1, 2, 3, 4* mRNA rely on publicly available mRNA data sets made available via BloodSpot (2.6) (Bagger et al. 2016).

3.2.1 *PFKFB1* mRNA expression does not change during normal haematopoietic differentiation

To determine the expression of human *PFKFB1* mRNA during normal haematopoiesis, I analysed the 207537-probe set using Bloodspot. As shown in Figure 3-1A, *PFKFB1* is expressed at relatively low levels in HSC, and the expression remains unchanged as human HSC differentiate towards myeloid cells. In contrast, *Pfkfb1* expression in primary mouse blood cells shows a different pattern of expression (Figure 3-1B). Here *Pfkfb1* mRNA expression is highest in granulocyte monocyte progenitors (GMP) compared to short term- haematopoiesis stem cells (ST-HSC) where it has lower expression. However, as mouse haematopoietic stem cells differentiate to the monocytic and granulocytic lineages, *Pfkfb1* mRNA expression decreases to similar levels as HSC. Figure 3-1 showed a weak biological significance for *PFKFB1* in normal haematopoiesis.

3.2.2 *PFKFB2* mRNA expression does not change during normal haematopoietic differentiation

I next analysed *PFKFB2/Pfkfb2* mRNA. As shown in Figure 3-2A, *PFKFB2* mRNA is expressed at low levels in normal HSC. Using probe set 1422090_at to analyse *Pfkfb2* in normal mouse haematopoiesis, Figure 3-2B shows that this gene is expressed at low levels and remains unchanged throughout normal mouse haematopoiesis. These patterns of expression showed a weak biological significance for *PFKFB2* in normal haematopoiesis.

3.2.3 *PFKFB3* mRNA expression increases along with differentiation in normal haematopoiesis

Probe set 202464_s_at was used to analyse the expression of *PFKFB3* in normal human haematopoiesis. A t-test was used to identify statistically significant differences

between expression levels of different subsets. Figure 3-3A shows that *PFKFB3* is expressed in normal human HSC and its expression increases as HSC differentiate into PMN and monocytes. PMN have the highest expression which is ~4-fold higher than HSC. Using probe set 1416432_at, I next analysed *Pfkfb3* mRNA in normal mouse haematopoiesis. As Figure 3-3B shows, *Pfkfb3* mRNA expression increases in GMP along with mouse HSC differentiation ($p < 0.05$). These patterns of expression imply that *PFKFB3* has a strong biological significance in normal haematopoiesis.

3.2.4 *PFKFB4* mRNA expression increases along with differentiation in normal haematopoiesis

Using 206246_at probe set to analyse the role of *PFKFB4* in normal human haematopoiesis, Figure 3-4A shows that *PFKFB4* is expressed at relatively low levels in human normal HSC but its expression increases as human HSC differentiate. Within the granulocytic lineages, *PFKFB4* expression is maintained at the same level as HSC, GMP and MMP, increasing significantly (around 2.5-fold) as cells reached PMN and monocyte developmental stages. I used 1456888_at probe set to analyse the role of *Pfkfb4* in normal mouse haemopoiesis (Figure 3-4B). As shown in Figure 3-4B, *Pfkfb4* is expressed in normal mouse haemopoiesis, and its expression slightly increases as cells differentiate. Within the monocytic and granulocytic lineages, *Pfkfb4* expression was the same as in HSC and LMPP.

In summary (Figure 3-8 B), *PFKFB1 and 2* mRNA are expressed in human & mouse normal haemopoiesis, and their expression remains unchanged as human HSC differentiate (Figure 3-1A, Figure 3-2A, Figure 3-1B, Figure 3-2B). *PFKFB3 and 4* expression increases with human HSC differentiation, being significantly elevated in monocytes and PMN (Figure 3-3A, Figure 3-4A), and also slightly increased in mouse HSC differentiation (Figure 3-3B, Figure 3-4B). However, I still need to compare the difference between expression levels of the *PFKFB/ Pfkfb* family in normal

haemopoiesis compared to AML to identify which family members may have a strong biological significance in AML proliferation. This will be described in next section.

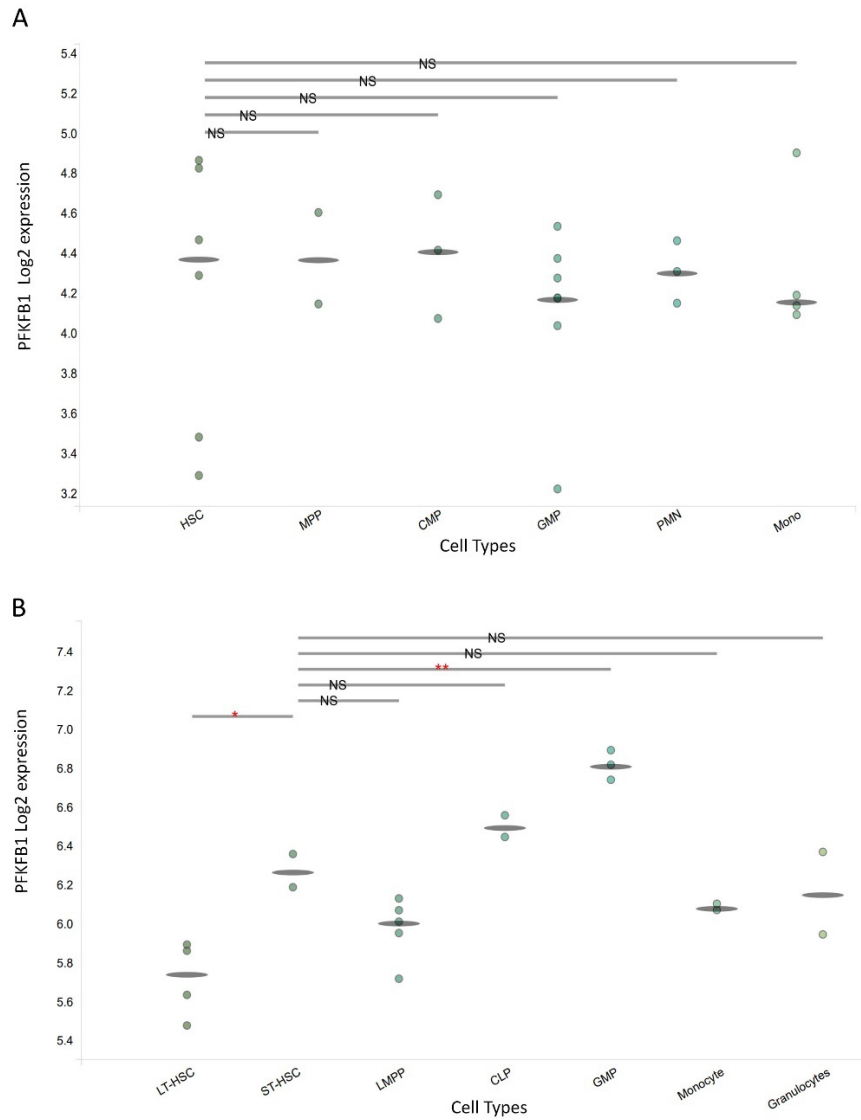


Figure 3-1 *PFKFB1/Pfkfb1* mRNA expression in normal haematopoiesis

- A. *PFKFB1* mRNA expression (Log₂) during normal human haematopoiesis. Determined by microarray and analysed using Bloodspot (GSE42519; Probe-set 207537_at;(Rapin et al. 2014)).
- B. *Pfkfb1* mRNA expression (Log₂) in normal mouse haematopoiesis. Determined by microarray and analysed using Bloodspot (GSE14833 and GSE6506; Probe-set 1417213_at; (Rapin et al. 2014)).

Abbreviations: common lymphoid progenitor (CLP); haematopoietic stem cell (HSC); multipotent progenitors (MPP); common myeloid progenitor (CMP); megakaryocyte-erythroid progenitor (MEP); granulocyte macrophage progenitor (GMP); polymorphonuclear cells (PMN); long term-haemopoietic stem cell (LT-HSC); short term-haemopoietic stem cell (ST-HSC). Monocyte (Mono). Statistical significance was determined by t-test. NS: non-significant; * $p < 0.05$; ** $p < 0.01$; *** $p < 0.001$ (2.6.2).

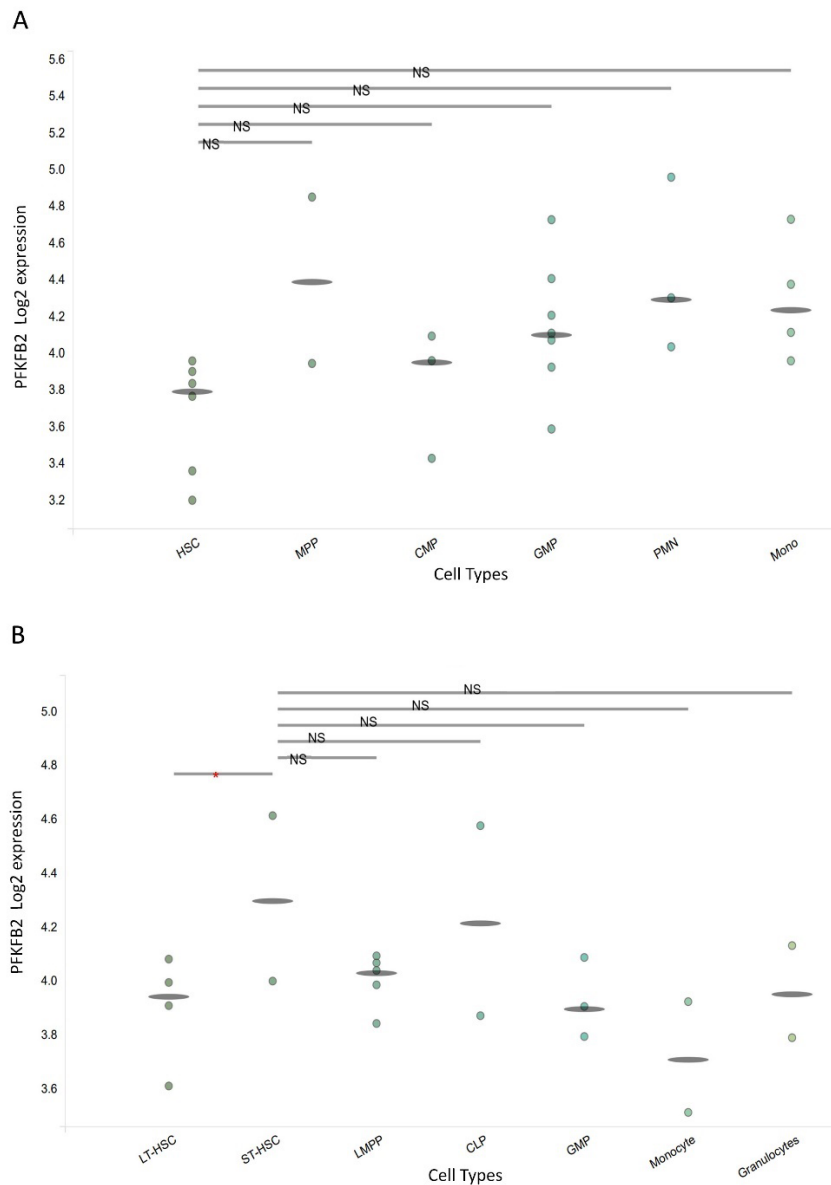


Figure 3-2 *PFKFB2/Pfkfb2* mRNA expression in normal haematopoiesis

- A. This plot shows *PFKFB2* mRNA expression (Log₂) during normal human haematopoiesis, which had been determined by microarray and analysed using Bloodspot (GSE42519; Probe-set 238450_at;(Rapin et al. 2014)).
- B. This plot shows *Pfkfb2* mRNA expression (Log₂) in normal mouse haematopoiesis, which had been determined by microarray and analysed using Bloodspot (GSE14833 and GSE6506; Probe-set 1422090_at; (Rapin et al. 2014)).

Abbreviations: common lymphoid progenitor (CLP); haematopoietic stem cell (HSC); (MMP); common myeloid progenitor(CMP); megakaryocyte-erythroid progenitor (MEP); granulocyte macrophage progenitor(GMP); polymorphonuclear cells(PMN); long term-haemopoietic stem cell (LT-HSC); short term-haemopoietic stem cell (ST-HSC). Monocyte (Mono). Statistical significance was determined by T-test. NS: non-significant; *p<0.05; **p<0.01; ***p<0.001(2.6.2)

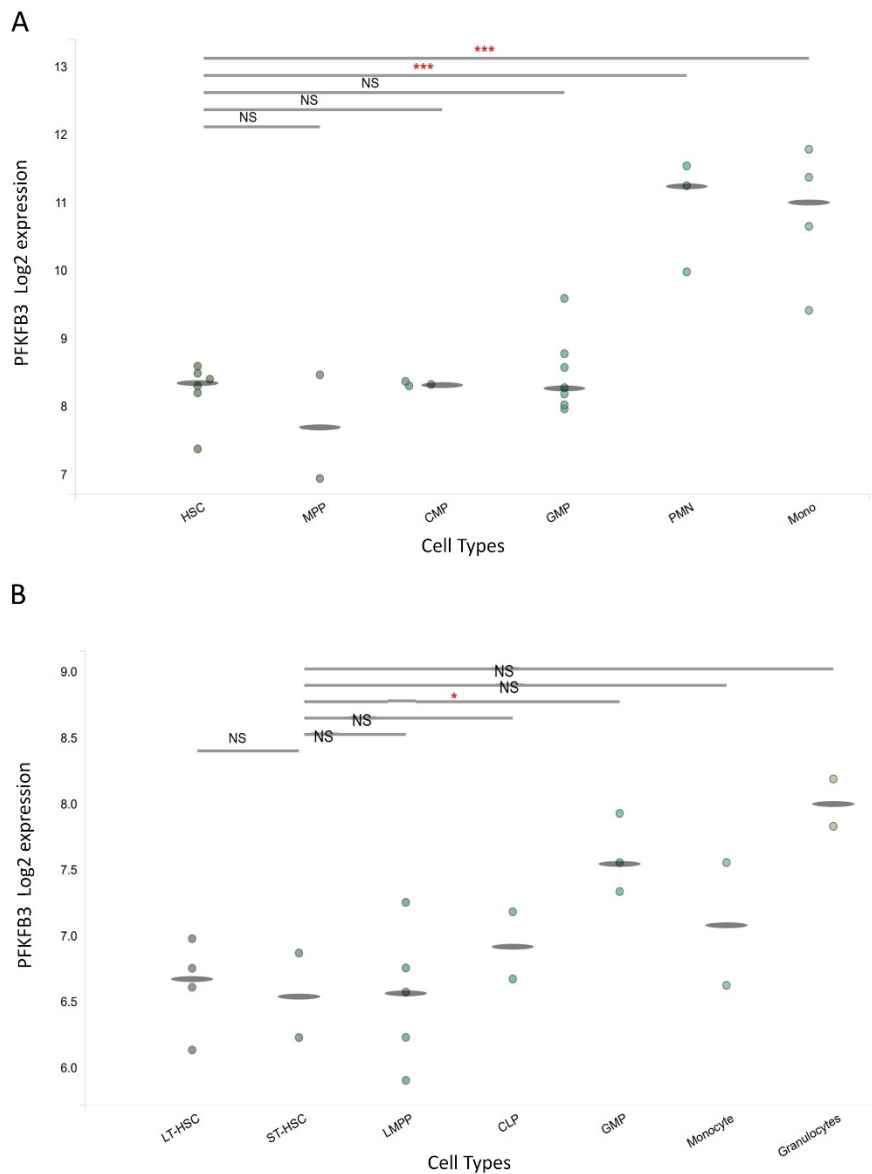


Figure 3-3 *PFKFB3/Pfkfb3* mRNA expression in normal haematopoiesis

- A. This plot shows *PFKFB3* mRNA expression (Log₂) during normal human haematopoiesis, which had been determined by microarray and analysed using Bloodspot (GSE42519; Probe-set 202464_s_at;(Rapin et al. 2014)).
- B. This plot shows *Pfkfb3* mRNA expression (Log₂) in normal mouse haematopoiesis, which had been determined by microarray and analysed using Bloodspot (GSE14833 and GSE6506; Probe-set 1456676_at; (Rapin et al. 2014)).

Abbreviations: common lymphoid progenitor (CLP); haematopoietic stem cell (HSC); multipotent progenitors (MMP); common myeloid progenitor (CMP); megakaryocyte-erythroid progenitor (MEP); granulocyte macrophage progenitor (GMP); polymorphonuclear cells (PMN); long term-haematopoietic stem cell (LT-HSC); short term-haematopoietic stem cell (ST-HSC). Monocyte (Mono). Statistical significance was determined by T-test. NS: non-significant; * $p < 0.05$; ** $p < 0.01$; *** $p < 0.001$ (2.6.2)

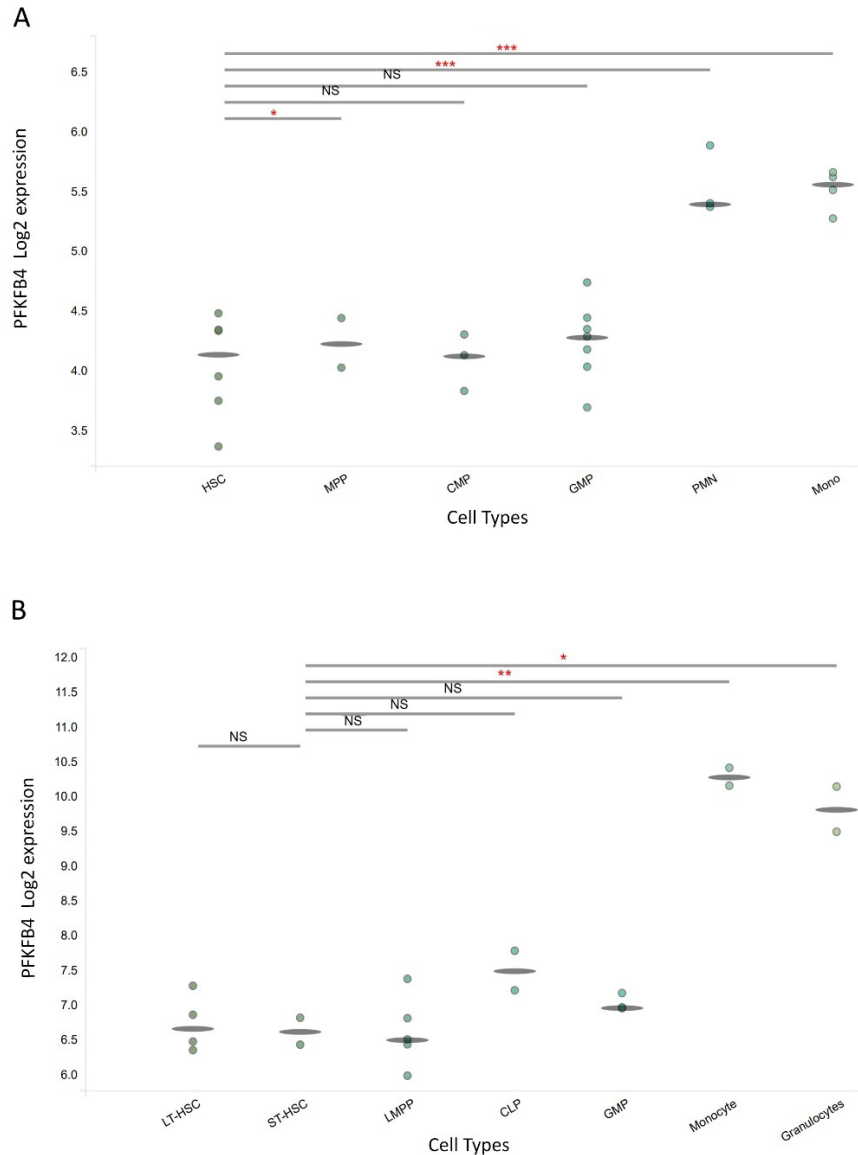


Figure 3-4 *PFKFB4/Pfkfb4* mRNA expression in normal haematopoiesis

- A. This plot shows *PFKFB4* mRNA expression (Log₂) during normal human haematopoiesis, which had been determined by microarray and analysed using Bloodspot (GSE42519; Probe-set 206246_at;(Rapin et al. 2014)).
- B. This plot shows *Pfkfb4* mRNA expression (Log₂) in normal mouse haematopoiesis, which had been determined by microarray and analysed using Bloodspot (GSE14833 and GSE6506; Probe-set 1456888_at; (Rapin et al. 2014)).

Abbreviations: common lymphoid progenitor (CLP); haematopoietic stem cell (HSC); multipotent progenitors (MPP); common myeloid progenitor (CMP); megakaryocyte-erythroid progenitor (MEP); granulocyte macrophage progenitor (GMP); polymorphonuclear cells (PMN); long term-haemopoietic stem cell (LT-HSC); short term-haemopoietic stem cell (ST-HSC). Monocyte (Mono). Statistical significance was determined by T-test. NS: non-significant; *p<0.05; **p<0.01; ***p<0.001(2.6.2)

3.3 *PFKFB3* mRNA expression is significantly higher in AML patient blasts compared to normal HSC

Amongst the *PFKFBs* analysed, the data above suggest that *PFKFB3* and *PFKFB4* may have a role in normal haematopoiesis. However, it remains unknown whether there is a change in expression (and activity) of *PFKFB* family group members in AML compared to normal HSC. To determine if any *PFKFB* family members are dysregulated in AML, I analysed the mRNA expression levels of the *PFKFB* family within different molecular AML subtypes (e.g. AML with t(15;17), inv(16)/t(16;16), t(8;21), t(11q23)/MLL, complex aberrant karyotype (Kohlmann et al. 2008; Kohlmann et al. 2010) which are annotated in the TCGA dataset database, and compared them to HSC *PFKFB* mRNA expression using the Bloodspot platform (Bagger et al. 2016).

Most of AML types have significant *PFKFB1* expression and insignificant *PFKFB2*, *PFKFB4* expressions (Figure 3-5 and Figure 3-6 respectively), while AML complex has strong *PFKFB3* expression (detail in below). Furthermore, whilst expression is statistically significantly higher in the majority of AML than in HSC, the overall fold change is negligible suggesting that the biological significance is weak. Taken together, these two genes do not seem to have a significant role in normal haematopoiesis and appear to be biologically insignificant in AML, suggesting that *PFKFB1* and 2 do not play an important role in AML malignant proliferation.

I next analysed *PFKFB3* mRNA expression in AML. Figure 3-7 suggests that *PFKFB3* is significantly overexpressed in AML t(15;17) and AML with complex aberrant karyotype (multiple recurrent chromosomal aberrations) compared to normal HSC. There are no significant statistical changes in expression in other represented AML subtypes. However, the distribution of *PFKFB3* mRNA expression is highly variable within each subtype suggesting that a proportion of AML patients have higher levels of *PFKFB3* compared to other AMLs and HSC. Considering that *PFKFB3* expression

increases as human HSC differentiate, especially when cells reach PMN and monocytic differentiation (3.2.3), this may suggest that *PFKFB3* expression could be associated with differentiation (also see Figure 3-3A).

Lastly, Figure 3-8B shows that *PFKFB4* is expressed at lower levels in AML with little significant expression in different AML subtypes.

PFKFBs expression in HSC was selected as the standard for the normalization of *PFKFBs* data in AML and healthy blood because patients with HSC, progenitor cells and mature cell components in AML blood are containing recurrent mutations leading to clonal expansion pre-LSC pool(Shlush et al. 2014a). Normal healthy blood cells are also differentiated from HSCs (1.1.2). It is concise and straightforward to use HSC data as a unified standard to anchor the next protein research direction, although cancer stem cells are not equal to normal stem cells and have their own characteristics(Hua et al. 2022): first, stem cell self-renewal has a negative feedback regulation mechanism to help its proliferation and the differentiation is balanced. However, the negative feedback mechanism of cancer stem cell has been destroyed, resulting in uncontrolled proliferation and differentiation of it. Second, cancer stem cells disordered in differentiate and mature, so cancer cells are often poorly differentiated compared with normal stem cells(Steinbichler et al. 2018). Third, cancer stem cells tend to accumulate replication errors, whereas normal stem cells prevent this in several ways(Sancho et al. 2016). Finally, some signal transduction pathways are different between the two(Ding et al. 2015).Taken together, of the *PFKFB* family members, it appears most likely that *PFKFB3* in AML complex has the strong biological significance. Therefore, the rest of the Chapter and thesis will explore the role of this isoform.

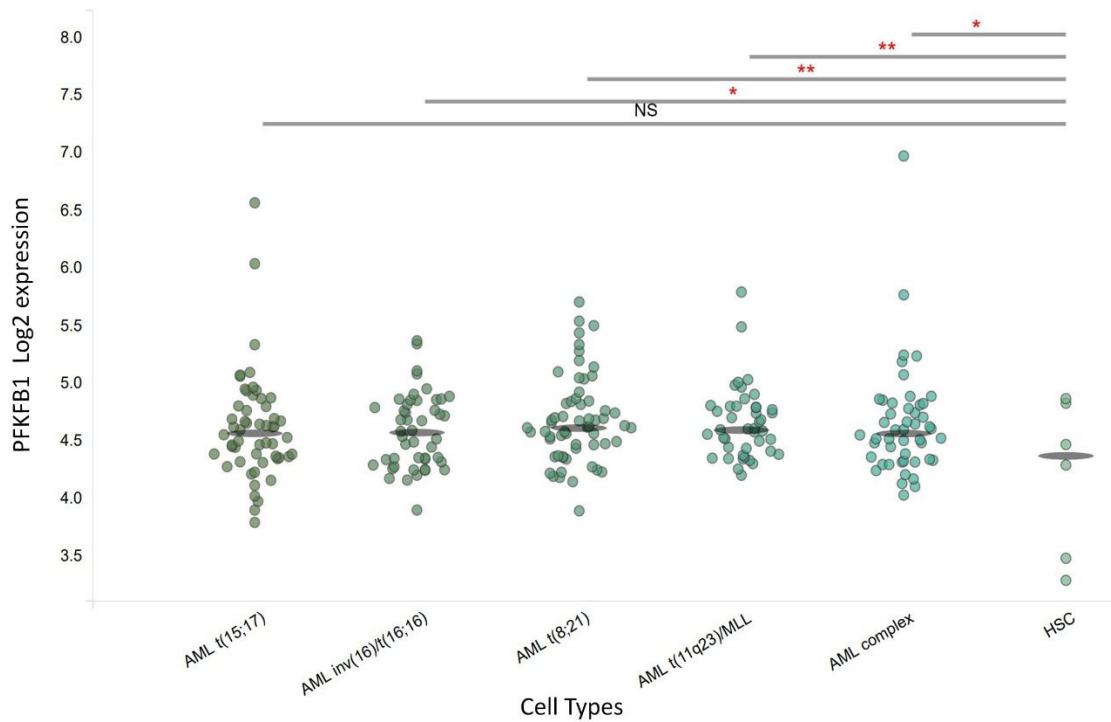


Figure 3-5 *PFKFB1* mRNA expression changed in AML compared to normal HSC

This plot shows *PFKFB1* mRNA expression (Log₂) during AML human haematopoiesis, which had been determined by microarray and analysed using Bloodspot (GSE42519; Probe-set 207537_at;(Rapin et al. 2014)).

AML t(15;17)(AML with *t(15;17)*); *AML inv(16)/t(16;16)* (AML with *inv(16)/t(16;16)*); *AML t(8;21)* (AML with *t(8;21)*); *AML t(11q23)/MLL*(AML with *t(11q23)/MLL*); *AML complex* (AML with complex aberrant karyotype); *HSC* (Hematopoietic stem cell). Statistic significance was determined by T-test. NS: non-significant; * $p < 0.05$; ** $p < 0.01$; *** $p < 0.001$ (2.6.2)

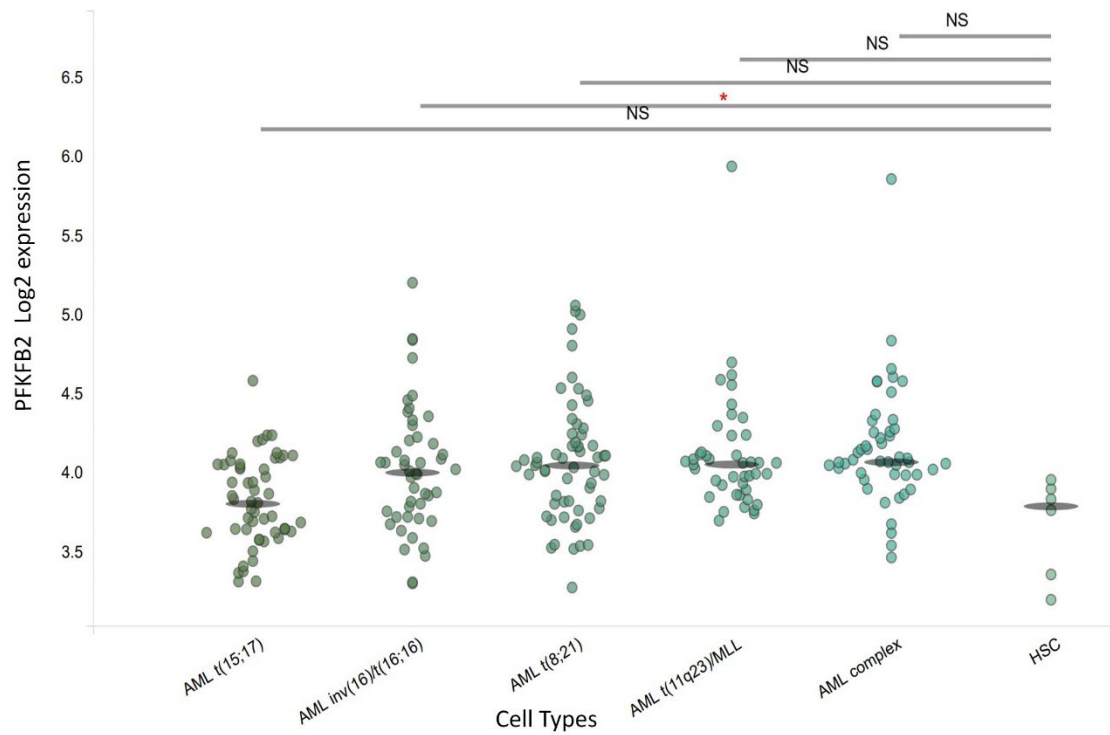


Figure 3-6 *PFKFB2* mRNA expression is not changed in AML compared to normal HSC

This plot shows *PFKFB2* mRNA expression (Log₂) during AML human haematopoiesis, which had been determined by microarray and analysed using Bloodspot (GSE42519; Probe-set 238450_at;(Rapin et al. 2014)).

AML t(15;17)(AML with *t(15;17)*); *AML inv(16)/t(16;16)* (AML with *inv(16)/t(16;16)*); *AML t(8;21)* (AML with *t(8;21)*); *AML t(11q23)/MLL*(AML with *t(11q23)/MLL*); *AML complex* (AML with complex aberrant karyotype); *HSC* (Hematopoietic stem cell). Statistical significance was determined by T-test. NS: non-significant; * $p < 0.05$; ** $p < 0.01$; *** $p < 0.001$ (2.6.2)

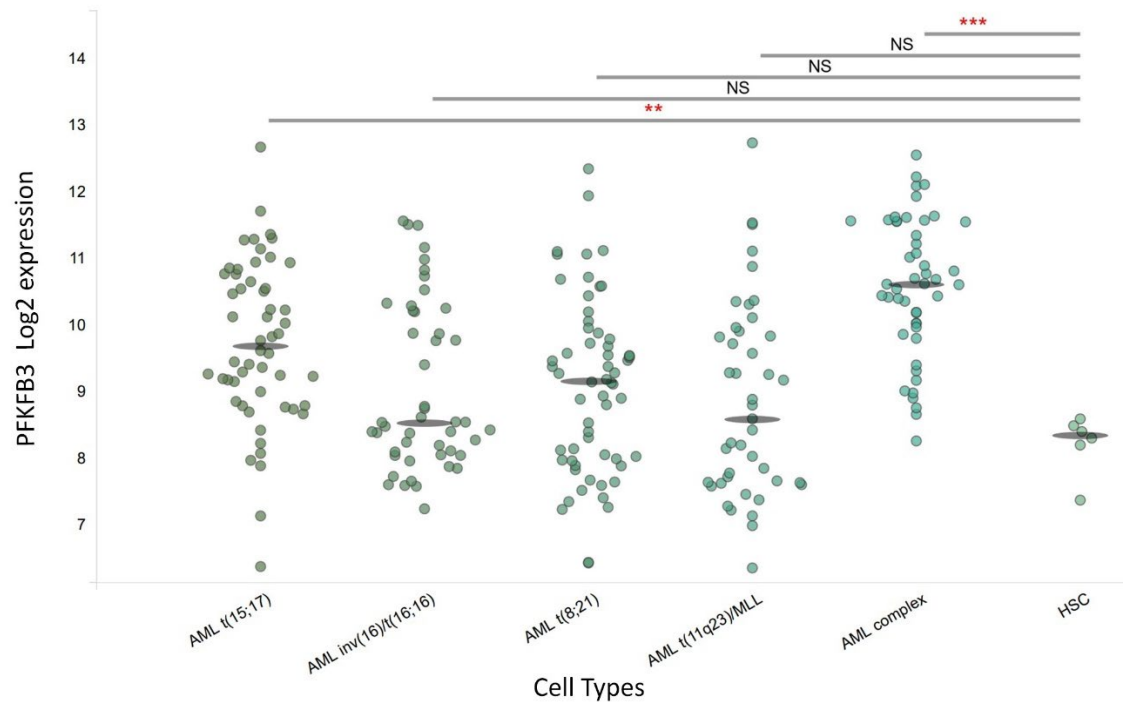


Figure 3-7 *PFKFB3* mRNA expression is higher in AML complex compared to normal HSC

This plot shows *PFKFB3* mRNA expression (Log₂) during AML human haematopoiesis, which had been determined by microarray and analysed using Bloodspot (GSE42519; Probe-set 202464_at;(Rapin et al. 2014)).

AML t(15;17)(AML with *t(15;17)*); *AML inv(16)/t(16;16)* (AML with *inv(16)/t(16;16)*); *AML t(8;21)* (AML with *t(8;21)*); *AML t(11q23)/MLL*(AML with *t(11q23)/MLL*); *AML complex* (AML with complex aberrant karyotype); *HSC* (Hematopoietic stem cell). Statistical significance was determined by T-test. NS: non-significant; *:p<0.05; ** p<0.01; *** p<0.001(2.6.2)

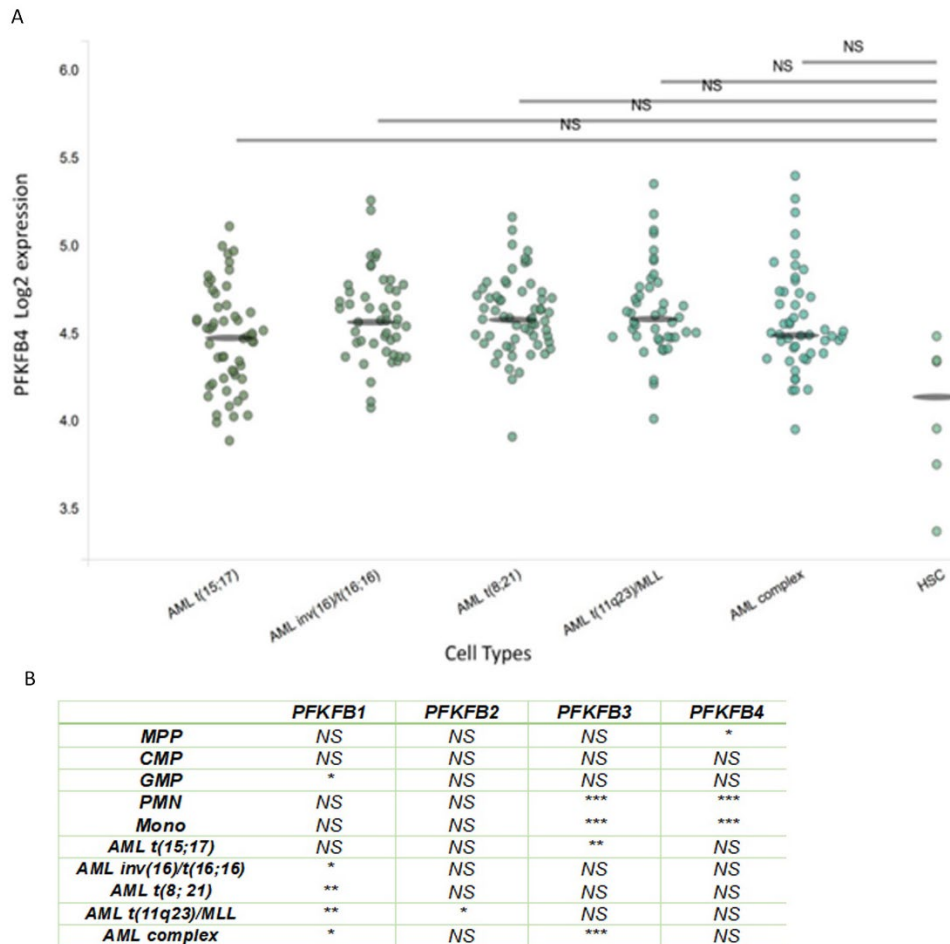


Figure 3-8 *PFKFB4* mRNA expression is not changed in AML compared to HSC and the summary

A: This plot shows *PFKFB3* mRNA expression (Log₂) during AML human haematopoiesis, which had been determined by microarray and analysed using Bloodspot (GSE42519; Probe-set 206246_at;(Rapin et al. 2014)). B: A summary table of expression of the *PFKFBs* in the different haematopoietic compartments.

*Abbreviations: common lymphoid progenitor (CLP); haematopoietic stem cell (HSC); (MMP); common myeloid progenitor(CMP); megakaryocyte-erythroid progenitor (MEP); granulocyte macrophage progenitor(GMP); polymorphonuclear cells(PMN) ; Monocyte (Mono). AML t(15;17)(AML with t(15;17)); AML inv(16)/t(16;16) (AML with inv(16)/t(16;16) ; AML t(8; 21) (AML with t(8;21)); AML t(11q23)/MLL(AML with t(11q23)/MLL); AML complex (AML with complex aberrant karyotype); HSC (Hematopoietic stem cell). Statistical significance was determined by T-test. Statistical significance was determined by T-test. NS: non-significant; * $p < 0.05$; ** $p < 0.01$; *** $p < 0.001$ (2.6.2)*

3.4 *PFKFB3* mRNA expression correlates with *CYBB* mRNA expression

A previous study by Robinson suggested that changes in ROS production influence the expression of *PFKFB3* expression in AML cell lines (Robinson et al. 2020). To further investigate the relationship between *PFKFB3* expression and NOX2-derived ROS production in AML patient blasts, I analysed pre-existing mRNA data. *CYBB* is a gene encoding the main catalytic subunit of NADPH oxidase 2 (NOX2) whose expression has previously been shown to correlate with NOX2 derived ROS production (Robinson et al. 2020)(1.3). The AML patient RNA-sequence TCGA database (Ley 2013) was downloaded, and I made a regression analysis graph of *CYBB* and *PFKFB3* expression (Figure 3-9). As shown in Figure 3-9, higher expression of *CYBB* mRNA is associated with higher *PFKFB3* mRNA expression and the Pearson value is 0.47. Overall, this concurs with Robinson's research (Robinson et al. 2020), supporting the hypothesis that *PFKFB3* expression and ROS are positively related. The next section will evaluate the association between high / low expression of *PFKFB3* and OS for AML subtypes (Figure 3-10).

3.5 *PFKFB3* expression does not correlate with overall survival in AML patients

The above data showed a positive correlation between *PFKFB3* and *CYBB* mRNA expression, and that some AML patients have higher levels of *PFKFB3* compared to HSC (Figure 3-7). I next analysed patient OS to determine whether there was a correlation of high or low *PFKFB3* expression with clinical outcome. Figure 3-10 shows similar patterns of OS in high and low *PFKFB3* expression groups. Furthermore, there was no statistical correlation between the expression level of *PFKFB3* and OS (Figure

3-10). Overall, this analysis suggests that *PFKFB3* expression does not correlate with AML patient OS.

3.6 High *PFKFB3* mRNA expression is linked to FAB groups M4, M5

Since *PFKFB3* was associated with normal differentiation, I wanted to see if expression in AML correlated with differentiated (FAB) subtypes. To determine the association of *PFKFB3* expression with different FAB group types and clinical parameters in AML, I analysed patient sample data from the TCGA database (Ley 2013). The data were stratified as above (2.6.1.2). Figure 3-11 shows that 100% of the M4 patients had high *PFKFB3* expression (acute myelomonocytic leukaemia), 60% in M5 (acute monocytic/monoblastic leukaemia), 50% in M0 (undifferentiated acute myeloblastic leukaemia) and the least in M1 (AML with minimal differentiation), with 19% of patients having increased expression. As shown above, *PFKFB3* expression is elevated in monocytes (Figure 3-3); it may be that in AML disease, *PFKFB3* expression has some of the developmental feature of normal monocytes that has higher *PFKFB3* expression in normal haematopoiesis monocytes than other normal haematopoiesis lineages.

In summary, *PFKFB3* expression increases with human HSC differentiation and is found to be significantly elevated in monocytes. *PFKFB3* may also play an important role in acute promyelocytic leukaemia and AML with complex cytogenetics. Further, *PFKFB3* and *CYBB* expression are positively related, which lays the foundation for investigating the relationship between ROS and *PFKFB3* protein expression in cell lines in the next chapter.



Figure 3-9 *PFKFB3* mRNA expression level correlates with *CYBB* expression in AML patients

This scatter plot shows *PFKFB3* mRNA expression in patient samples from the TCGA 2013 dataset (Ley 2013). The Pearson value is 0.47, indicating a correlation between *CYBB* and *PFKFB3* mRNA expression; R^2 value is 0.2217 which indicates that only a small proportion of variance in *PFKFB3* can be explained by *CYBB*. The relationship between *CYBB* and *PFKFB3* is represented by the equation $y = 0.5235x - 0.0411$.

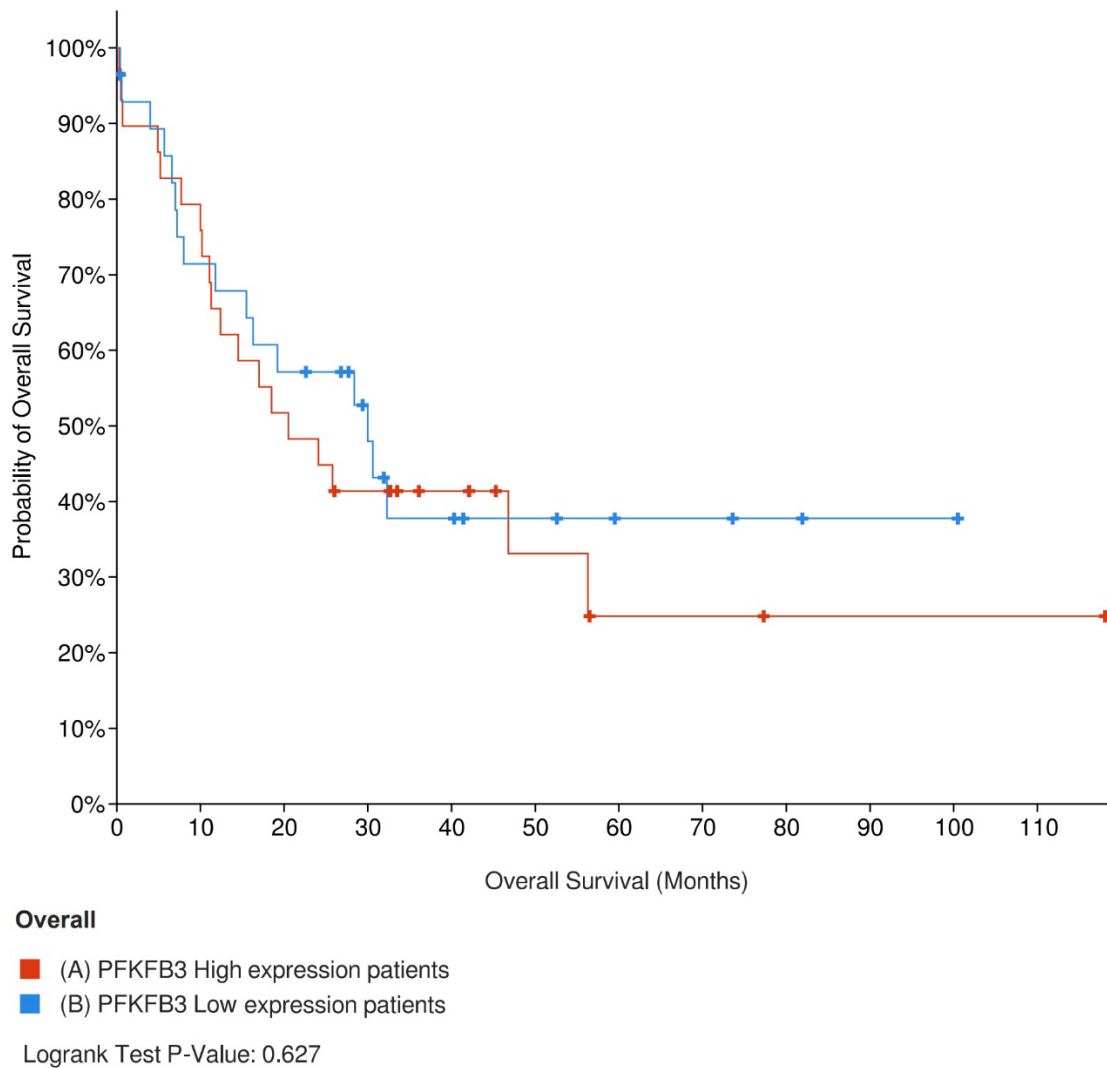


Figure 3-10 PFKFB3 mRNA expression level does not relate with overall survival

Kaplan-Meier survival curve showing *PFKFB3* mRNA expression in patient samples from TCGA 2013 dataset (Ley 2013). All patients were divided into high expression group (30 samples) and low expression group (30 samples) according to above/below median expression level of *PFKFB3*. Statistical significance was determined using a Log-Rank Test and was deemed insignificant based on the P-value of 0.627. Data was obtained using cBioPortal (Cerami et al. 2012; Gao et al. 2013)(see in 2.5).

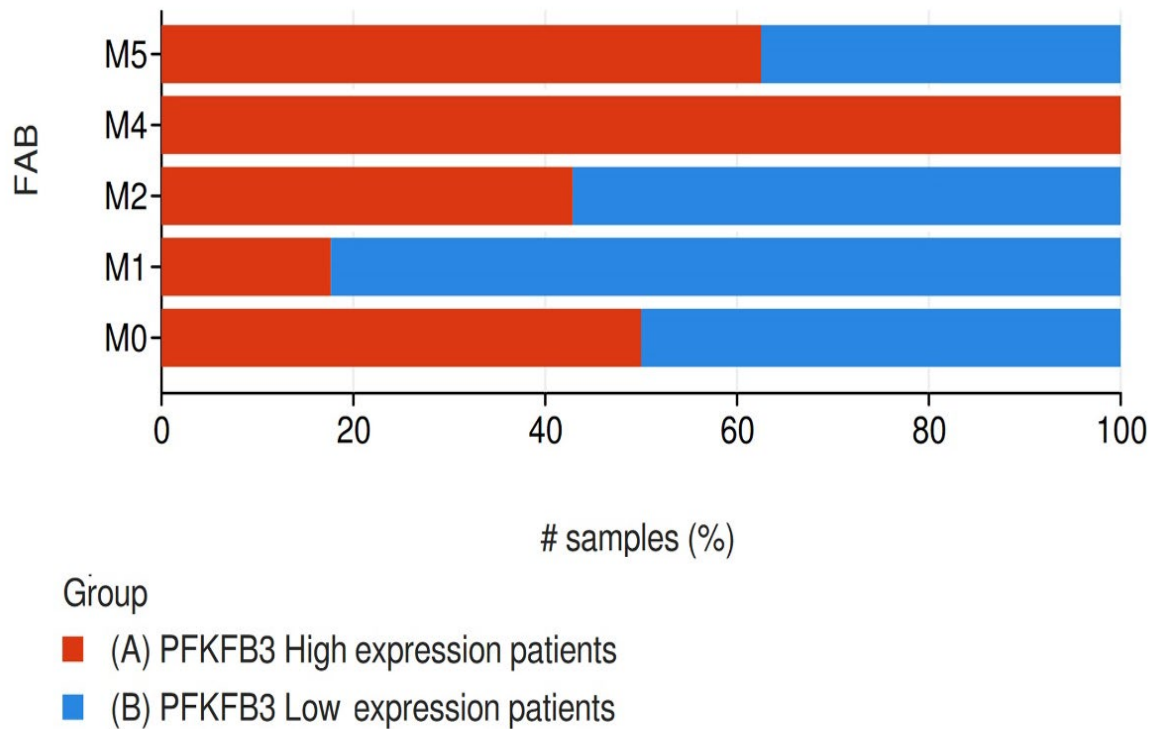


Figure 3-11 High and low *PFKFB3* mRNA expression in AML disease subtypes

Bar graph represents the number of patients with different FAB subtypes of AML (M0-M7) for samples from the TCGA 2013 dataset (Ley 2013). All patients were divided into high expression group (30 samples) and low expression group (30 samples) according to above/below the median expression level of PFKFB3. Data was obtained using cBioPortal (Cerami et al. 2012; Gao et al. 2013). The horizontal axis represents the percentage of each group occupying the subtype. M6, M7 did not appear in the bar graph because they were not represented in the data set. FAB: French American British Classification of AML. Number of patients in different categories (High PFKFB3 patient group/Low PFKFB3 patient group) : M0: 3/3; M1: 3/14; M2: 6/8; M4: 11/0; M5: 5/3; M6: 1/0.

3.7 Discussion

Malignant proliferation of AML blasts was previously shown to be associated with extracellular ROS production (Hole et al. 2010). Recently, Robinson *et al.*, showed that changes in expression of PFKFB3 were associated with ROS production in a human HSPC model (Robinson et al. 2020). However, little is yet known regarding the expression of other PFKFB family members in haematopoietic development, or their association with AML development. This chapter analyses the mRNA expression of the *PFKFB* family (*PFKFB1*, 2, 3 and 4). Interestingly, only *PFKFB3* and *PFKFB4* mRNA expression changed during haematopoiesis, and only *PFKFB3* mRNA expression significantly changed in AML. Importantly, this chapter found that *PFKFB3* mRNA was significantly associated with *CYBB* expression in AML blasts. However, *PFKFB3* expression shows no association with OS. There is even a trend that the OS of the high expression group is lower than that of the lower expression group, but the sample size 30 is at boundary of small and large, increase the sample size might reach the statistical significance.

The results in this chapter were obtained using the freely available primary material data from the BloodSpot database and TCGA database, so no RNA isolation was required, thus making my progress more economical and faster. I used the BloodSpot data to compare the expression differences of both *PFKFBs* mRNA in human and mouse in normal haemopoiesis, so that mouse data can be compared to *PFKFB* expression in human normal haemopoiesis.

PFKFB1 and 2 are expressed in human mouse normal haemopoiesis, and their expression remains unchanged as human HSC differentiate (Figure 3-1A, Figure 3-2A, Figure 3-1B, Figure 3-2B). Expression of *PFKFB3* and 4 increases with human HSC differentiation and is found to be significantly elevated in monocytes and PMN (Figure 3-3A, Figure 3-4A), and slightly increased with mouse HSC differentiation

(Figure 3-3B, Figure 3-4B). From the results, the expression of *Pfkfb* mRNA in normal haemopoiesis of mice is always up-regulated along with the HSC differentiation, which indicates conservation of their roles between human and mouse genes. In normal tissues, differences in mRNA expression between humans and mice have also been mentioned in other studies. For example, there is a report in the mRNA distribution and gene mapping study of mouse and human precortistatin which found that this region of chromosome 4 shows a conserved homology to human 1p36, but the human cortistatin peptide has an arginine for lysine substitution and is N-terminally extended by 3 amino acids compared to the mouse product (de Lecea et al. 1997). Similarly, Clofibrilic acid (CLO) treatment that induces upregulation of the I-fatty acid binding protein gene in mouse and human hepatocytes (Richert et al. 2003) show differences in its effects between species; whilst the genes involved in the cytoplasmic, microsomal and mitochondrial pathways involved in fatty acid transport and metabolism were up-regulated by CLO in both cell cultures, the genes in the peroxisomal pathway of lipid metabolism were only up-regulated in mice (Richert et al. 2003). As introduced in 1.4 and 1.5.2, the lipid metabolism peroxisomal pathway is associated with glycolysis for the production of hydrogen peroxide. There is potential that glycolysis-related enzymes are more active or more sensitive to external regulators in normal mouse tissue than in normal human tissue, which is similar to the expression of *Pfkfb* mRNA in normal haemopoiesis of mice always being slightly up-regulated along with HSC differentiation. Furthermore, the quantitative RTqPCR analysis of *Pfkfb* 1, 2, 3, and 4 expressions in *Xenopus* embryos showed increased expression during late organogenesis and the tadpole stage (late stem cell differentiation) (Pegoraro et al. 2013). This is consistent with the mouse data (Figure 3-1B, Figure 3-2B, Figure 3-3B, Figure 3-4B) in this chapter. Thus, the comparison between human and mouse genes allows the expression of *Pfkfb* 1, 2, 3, and 4 in mice to provide a reference for judging whether human *PFKFBs* mRNA expression results are consistent with the human because they are broadly similar.

The changes of expression of *PFKFB* in other tissues in relation to differentiation from blood stem cells have not yet been studied in detail. However, there is a study about *PFKFB3* expression regulated by hypoxia factor in different normal human tissues (Chesney et al. 2014). *PFKFB1* is highly expressed in liver and skeletal muscle; *PFKFB2* is highly expressed in heart, lung, skeletal muscle, kidney, pancreas and testis; *PFKFB3* is expressed at very low levels in all tissues (except leukocytes), but is inducible and ubiquitous and *PFKFB4* is highly expressed in placenta, lung, skeletal muscle, pancreas, spleen, prostate, testis, ovary, colon and leukocytes (Chesney et al. 2014). This is consistent with the results we obtained in this chapter (Figure 3-1A, Figure 3-2A, Figure 3-3A, Figure 3-4A). Blood cells are not in the range of high expression tissues of *PFKFB1,2* mRNA, so their expression levels do not change significantly with HSC differentiation. But leukocytes are in the high expression range, so *PFKFB3,4* mRNA expression increases with human HSC differentiation and is found to be significantly elevated in monocytes and PMN (late stage of differentiation, relatively mature morphology).

However, the above discussion about mRNA does not fully represent the functions of *PFKFB* proteins. Abreu *et al.*, and Affymetrix found that protein and mRNA expression levels had a correlation of 0.4 in *H. sapiens* by immunohistochemistry with Affymetrix and agilent microarrays (de Sousa Abreu et al. 2009). In the statistical analysis of mRNAs that were expressed differentially to proteins, it was found that some factors (transcription factors, cell cycle, up-stream regulators, etc.) affected the protein expression, especially the multi-structural mRNAs (Maier et al. 2009). Differentially expressed mRNAs influence their respective experimental conditions through protein differences (Koussounadis et al. 2015). We should also consider the advantages of mRNA detection compared to protein detection which, whilst taking lesser time and having lower cost and lower sample requirements, can nonetheless provide raw upstream information from genes in molecular research. Scientists do recognize the

importance of a more accurate detection of mRNA expression. Several new strategies have also been proposed recently. A method called REAP-seq combined with total-seq (CITE-seq) has been reported to have a better effect than single-cell mRNA sequencing by using DNA-tagged antibodies and droplet microfluidics to measure gene and protein expression levels in individual cells. Ab-seq assay is unique in exploring the relationship between protein and mRNA. Ab-seq was tested in 2020, validating its results to the Total-seq and enabling the intuitive visualization of protein-transcript relationships at the single-cell level (Mair et al. 2020). In addition, the combined use of the above methods is suggested to be more effective in improving the quality of mRNA expression measurement (Li et al. 2020a).

The analysis of *PFKFBs* mRNA in normal haemopoiesis laid the groundwork for my next comparison of *PFKFBs* mRNA in AML haemopoiesis. The expression of *PFKFBs* in AML has three main trends from the Bloodspot database: Comparing with HSC, *PFKFB4* has no difference in expression at all (Figure 3-8); *PFKFB1 and 2* (Figure 3-5, Figure 3-6) have a small increase in expression in specific AML subtypes; *PFKFB3* also has significantly increased expression in specific AML subtypes (Figure 3-7). Specifically, *PFKFB1* was raised in AML t(11q23)/MLL, AML t(8;21) and AML with complex cytogenetics. *CYBB* and *PFKFB2* both showed an increase in AML inv(16)/t(16;16) and t(8;21). AML with inv(16)/t(16;16) and t(8;21) are often considered together as 'core binding factor leukaemias' because of relatively small patient populations and similarity of pathogenetic mechanisms and treatment outcomes) (Nguyen et al. 2002). t(8;21) is generally associated with a relatively low risk of recurrence (Reikvam et al. 2011). This chromosomal abnormality results in the formation of the RUNX1::ETO fusion protein, which upregulates connexin 43 (Cx43). Cx43 could help AML malignant proliferation because Cx43 is closely related to inflammatory factors, and the report observed that during hypoxia and inflammation, PMNs release ATP from Cx43 through an activation-dependent pathway, regulating

adenosine-dependent endothelial cell function (Eltzschig et al. 2006). *PFKFB1* mRNA expression is also up-regulated significantly along with inflammatory marker genes (including NOS2, TNF, IL-1b and CD86), and the anti-inflammatory marker gene IL-10 was significantly up-regulated in mouse arthritic tissues, which caused long term inflammation (Saeki and Imai 2020). Thus, this might offer a potential explanation why *PFKFB1* is expressed at slightly higher levels in AML with inv(16)/t(16;16) and t(8;21).

Similarly, *PFKFB2* mRNA is also significantly upregulated in tissues in disc degeneration, accompanied by oxidative stress (Cao et al. 2021), but mostly in non-cancer disease, such as, upregulation of *PFKFB2* mRNA under chronic hypoxia assists pulmonary artery smooth muscle cell proliferation, resulting in reduced pulmonary artery lumen leading to poor blood flow and cardiac overload (Parra et al. 2017). The QRT-PCR analysis of patients with chronic progressive right ventricular pressure overload and shunt hypoxemia showed significantly elevated *PFKFB2* mRNA levels and decreased lipid metabolism-related mRNA levels (Xia et al. 2013). On the other hand, *PFKFB1,2* (Figure 3-5, Figure 3-6) increased AML subtypes share a common feature: good prognosis and low-risk mutation categories (Nguyen et al. 2002; Reikvam et al. 2011; Chen et al. 2013). Therefore, the expression of *PFKFB1, 2* (Figure 3-5, Figure 3-6) slightly increased in AML may be related to hypoxia, long-term inflammation environment.

PFKFB4 mRNA expression remained unchanged in AML compared to HSC (Figure 3-8) but increased along with differentiation as discussed above in this section (Figure 3-4). However, *PFKFB4* mRNA has different roles in diseases other than AML, which is more related to cell signalling. It has been reported that upregulation of *PFKFB4* mRNA expression drives cytokine release syndrome in response to cellular immunotherapy and malignant cells (Shao et al. 2022). *PFKFB4* mRNA is also involved in the hydroxycarboxylic acid receptor2 regulatory pathway in the form of promoting glycolytic flux (Warburg effect)(Rabe et al. 2022). Studies have also shown

that the key target *PGMA1* in breast cancer is regulated indirectly (by affecting multiple kinases, miRNAs and transcription factors) by *PFKFB4* by GSEA analysis (Wang et al. 2021). Similarly, there are effects of long noncoding RNAs on cell proliferation and glycolysis by enhancing *PFKFB4* mRNA transcription and expression (Shen et al. 2021). . The overexpression of *PFKFB4* mRNA under hypoxic conditions found in melanoma with a 148-base spliced isoform inserted in the amino-terminal region of high composition type (Minchenko et al. 2005). *PFKFB4* mRNA was implicated in acquired drug resistance in paediatric retinal tumours (Song et al. 2020). In conclusion, *PFKFB4* mRNA has specific performance in different diseases other than AML.

An important finding in this Chapter is that *PFKFB3* mRNA expression is significantly increased in AML with complex karyotype and in acute promyelocytic leukaemia (AML with [15;17]) compared to HSC (Figure 3-7). AML (15;17) mutation is associated with promyelocytes and a differentiation block preventing cells from getting beyond that stage (Morikawa et al. 2003), but there is no sample shows the connection between the *PFKFB3* high and low expression groups and the FAB (Figure 3-11) in the form of TCGA data. *PFKFB3* mRNA is widely expressed in cancer/disease and healthy tissues, especially in cancer tissues to provide nutrients and signals in conjunction with other disordered molecules. *PFKFB3* mRNA was found to be associated with drug resistance in colorectal cancer (Gao et al. 2022). But it is not associated with drug resistance since it does not show an OS difference in AML (Figure 3-10). There are therapeutic regimens for hepatocellular carcinoma using inhibition of *PFKFB3* mRNA in combination with sildenafil (a type 5 phosphodiesterase inhibitor) (Liu et al. 2021). *PFKFB3* mRNA was incorporated into the reference index in the hepatobiliary cancer prognosis prediction model (Ran et al. 2022). But High *PFKFB3* mRNA expression does not affect OS in TCGA data (Figure 3-10). Importantly, *PFKFB3* was significantly higher in AML compared to normal HSC. This data supports Robinson et al, who found higher *PFKFB3* expression levels in ROS producing AML lines (Robinson et al. 2020).

Indeed, when I analysed ~160 AML patient blast samples stratified according to *CYBB* expression, I found a correlation between *CYBB* expression and *PFKFB3*. Previously expression of *CYBB/NOX2* has been shown to correlate with ROS production expression (Figure 3-9). However, the relationship between ROS production using Diogenes and *PFKFB3* protein expression in AML blasts needs to be confirmed (this was the intent of Chapter 4). Interestingly, in 66 individual tumours, *PFKFB3* mRNA levels were much higher than *PFKFB4* (Kessler et al. 2019). This data supports my study in which I observed little difference in *PFKFB4* expression in AML compared to normal haemopoiesis.

In summary, I investigated the expression of *PFKFBs* in normal and human haemopoiesis using the Bloodspot and TCGA databases in this chapter. It was found that *PFKFB3* expression has strong biological significance in some AML and is related to ROS expression. In the next chapter, I will focus on investigating the relationship between *PFKFB3* protein expression and ROS in AML cell lines.

Chapter 4 PFKFB3 protein expression is associated with NOX2 derived ROS in AML

4.1 Introduction

Using a normal human haematopoietic cell model, Hole *et al.*, showed that activated RAS (a common abnormality in AML) stimulates extracellular ROS production through the membrane bound enzyme NOX2 (Hole et al. 2010) (1.3). The authors further demonstrated that ROS production promoted the proliferation of normal human haematopoietic progenitor cells (Hole et al. 2010). More recently, using the same model, higher levels of ROS were shown to lead to changes in carbohydrate metabolism (Robinson et al. 2020). Specifically, using a single cell line as a model, culture with ROS increased glucose uptake and altered the expression of a key regulatory glycolytic enzyme, *PFKFB3* (1.4.3.3). The *PFKFB* family is comprised of four bifunctional enzymes (*PFKFB1-4*); *PFKFB3* is the only isoform with stronger kinase activity than phosphatase activity, which can better promote glycolysis, regulate cell cycle and control autophagy (reviewed by (Lu et al. 2017)). *PFKFB3* is frequently involved in oncogenesis where it promotes proliferation. It is commonly defined in many 'cancer signatures' and linkage marker studies such as pancreatic (Ozcan et al. 2021) and lung cancers (Li et al. 2018b). Therefore, targeting *PFKFB3* is emerging as an anticancer therapeutic strategy.

In Chapter 3, I analysed the *PFKFB* family of genes for mRNA expression during normal haematopoietic development. Further I compared *PFKFB3* mRNA expression in normal cells to mRNA expression in AML blasts. The most significant finding was that *PFKFB3* was expressed during haematopoietic development; expression

increased as HSC differentiated into terminally differentiated myeloid cells. Importantly, *PFKFB3* mRNA expression in AML blasts positively correlated with *CYBB* mRNA (also known as NOX2). However, it remains to be verified whether PFKFB3 protein expression correlates with ROS production in a larger panel of AML cell lines and primary AML blasts.

Given that previous studies only examined two AML cell lines (THP-1 and Mv4;11) (Robinson et al. 2020), I initially investigated the expression of PFKFB3 protein by western blot in a larger panel of AML cell lines. Using this data, I developed an assay to detect intracellular PFKFB3 expression at the single-cell level so PFKFB3 expression could be analysed in AML patient subpopulations in subsequent studies.

4.1.1 Aims and objectives

The main aim of this Chapter was to determine the relationship between extracellular ROS production and PFKFB3 protein expression in AML. To achieve this goal, this chapter had the following objectives:

- **Determine extracellular superoxide production in AML cell lines**

To investigate the relationship between PFKFB3 expression and ROS in AML cell lines, I measured extracellular ROS (superoxide) production using the chemiluminescent probe Diogenes in 10 AML cell lines.

- **Determine PFKFB3 protein expression in AML cell lines**

PFKFB3 protein expression in AML cell lines (those analysed above) were analysed by western blot. Initially PFKFB3 protein detection was optimised using cell lines ectopically expressing PFKFB3 as a positive control. The MV4;11 cell line was also used given its low PFKFB3 endogenous expression. Subsequently, PFKFB3 protein expression in AML cell lines was measured using optimised Western Blot conditions.

- **Determine the relationship between PFKFB3 protein expression and extracellular superoxide production in AML cell lines**

To investigate the relationship of PFKFB3 protein expression and ROS production in AML cell lines, I used Pearson linear regression analysis using data collected above; ROS by Diogenes and PFKFB3 expression by Western blot.

- **Develop a flow cytometry assay to detect intracellular PFKFB3 expression**

Developing a flow cytometry assay to detect PFKFB3 protein expression at the single cell level can overcome the challenge of insufficient AML cells and/or heterogenous cell populations in AML patient samples which can be a limitation for western blot testing. MV4;11-PFKFB3 knock in samples were used as a positive control to test whether the intracellular staining protocol is successful. Optimal conditions were used to detect PFKFB3 expression by flow cytometry in 10 AML cell lines. Due to time constraints, it was not possible to analyse PFKFB3 expression correlates with extracellular ROS production

4.2 AML cell lines produce varying amounts of extracellular superoxide

The Diogenes assay was used to measure ROS production (extracellular superoxide) in 10 AML cell lines (2.3). Previous studies have validated the use of Diogenes to measure extracellular superoxide (ROS) (Hole et al. 2010). As shown in Figure 4-1B, NOMO-1 cells produced the highest levels of extracellular ROS amongst the 10 AML cell lines analysed. HEL, OCI-AML2 and U937 produced the least amount of ROS. KG-1, PLB985, THP-1 produced ROS levels around the median. Overall, the 10 AML cell lines analysed produced variable levels of superoxide, which might relate to

different molecular abnormalities, or expression of key related proteins or pathways (1.3.4).

4.3 PFKFB3 expression in cell lines by western blot

The above data analysed NOX2 derived ROS from AML cell lines. In order to correlate ROS production with PFKFB3 expression, western blotting was performed on the same lines analysed above.

I first optimised several conditions of the western blot assay for PFKFB3 protein expression including the use of Beta-Actin antibody as an internal reference protein. I tested the optimal clone for PFKFB3 detection; I used MV4;11 cell line as a low expressing control as it has previously been reported to have low or undetectable levels of PFKFB3 by western blot (Robinson *et al.* 2020). I used a MV4;11 PFKFB3 Knock In (KI) cell line as a positive control.

Initially I focussed on beta actin. As shown in Figure 4-2, a dilution of 1/10,000 was optimal for detection of actin as this gave a strong signal to background noise at a dilution that was cost effective. Secondly, I focussed on optimising PFKFB3 detection by western blot. As shown in Figure 4-3, the clone purchased from Abcam (Ab181861 rabbit monoclonal antibody), had good specificity with the highest signal to noise ratio. The remaining antibody clones tested showed several nonspecific bands. The optimal dilution for Abcam PFKFB3 antibody was 1/2000 (Figure 4-4). Similar data is also shown in Mv4;11 cells where PFKFB3 was over-expressed (PFKFB3 positive control) (Figure 4-5).

Overall, these data show that Abcam PFKFB3 antibody at 1/2000 dilution was specific and optimal for target protein detection. A 1/10,000 dilution was used for beta-actin for internal reference protein. To detect the PFKFB3 protein in different AML cell lines, I

performed SDS PAGE coupled with the optimised condition for western blot as above. As show in Figure 4-6, the immunoblot shows variable levels of PFKFB3 protein expression in a panel of AML cell lines. PFKFB3 was the most expressed in NOMO-1, followed by OCI-AML5, SKNO1 and THP-1, and U937 the least.

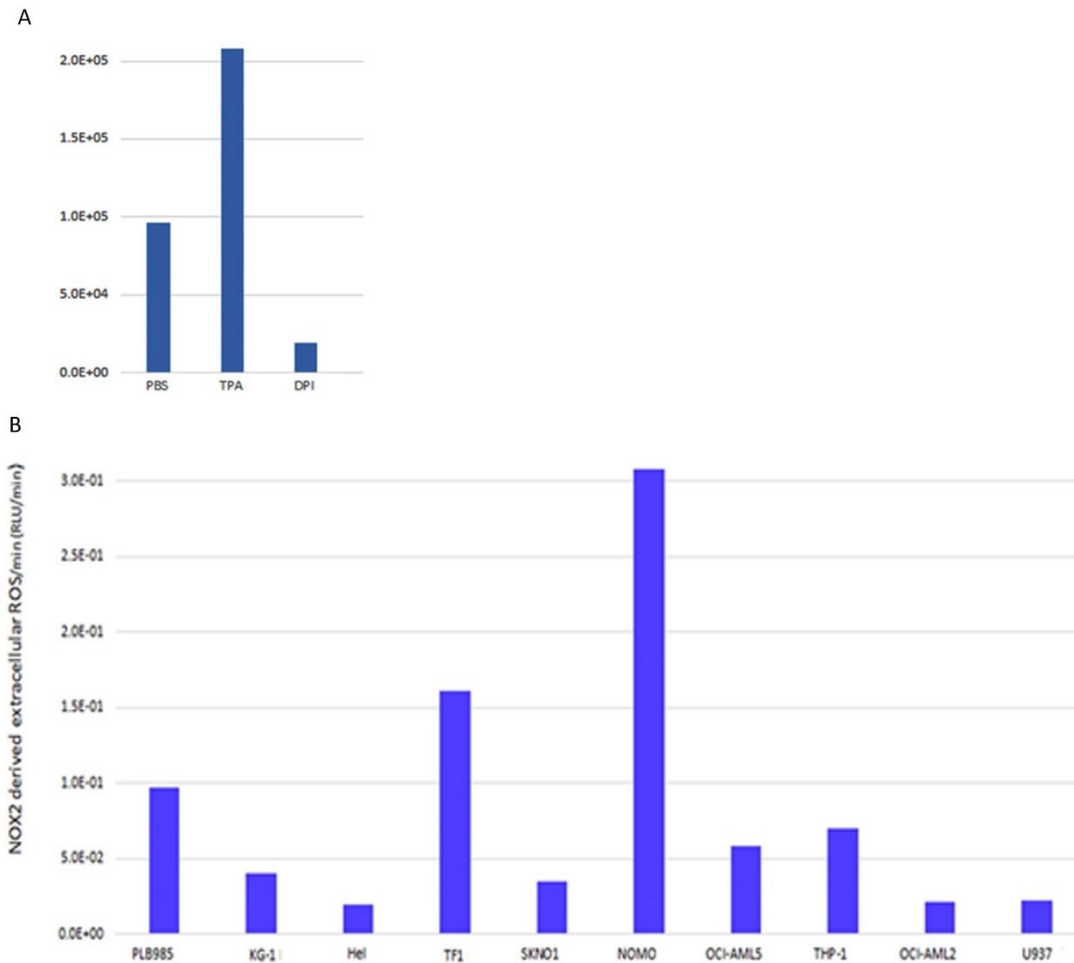


Figure 4-1 Extracellular superoxide production in AML cell lines

A: Extracellular superoxide production in Nomo cells. ROS production (initial rate in relative luminescent units/min (RLU/min)) was measured in NOMO-1 cells using Diogenes. PBS (No treatment group), TPA (NOX2 agonist group), DPI (NOX2 inhibitor group) were used to determine NOX2-derived ROS production. Samples were analysed with three technical replicates. However, the experiment was performed once (n=1). B: Peak ROS production (relative luminescent units /min (RLU/min)) was measured in AML cell lines using Diogenes. DPI (NOX-2 inhibitor) was used to determine NOX-2 specific derived ROS production (details in 2.2). Samples were analysed with three technical replicates. The experiment was performed once (n=1).

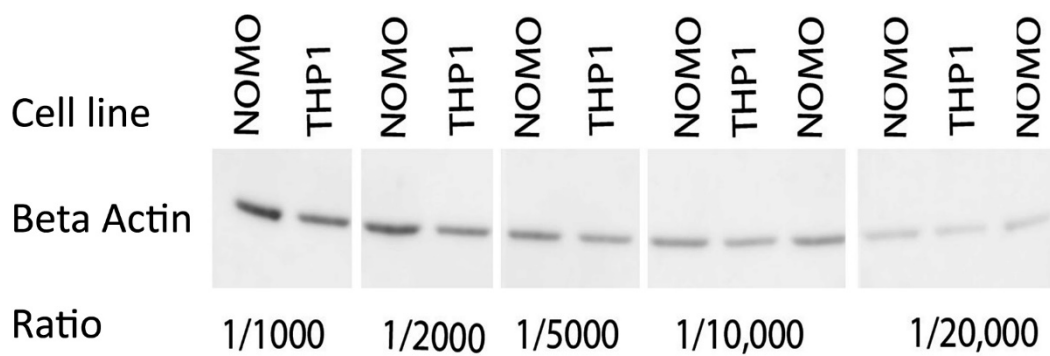


Figure 4-2 Optimisation of the best beta-actin detecting dilution by western blot

Immunoblot showing optimisation of beta-actin primary antibody dilutions in NOMO-1 and THP1 AML cell lines. 10 μ g of protein was loaded into each well. Beta-actin monoclonal antibody 5-15739-D680 dilutions of 1/1000; 1/2000; 1/10,000; 1/20,00 were assayed as indicated. The molecular mass of beta actin is 42 KDa. n=1.

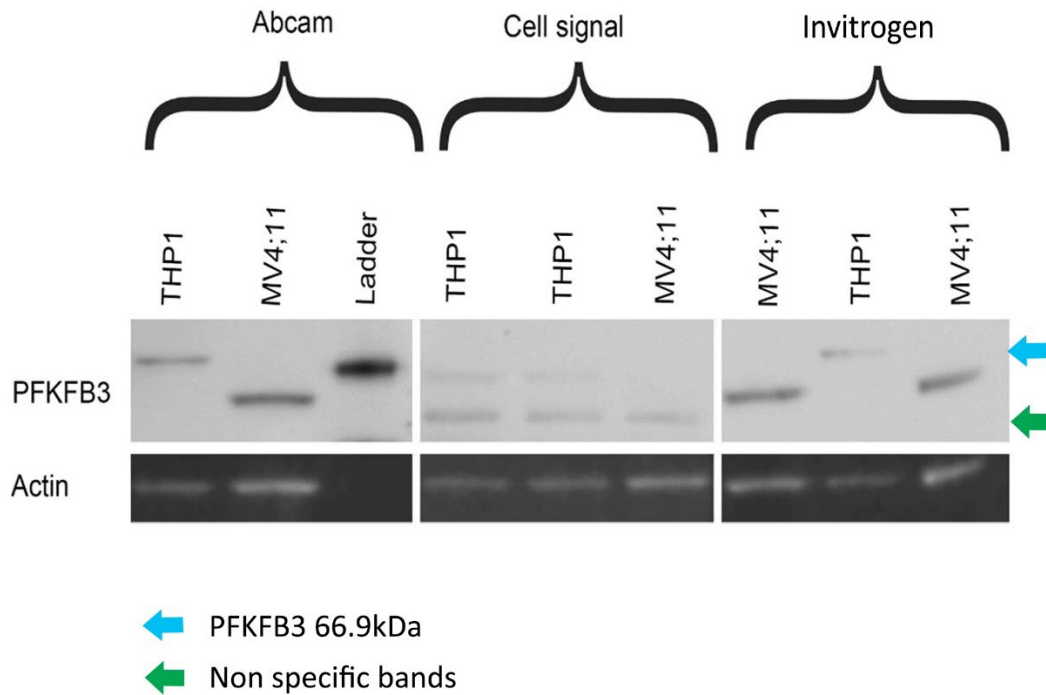


Figure 4-3 Determination of optimal clone of antibody to detect PFKFB3 by western blot

Immunoblot showing optimised clone of antibody to use to detect PFKFB3. Clones were obtained from Abcam (Ab181861 rabbit monoclonal antibody), Cell Signaling (D7H4Q; rabbit monoclonal antibody), Invitrogen (5-35419; rabbit monoclonal antibody). PFKFB3 molecular mass is 66.9 KDa (Blue arrow) Actin (monoclonal antibody 5-15739-D680) as loading control. Antibodies were used at 1/1000 dilution as recommended by supplier (2.1). Green arrows indicate non-specific bands. n=1.

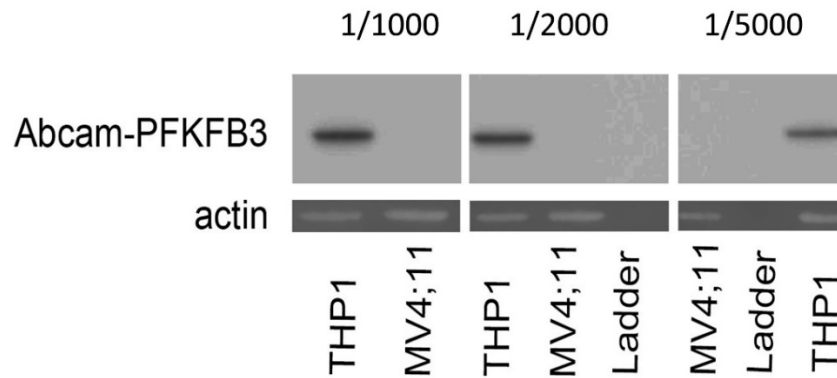


Figure 4-4 Determination of optimal Abcam PFKFB3 antibody dilution in THP1 cells

Immunoblot showing detection of PFKFB3 using Abcam's anti-PFKFB3 antibody (Ab181861 rabbit monoclonal antibody) at different dilutions: 1/1000; 1/2000; 1/5000. THP1 is the positive control. MV4;11 is the negative control cell line sample (Robinson et al. 2020). Actin (monoclonal antibody 5-15739-D680) used as a loading control. THP1 is known to have higher levels of PFKFB3. PFKFB3 molecular mass is 66.9 KDa. Ladder is Magic Mark GSEA. n=1.

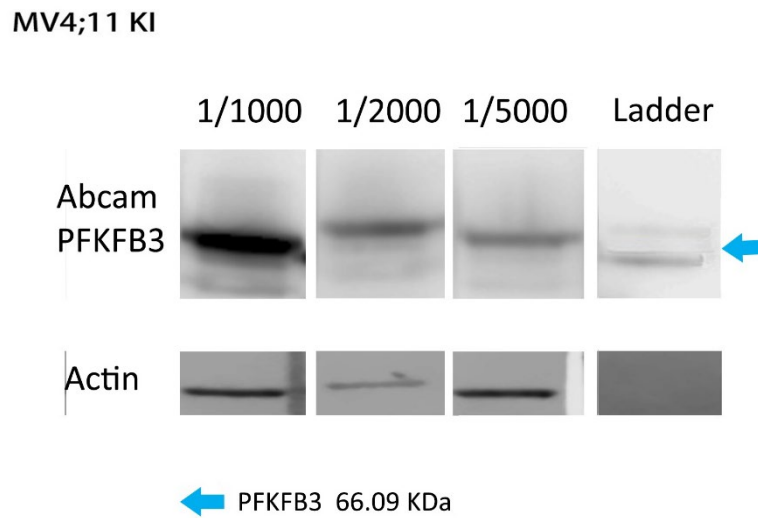


Figure 4-5 Determination of optimal Abcam PFKFB3 antibody dilution in M4v;11 PFKFB3 Knock In cells over expressing PFKFB3

Immunoblot showing PFKFB3 detection using Abcam anti-PFKFB3 antibody (Ab181861 Rabbit Monoclonal antibody) and different dilutions using Mv4;11(KI)-PFKFB3 cells transduced with PFKFB3 over-expressing vector. MV4;11(KI)-PFKFB3 cell line was kindly provided by Dr Robinson (Cardiff University), (Robinson et al. 2020). Actin (monoclonal antibody 5-15739-D680) was used as a loading control. Each lane was loaded with 10 μ g protein lysate. PFKFB3 molecular mass is 66.9 KDa. (Blue arrow pointed to it). Data shown is n=1.

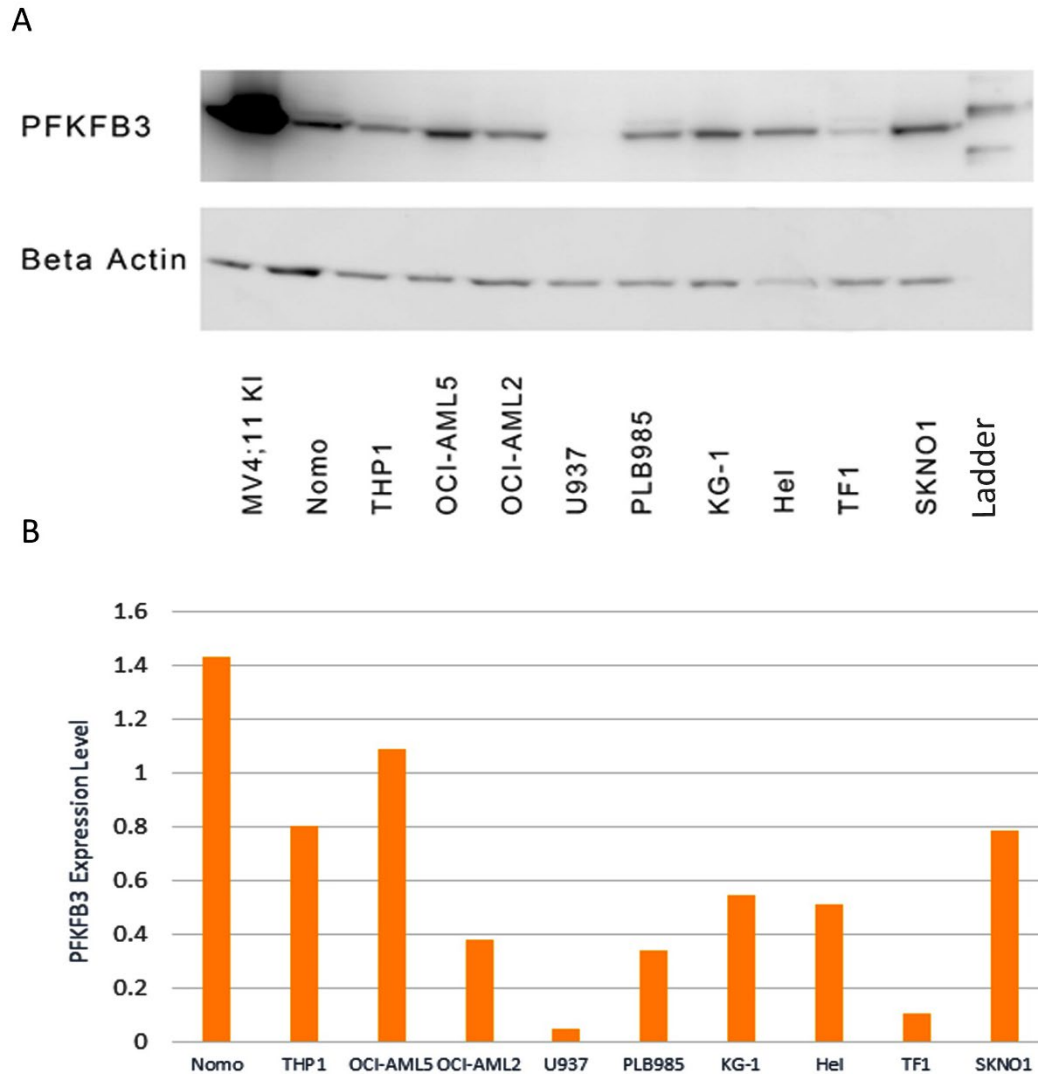


Figure 4-6 PFKFB3 expression in AML cell lines detected by Western Blot

- A. Immunoblot showing PFKFB3 protein expression in 10 AML cell lines in which total protein was extracted from the cells. MV4;11-PFKFB3- over expressing cells were used as a positive control and kindly provided by Dr Robinson (Cardiff University). Actin was used as the internal reference protein to control for loading.
- B. Bar chart showing densitometry analysis of PFKFB3 expression level across the cell lines semi-quantified by ImageJ. PFKFB3 expression were determined by normalising each sample to actin. (n=1).

4.4 PFKFB3 protein expression correlates with ROS production in AML cell lines

To investigate the relationship between NOX derived ROS and PFKFB3 protein expression, I correlated the levels of PFKFB3 protein expression (Figure 4-7) with ROS production (4.2.1). As shown in Figure 4-7, a significant positive correlation was observed. Overall, this suggests that PFKFB3 expression is positively associated with production of ROS. However, this association is likely driven by the high levels of ROS/PFKFB3 in NOMO-1 cells. To further investigate this association, I will also verify the expression level of PFKFB3 in single cells using flow cytometry in the next section.

4.5 Development of an assay to measure intracellular PFKFB3 protein expression by flow cytometry

Given that AML blasts samples can be composed of heterogenous populations and or be limited in available material to derived protein extracts, I developed a single cell flow cytometric assay to measure PFKFB3 protein expression.

4.5.1 Development of a positive control for intracellular PFKFB3 protein expression

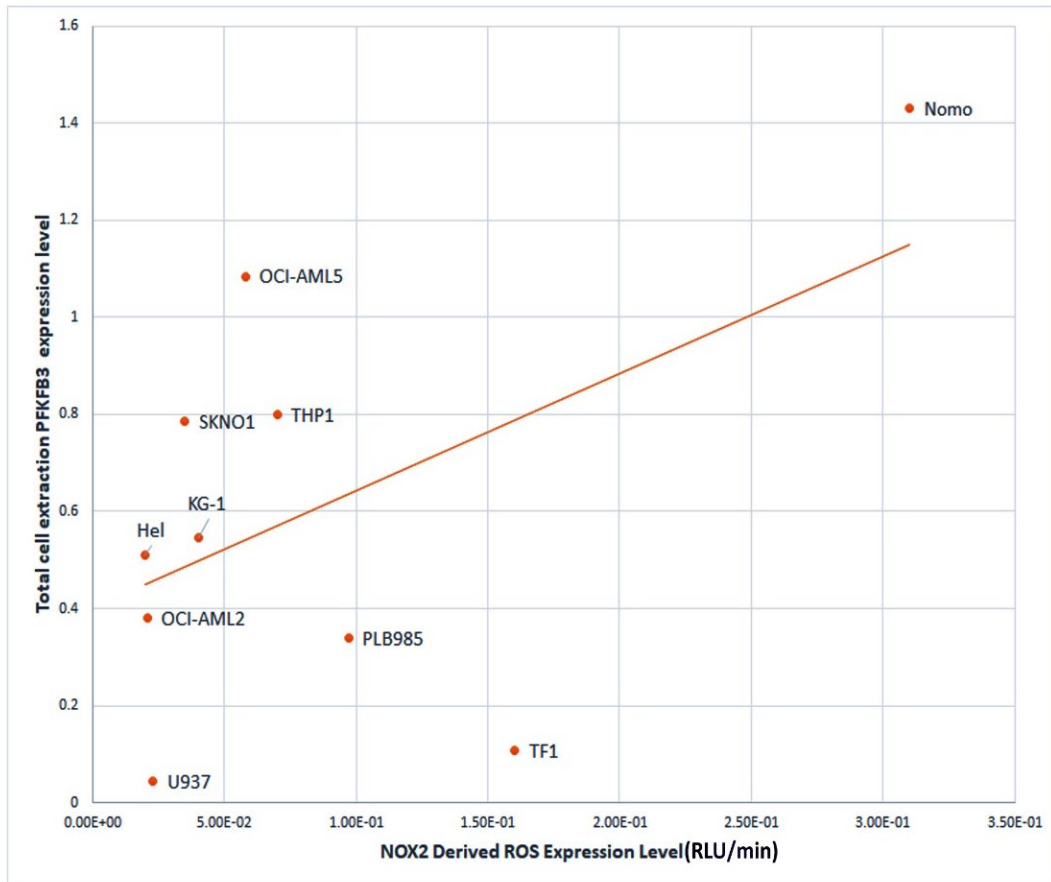
Initially, I used MV4;11 KI(PFKFB3) cells in which PFKFB3 was ectopically expressed (a positive control) to optimise the technique. As shown in Figure 4-8, MV4;11 PFKFB3 was detectable by flow cytometry. This demonstrates that this approach may be used to detect intracellular PFKFB3.

4.5.2 Intracellular PFKFB3 protein expression in AML cell lines

I next assayed intracellular PFKFB3 protein expression in 10 AML cell lines (analysed above). As shown in Figure 4-9, the expression of PFKFB3 determined by flow cytometry for each cell line was not variable which is in contrast to western blotting (Figure 4-6). To support this, I compared intracellular PFKFB3 expression by flow cytometry with total extracts analysed by western blotting. As shown in Figure 4-10, no correlation was observed. This data suggests that the flow cytometry assay may not be optimal using the current methodology. I hypothesized whether the permeabilization of the nuclear membrane was sub-optimal and therefore flow cytometry was under estimating PFKFB3 expression, though the technical replicates showed considerable variability for some cell lines (CV >10%; data not shown) making definitive conclusions difficult. Further development of the assay is required for consistent valid data (4.3.4).

4.5.3 PFKFB3 is mainly expressed in the nucleus in some cell lines which affected the result of intracellular staining assay

Given that not all PFKFB3 maybe detected by flow cytometry (ie. underestimating nuclear PFKFB3 expression), I next analysed PFKFB3 nuclear expression by western blot using nuclear fractions of AML cell lines. As shown in Figure 4-11, I found that PFKFB3 is expressed in the nucleus of NOMO-1 cells. Most AML lines have expression of PFKFB3 in the nucleus and this supports the hypothesis that the flow cytometry method is underestimating PFKFB3 protein expression.



Pearson Value $r=0.51$
 Pearson Value with out Nomo $r^*=-0.24$
 P Value = 0.0012

Figure 4-7 PFKFB3 protein expression (Western Blot) correlation with ROS production in AML cell lines

Correlation between PFKFB3 protein expression in 10 cell lines and ROS production. PFKFB3 expression was determined from western blot and semi-quantified by ImageJ as shown in Figure 4-6. NOX2 derived ROS was determined by peak superoxide production (relative luminescent units/min (RLU/min)) in AML cell lines by Diogenes (Figure 4-1). The Pearson correlation coefficient is recorded as r . The statistical object represented by r^* does not contain NOMO-1 data. Data shown is $n=1$. See details in 2.6.2.

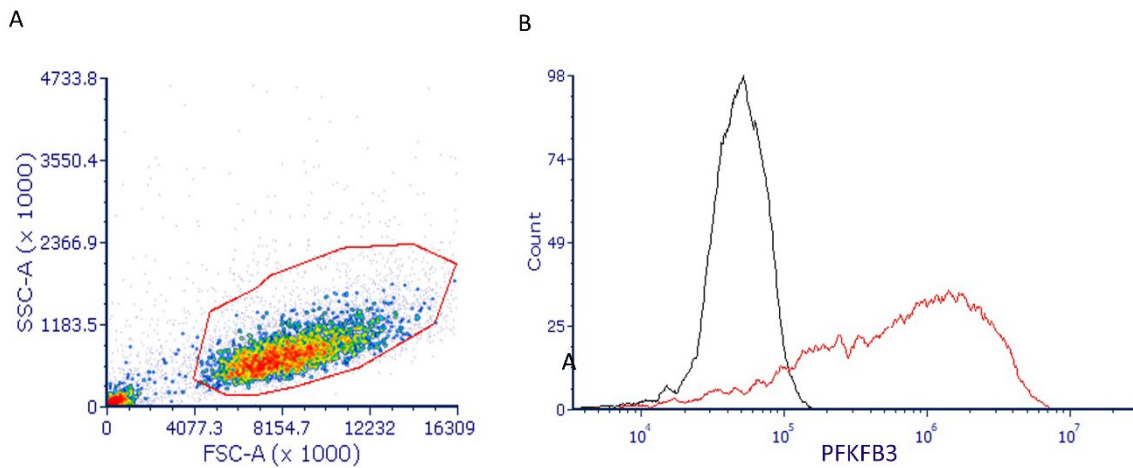


Figure 4-8 Intracellular PFKFB3 expression detected by flow cytometry using MV4;11 in which PFKFB3 was ectopically expressed

- A. Events were initially gated to exclude debris based on forward scatter (FSC) and side scatter (SSC).
- B. An example histogram plot showing PFKFB3 expression in Mv4;11 cells ectopically expressing PFKFB3. Events were gated on FSC/SSC (A). The black histogram represents IgG-APC background staining. Red histogram represents cells stained with anti-PFKFB3-APC. Rabbit polyclonal Isotype control antibody enabled an estimation of non-specific binding of rabbit polyclonal antibody. The ratio calculation consists of dividing the median of the net PFKFB3 signal by the median of the IgG signal (see 1.3.2) $n=2$.

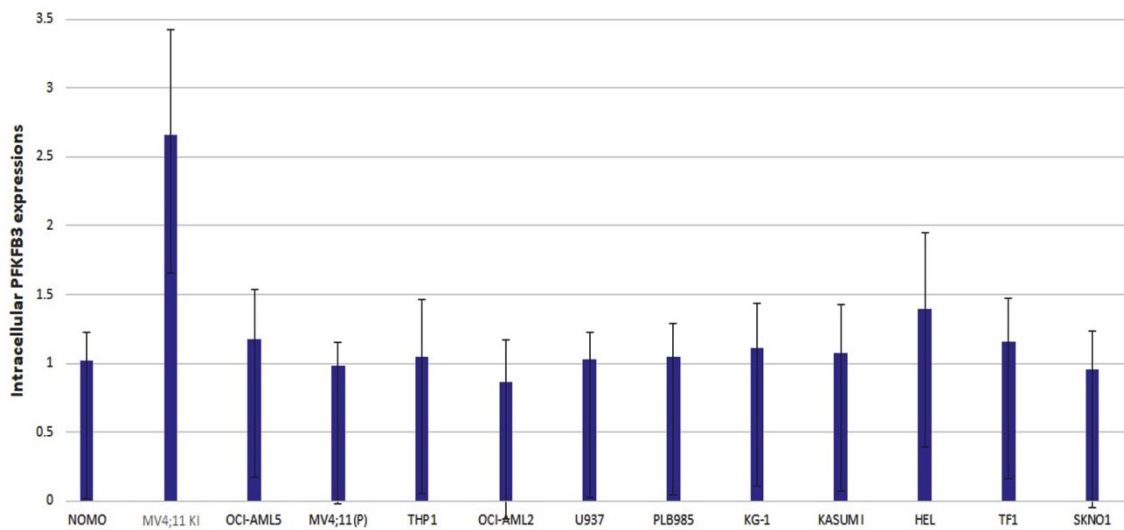
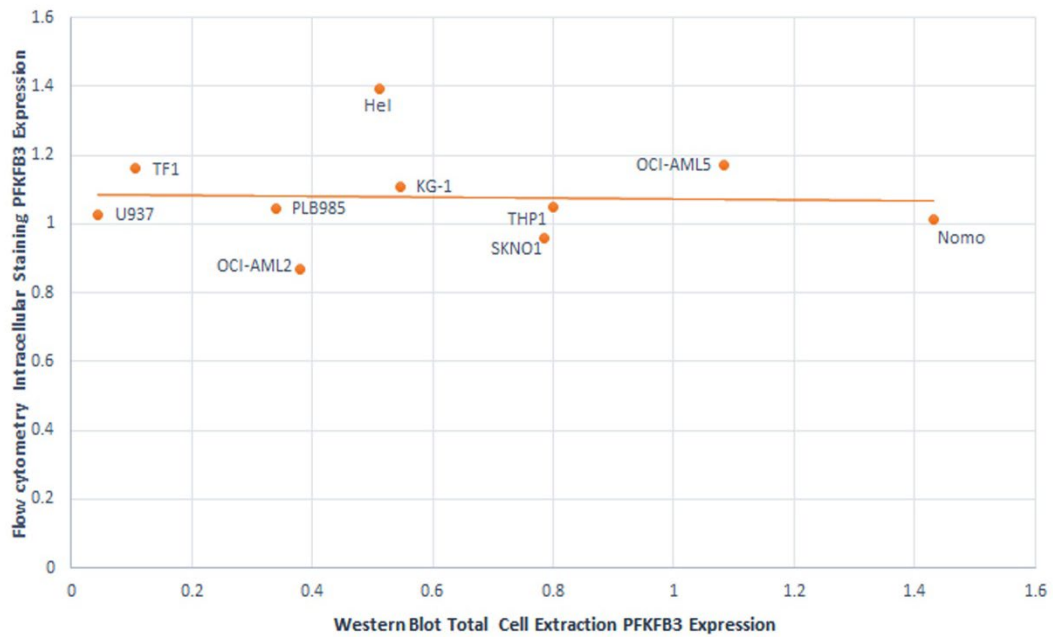


Figure 4-9 Intracellular PFKFB3 expressions detected by flow cytometry

Summary of PFKFB3 intracellular protein expression in different AML cell lines. MV4;11(P) means MV4;11 parental that have not been transduced. MV4;11 KI indicates MV4;11 with PFKFB3 over-expressed. The y-axis is a ratio of intracellular PFKFB3 median signal to background IgG median signal (see 1.3.2). Data shown includes mean + 1 SD (2.3), n=5.



Pearson Value = - 0.04

Figure 4-10 Intracellular PFKFB3 expression does not correlate with western blot total cell extraction PFKFB3 expression in AML cell lines

This plot shows the relationship between intracellular PFKFB3 expression by flow cytometry and western blot total cell extraction PFKFB3 expression in AML cell lines. The Pearson correlation coefficient is -0.04 (see 2.6)

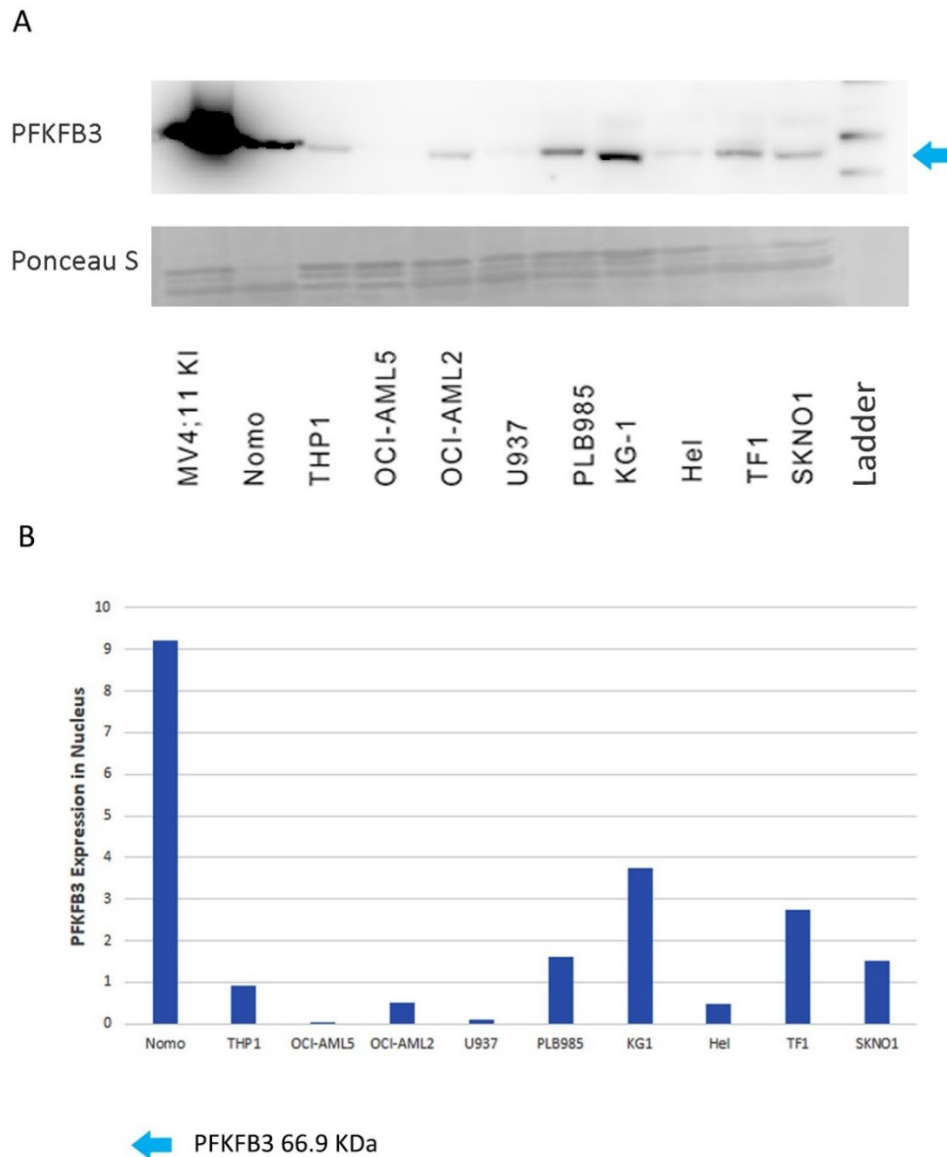


Figure 4-11 PFKFB3 expression in nucleus detected by western blot

- A. Immunoblot showing PFKFB3 protein expression in the nucleus of 10 AML cell lines (see 1.4.2). MV4;11-PFKFB3- knock in was used as a positive control and kindly provided by Dr Robinson (Cardiff University). Ponceau S stained histone banding was used as a loading control. PFKFB3 molecular mass is 66.9 KDa (blue arrow).
- B. Bar chart showing densitometry analysis of PFKFB3 expression level across nuclear AML cell lines semi-quantified by ImageJ. PFKFB3 expressions were determined by normalising each sample to total Ponceau S histone signal. (n=1).

4.6 Discussion

Recently, Robinson *et al.*, showed that changes in expression of PFKFB3 was associated with ROS production in a human HSPC model (Robinson et al. 2020). Further, my previous chapter established that *PFKFB3* mRNA expression was significantly higher in AML in which ROS production was high compared to low ROS producing AML; with the caveat that ROS production was indirectly established using *CYBB* mRNA expression. To further substantiate this data, this current chapter found that PFKFB3 protein expression also positively correlated with ROS production in AML cell lines measured by chemiluminescence. I also attempted to establish a flow cytometry assay to measure PFKFB3 protein expression in primary AML. However, due to inconsistencies in the method and the fact that PFKFB3 is also expressed in the nucleus, I was unable to validate the findings in primary AML blasts since time constraints limited further development of this assay.

ROS production was assayed using the chemiluminescent probe, Diogenes. The probe is based on luminol enhanced chemiluminescence and is specific for the measurement of superoxide (Hole et al. 2010). This assay has previously been validated to measure ROS (Hole et al. 2010; Robinson et al. 2020). I showed in this chapter that ROS was produced to varying amounts in different AML cell lines (Figure 4-1). Interestingly, NOMO-1 was the only cell line with orders of magnitude of ROS production higher than other cell lines. It is not clear why this is the case as I was unable to correlate ROS production to specific molecular abnormalities (data not shown). However, the sample size was small (n=10 AML cell lines). This is consistent with Hole et al., where in AML patient samples (n=60) no significant association was found with AML subtypes (Hole et al. 2010). Interestingly, THP-1 and NOMO-1 carry a similar mutation t(9;11) (p22;q23) and THP-1 cells do produce higher levels of ROS than many other cell lines but not to the same magnitude as NOMO-1.

Preliminary evidence by Robinson *et al*, showed that higher levels of ROS increased PFKFB3 expression using the NOMO-1 cell line (Robinson et al. 2020). To establish this in a larger AML panel of lines, I correlated ROS production with PFKFB3 expression (determined by Western Blot). The data suggested there was a positive correlation. However, this effect could be driven by the much higher levels of superoxide produced by NOMO cells compared to that of the other lines. When NOMO-1 data was removed from the analysis, no significant correlation was observed. Whilst cell lines might represent the disease of interest they don't always faithfully replicate in vivo or ex vivo primary AML (Nguyen et al. 2002). To provide evidence this was the case, I aimed to establish a similar correlation using primary AML (see below) but due to time constraints, issues with supply chain (as a result of COVID19 interruptions) and inconsistencies in measuring PFKFB3 protein expression by flow cytometry I was not able to achieve this. The positive association between PFKFB3 and ROS is potentially supported by other studies which found that the overexpression of TP53-induced glycolysis and apoptosis regulator (TIGAR) can inactivate related genes (including PFKFB3), increase GSH after PPP activation, and reduce ROS levels (Qian et al. 2016). However, the hypothesis that the PFKFB3 expression is positively associated with ROS expression in AML cell lines remains undetermined, other than NOMO-1 (Robinson et al. 2020). Interestingly, the expression of PFKFB3 is cooperatively affected by multiple regulators, such as: HIF (Feng and Wu 2017), GLUT1 (Bonello et al. 2007; Mucaj et al. 2012), DHODH (Jóźwiak et al. 2014). Therefore, it would be important to determine the relationship in cells cultured under hypoxia conditions.

The intracellular staining for PFKFB3 expression by flow cytometry had limited success. Whilst the initial assays were promising where I was able to detect expression of PFKFB3 in Mv4;11 cell lines (ectopically expressing the protein), there was considerable variations in the replication of the analysis. This could be one reason

why PFKFB3 expression by Western Blot within AML cell lines did not correlate with the flow cytometry data (Figure 4-10). The Western Blot total cell extraction data has been well established and routinely used within the lab and therefore it is likely that the flow cytometry assay needs further optimisation. For example, the reason for the inaccurate intracellular staining data maybe partly due to incomplete permeabilization since PFKFB3 is also located in nucleus where the fixative solution (methanol) is less effective. Western Blot of nuclear extractions supported the notion that significant expression of PFKFB3 is found in the nucleus of AML cell lines (Figure 4-11).

Studies of synchronized changes in the cell cycle and cancer metabolism have found that PFKFB3 periodically translocates into the nucleus where it influences cell cycle regulators (Icard et al. 2019). But after its sequential translocation in the nucleus with other metabolic enzymes (PKM2, PFKFB3, ALDO, GAPDH) creates a vicious circle linking metabolism and cell cycle regulators to cancer genes (K-ras and c-Myc)(Icard et al. 2019). PFKFB3-mediated cell cycle activity provides cancer cells with a parallel mode of proliferation. Continued glycolysis can lead to NADPH deficiency allowing excess ROS production, resulting in cell cycle arrest (Yamamoto et al. 2014). In a highly competitive environment where both cancer cells and healthy cells require nutrients, PFKFB3, which is highly expressed in cancer cells and can help cancer cells gain a proliferative advantage (Yamamoto et al. 2014). High nuclear expression of PFKFB3 in hepatoma cells was also shown to be required for DNA repair mediated by AKT (Shi et al. 2018). PFKFB3 has also been identified as a key factor aiding in the repair of broken DNA by homologous recombination (Gustafsson et al. 2018). PFKFB3 has been reported to share the same localization with ionizing radiation-induced nucleus foci (with DNA damage) and homologous recombination repair proteins. Inhibition of PFKFB3 affects the recruitment of ribonucleotide reductase M2 and deoxynucleotides during homology repair (Gustafsson et al. 2018). PFKFB3 has a nuclear localization signal at residues 472-475 that directs it to shuttle from the

cytoplasm to the nucleus (Yalcin et al. 2009). Nucleus PFKFB3 then allows cell cycle-dependent kinase 1 to amplify and downregulate the cell cycle inhibitor p27. This action affects cell cycle progression by increasing cell proliferation (Yalcin et al. 2009). However, lysine acetylation regulated by the acetyltransferases GCN5 and PCAF and the deacetylase SIRT1 is an important mechanism that hinders the translocation of PFKFB3 from the cytoplasm into the nucleus (Li et al. 2018a). Acetylation of PFKFB3 results in its retention in the cytoplasm, which favours its phosphorylation and activation of AMPK. The mechanism of PCAF and DNA damage or combined GCN5 activation remains to be explored (Li et al. 2018a).

As a key enzyme in glycolysis, PFKFB3 plays a major role in malignant proliferation, vascularization, and migration in cancer (Gu et al. 2017; Li et al. 2020c). For example, in human adenocarcinoma tissues, the expression of PFKFB3 correlates with its clinical characteristics and overall survival and is identified as a regulatory element of lung adenocarcinoma (Li et al. 2018b). Targeting PFKFB3 may be a tractable strategy given that some AML cells have higher levels of PFKFB3. There are some examples of small peptide PFKFB3 inhibitors in development (Macut et al. 2019; Jones et al. 2022). A series of small peptides that act by allosterically activating its bisphosphate activity have been proposed as novel indirect inhibitors of PFKFB3 (Macut et al. 2019). These peptides reduce the overall glycolytic function of cancer cells by driving the kinase vs phosphatase activity ratio of PFKFB3 in the opposite direction (reviewed in (Jones et al. 2022)). However, these increases may not be enough to overcome the very high kinase activity of PFKFB3 to affect cancer cell proliferation (Macut et al. 2019). This feature could be used to overcome the uncertainty caused by multiple regulatory factors and flexibly regulate the ratio of PFKFB3 kinase/phosphatase by changing the dose according to the experimental requirements.

In summary, PFKFB3 is positively correlated with ROS expression, which is consistent with the mRNA results in Chapter 3 (Figure 3-9), although the conclusion is provisional

given the low number of experimental replicates. NOMO-1 and THP-1 carrying the same mutation did generate higher ROS than the other cell lines. The intracellular staining for PFKFB3 expression by flow cytometry had limited success, although it was able to detect PFKFB3 in the overexpression control. I also found that PFKFB3 might mainly expressed in the nucleus in AML cell lines, but yet to confirm.

Chapter 5 General Discussion

There are many sources of ROS including peroxisomal enzymes, lipoxygenase enzymes, and through mitochondrial respiration as part of the ETC. Importantly, ROS is also produced via NOX enzymes which can have different sub-cellular locations and include NOX2 (a plasma membrane bound form) (1.4), such as: sub-membranous phagosomes in neutrophils, and in caveolae on the leading edge of lamellipodia in endothelial cells and endosomes (Brown and Griending 2009). In the ETC, the primary cause of ROS production is the premature leakage of electrons from complexes I, II and III to mediate the one-electron reduction of oxygen to superoxide, which can then dismutate to H₂O₂ (Nolfi-Donagan et al. 2020). NOXs transfer electrons from NADPH in the cytoplasmic matrix to extracellular oxygen to generate superoxide which again dismutate to H₂O₂ through SOD (1.4). The purpose of the NOX2 enzyme as traditionally been thought of as a host defence mechanism. ROS is released within the phagolysosome to help fight infection. (Bosgra et al. 2005).

Redox homeostasis is the result of a tightly regulated balance between ROS production and detoxification and alterations in either part of this process has been established in AML. Excessive production of NOX-derived ROS can promote proliferation of AML and is associated with decreased glutathione antioxidant level (Hole et al. 2013). Overproduction of ROS is often activated by oncogenes which are expressed in various malignant tissues (An et al. 2019). For example, activated Ras strongly upregulates superoxide and H₂O₂ production by stimulating NOX activity (Hole et al. 2010). Hole *et al.*, showed in normal human CD34⁺ haematopoietic progenitor cells, in the presence of RAS oncogene activation, that excessive ROS production promoted the proliferative response of these cells (Hole et al. 2010). Interestingly, a recent report found that although *CYBB* (NOX2) knockdown blocked

the induced NOX2 activity, it did not affect the proliferation and differentiation of THP-1 cells (Dakik et al. 2021). This found that NOX2 requires exogenous PMA stimulation to help the THP1 cell line to proliferate (Dakik et al. 2021). Supporting the studies by Hole, Dakik *et al*, found that *CYBB* Knock down in primary AML cells resulted in slower proliferation with induced differentiation *in vitro* and reduced leukaemia burden after xenografting *in vivo* (Dakik et al. 2021). It may be that different experimental methods lead to opposite result to Robison *et,al*. found that NOX-ROS help AML proliferation (Robinson et al. 2020); Temperature might be one of variables, Dakik *et al* measured the NOX activity every minute for 2 h at 25 °C using a luminescence ClarioStar microplate reader as opposed to studies by Hole et al that assayed ROS over 3h at 37 °C.

Robinson *et al*, also showed that extracellular derived ROS, drives proliferation in AML via changes in carbohydrate metabolism, albeit using a limited pair of cell lines (one cell line capable of ROS production (THP1) vs one cell line (Mv;411) with no significant detection of extracellular ROS). These model systems showed that culture of low ROS producing cells with ROS (in the form of GOX) increased glucose uptake. In contrast, NOX inhibition or KD reduced glucose uptake (Robinson et al. 2020). Preliminary data suggested that expression of the glycolytic regulator, PFKFB3, was increased in response to ROS in THP1 cells. Supporting this data, Robinson *et al.*, found that NOX2 expression is higher in AML patient blasts which produce extracellular ROS production and that PFKFB3 expression correlated with NOX2 expression (Robinson et al. 2020). PFKFB3 is frequently associated with oncogenic activating mutations where it promotes proliferation. It is commonly defined in many 'cancer signatures' and linkage marker studies such as pancreatic (Ozcan et al. 2021) and lung cancers (Li et al. 2018b). PFKFB3 inhibition combined with chemotherapy or targeted therapy may enhance the therapeutic effect in different types of cancer by targeting the cell's

metabolism (Wang et al. 2020). Therefore, targeting PFKFB3 is becoming important in anticancer therapeutic strategy in these cancers, which might include AML.

ROS has also previously been shown to drive proliferation by activating the PI3K/AKT/mTOR and MAPK mitogenic signalling cascades. For example, oxidation of PTEN and PTP1B impairs their inhibition of PI3K and leads to hyperactivation of AKT and mTOR (Lee et al. 2002; Barford et al. 2003; Satooka and Hara-Chikuma 2016); ROS can activate Apoptosis signal-regulating kinase 1, protein kinase GFF and c-Jun NH-terminal kinases which further stimulates the downstream mitogen-activated protein kinase mitotic cascades (Liu et al. 2000; Kamata et al. 2005; Frigolet et al. 2017). Metabolic changes in cancer and LSC in response to ROS are well described and introduced in detail in 1.2.3.

Given the above observations, the association of PFKFB3 expression in AML cells required further substantiation in a larger panel of AML cell lines and AML primary blasts. In addition, little is known regarding the expression of PFKFB family members in normal haematopoietic development and AML. I therefore initially analysed the mRNA expression of the *PFKFB* family (*PFKFB1*, *2*, *3* and *4*) in AML and normal haematopoiesis (Chapter 3). Interestingly, only *PFKFB3* and *PFKFB4* mRNA expression was upregulated during normal haematopoiesis. Only *PFKFB3* mRNA expression significantly changed in AML compared to normal HSC. Interestingly, solid tumour studies have showed increases in glycolysis to be associated with poorer prognosis in lung cancers (Giatromanolaki et al. 2017). However, I did not find an association of higher PFKFB3 expression with overall survival in AML. Glycolytic enzymes are also dysregulated in many solid tumours compared to healthy tissue (El Hassouni et al. 2020; Alharbi et al. 2021; Curcio et al. 2021). Higher expression of PFKFB3 has been detected in prostate cancer, ovarian cancer and thyroid cancer (Atsumi et al. 2002). Altering glycolysis not only provides energy to cancer cells, but also produces metabolic intermediates necessary for malignant cell proliferation,

which are achieved by promoting macromolecular synthesis during metabolism (1.5). Multiple cancer stem cells rely on the glycolytic pathway rather than oxidative phosphorylation (Pacini and Borziani 2014; Shi et al. 2017). For example, breast cancer stem cells expressed higher levels of PFKFB3 and PFK1 compared to induced pluripotent stem cells or normal cells, which potentially indicated that PFKFB3 activity is different in the cancer stem cells (Cieślak-Pobuda et al. 2015).

Given the importance of PFKFB3 in normal haematopoiesis and AML, the next chapter (Chapter 4) focussed on this family member and protein expression by western blot in a larger panel of AML cell lines. PFKFB3 was most expressed in NOMO-1 cells, followed by OCI-AML5, SKNO1 and THP-1, with U937 having the lowest expression. In this study, NOX-derived ROS positively correlated with PFKFB3 expression in AML cell lines (Figure 4-7). However, this effect could be driven by the much higher levels of ROS generated by NOMO-1 cells compared to that of the other lines. No significant correlation was observed when NOMO-1 data was removed from the analysis. This might be that cell lines don't always represent faithfully replicate *in vivo* or *ex vivo* primary AML (Nguyen et al. 2002). To provide evidence, I aimed to establish a similar correlation using primary AML but due to time constraints, issues with supply chain (as a result of COVID19 interruptions) and inconsistencies in measuring PFKFB3 protein expression by flow cytometry I was not able to achieve this. The flow cytometry assay which would have been used to measure PFKFB3 protein expression in primary AML can detect clear fluorescence signals in AML cell lines, but the results of each replicate experiment have a large variance. This might be due to inconsistencies in the method and the fact that PFKFB3 is also expressed in the nucleus. The model was not very successful in this experiment, and I discuss the improvements in detail in 4.3.4

5.1 Future directions

Testing inhibitors of PFKFB3 was always an aim of this thesis, but it was not carried out due to lack of time. Robinson *et al.* have tested PFK158 (a PFKFB3 inhibitor) alone in a single AML cell line (THP1), but found no alternation in glucose uptake (Robinson *et al.* 2020). However, PFK158 combined treatment strategies have been shown to be effective in solid cancers. PFK158 showed antiproliferative activity in combination with the EGFR-targeting drug erlotinib in non-small cell lung cancer cells (Li *et al.* 2018b). PFK158 induced apoptosis (Imbert-Fernandez *et al.* 2014) in combination with Faslodex® (an antioestrogen) or paclitaxel in breast cancer cells (Doménech *et al.* 2015). A synergistic effect from chemotherapy combined with a PFKFB3 inhibitory drug was also shown in endometrial and ovarian cancers (Mondal *et al.* 2019; Xiao *et al.* 2021). These data suggest that PFK158 should be tested in primary AML possibly in combination with chemotherapeutic drugs.

In addition, it will be important to test other inhibitors, perhaps combining PFKFB3 inhibition with the mTOR inhibitor rapamycin which may give synergistic antiproliferative effects in AML cells (Feng and Wu 2017). AstraZeneca and CRT Discovery Laboratories tested multiple inhibitors of PFKFB3 and showed that AZ67 (which crystal structure analysis shows to bind to the catalytic pocket of PFKFB3) reduces proliferation and glucose uptake in MDA-MB-231 breast cancer cells, and alleviates symptoms in mice with blood reperfusion injury (Boyd *et al.* 2015). Testing this agent in ROS producing cells would be interesting and informative given its improved specificity over currently available inhibitors. A potential risk for using PFKFB3 inhibitors involves off-target effects involving cross-reaction with other PFKFB isoforms, which has been reported in studies of PFKFB3 inhibitor 3PO compounds (Emini Veseli *et al.* 2020). In addition to using inhibitors, using activators is one way to differentiate PFKFB⁺ cancer cells from healthy cells in the therapy. In

other diseases treatment, a powerful activator iPFK-2/PFKFB3 causes strong PFKFB3 protein phosphorylation in adipocytes (Atsumi et al. 2005) and PFKFB3 activator upregulates amyloid accumulation and astrocytes cytotoxicity (Atsumi et al. 2005; Fu et al. 2015) that rely on large amounts of glycolysis to maintain body health and interact with neurons in the brain.

Flow cytometry for single cell detection of PFKFB3 did not perform reliably (Figure 4-9, 4-10). There are many potential reasons: (1) possibly the methanol step cannot effectively permeabilise the inner nuclear membranes to allow antibodies to enter to bind PFKFB3 in the nucleus; (2) unstable experimental factors caused by procedures, reagents and antibodies, such as manual mediation of tubes results in different degrees of mixing and potentially different room temperatures. Alternatively, single cell westerns is a potential method for more accurate detection of target proteins (Hughes et al. 2014). Single cell westerns lysed single cells in situ in microwells, performed gel electrophoresis on microscope slides in 30 µm thick light-sensitive polyacrylamide gels, and light-induced blotting (Hughes et al. 2014). The advantages of this method are: support for low starting cell numbers when integrated with BD FACS Software; single-cell analysis of target protein seats up to 11; reduced dependence on the quality of antibody probes to avoid cross-reactions; Cell behaviour is masked by complex population characteristics; the scalable open microwell array architecture allows for the simultaneous detection of approximately 2,000 cells within 4 hours, which is beneficial when the target protein is in the nucleus and patient samples are few (Hughes et al. 2014). Notably, single cell westerns could identify two putative nesting isoforms and report the structure (Cohen et al. 2009). This might be a potential tool to identify the PFKFB3 kinase/enzyme (1.5.3). But whether this method can be used on blood cells remains to be verified, because the test of this experimental method was done with neural stem cells.

5.2 Conclusion

In conclusion, the expression of *PFKFB1-4* was established during normal haematopoiesis. Expression of *PFKFB 1,2,4* was not significantly changed in AML. On the other hand, *PFKFB3* mRNA expression was upregulated in AML with complex cytogenetics compared to normal hematopoietic stem cells. I demonstrated by western blotting that NOX-derived ROS positively correlated with PFKFB3 protein expression in AML cell lines. This study shows that PFKFB3 expression is altered in larger set of AML cell lines, and further studies are needed to determine whether PFKFB3 may represent a potential target for AML therapy.

References

Abdel-Wahab, A. F., Mahmoud, W. and Al-Harizy, R. M. 2019. Targeting glucose metabolism to suppress cancer progression: prospective of anti-glycolytic cancer therapy. *Pharmacological research* 150, p. 104511. doi: 10.1016/j.phrs.2019.104511

Alharbi, M. et al. 2021. Extracellular vesicle transmission of chemoresistance to ovarian cancer cells is associated with hypoxia-induced expression of glycolytic pathway proteins, and prediction of epithelial ovarian cancer disease recurrence. *Cancers* 13(14), p. 3388. doi: 10.3390/cancers13143388

Alter, B. P., Rosenberg, P. S., Giri, N., Baerlocher, G. M., Lansdorp, P. M. and Savage, S. A. 2012. Telomere length is associated with disease severity and declines with age in dyskeratosis congenita. *Haematologica (Roma)* 97(3), pp. 353-359. doi: 10.3324/haematol.2011.055269

An, A. R. et al. 2019. Association between Expression of 8-OHdG and Cigarette Smoking in Non-small Cell Lung Cancer. *Journal of pathology and translational medicine* 53(4), pp. 217-224. doi: 10.4132/jptm.2019.02.20

Arber, D. A. et al. 2016. The 2016 revision to the World Health Organization classification of myeloid neoplasms and acute leukemia. *Blood* 127(20), pp. 2391-2405. doi: 10.1182/blood-2016-03-643544

Atsumi, T. et al. 2002. High expression of inducible 6-phosphofructo-2-kinase/fructose-2,6-bisphosphatase (iPFK-2; PFKFB3) in human cancers. *Cancer research (Chicago, Ill.)* 62(20), pp. 5881-5887.

Atsumi, T. et al. 2005. Expression of Inducible 6-Phosphofructo-2-Kinase/Fructose-2,6-Bisphosphatase/PFKFB3 Isoforms in Adipocytes and Their Potential Role in Glycolytic Regulation. *Diabetes (New York, N.Y.)* 54(12), pp. 3349-3357. doi: 10.2337/diabetes.54.12.3349

Augsburger, F., Filippova, A. and Jaquet, V. 2019. Methods for Detection of NOX-Derived Superoxide Radical Anion and Hydrogen Peroxide in Cells. *Methods in molecular biology (Clifton, N.J.)* 1982, pp. 233-241. doi: 10.1007/978-1-4939-9424-3_13

Bagger, F. O. et al. 2016. BloodSpot: A database of gene expression profiles and transcriptional programs for healthy and malignant haematopoiesis. *Nucleic acids research* 44(1), pp. D917-D924. doi: 10.1093/nar/gkv1101

Baker, D. J. et al. 2016. Naturally occurring p16Ink4a-positive cells shorten healthy lifespan. *Nature (London)* 530(7589), pp. 184-189. doi: 10.1038/nature16932

Balmer, G. M. and Riley, P. R. 2012. Harnessing the Potential of Adult Cardiac Stem Cells: Lessons from Haematopoiesis, the Embryo and the Niche. *Journal of cardiovascular translational research* 5(5), pp. 631-640. doi: 10.1007/s12265-012-9386-3

Bancirova, M. and Lasovský, J. 2011. The photodynamic effect: the comparison of chemiexcitation by luminol and phthalhydrazide. *Luminescence (Chichester, England)* 26(6), pp. 410-415. doi: 10.1002/bio.1245

Barford, D., Salmeen, A., Andersen, J. N., Myers, M. P., Meng, T.-C., Hinks, J. A. and Tonks, N. K. 2003. Redox regulation of protein tyrosine phosphatase 1B involves a sulphenyl-amide intermediate. *Nature (London)* 423(6941), pp. 769-773. doi: 10.1038/nature01680

Bartosz, G. 2006. Use of spectroscopic probes for detection of reactive oxygen species. *Clinica chimica acta* 368(1), pp. 53-76. doi: 10.1016/j.cca.2005.12.039

Begicevic, R.-R. and Falasca, M. 2017. ABC transporters in cancer stem cells: Beyond chemoresistance. *International journal of molecular sciences* 18(11), p. 2362. doi: 10.3390/ijms18112362

Belambri, S. A., Rolas, L., Raad, H., Hurtado-Nedelec, M., Dang, P. M. C. and El-Benna, J. 2018. NADPH oxidase activation in neutrophils: Role of the phosphorylation of its subunits. *European journal of clinical investigation* 48(S2), pp. e12951-n/a. doi: 10.1111/eci.12951

Belisario, D. C., Kopecka, J., Pasino, M., Akman, M., De Smaele, E., Donadelli, M. and Riganti, C. 2020. Hypoxia Dictates Metabolic Rewiring of Tumors: Implications for Chemoresistance. *Cells (Basel, Switzerland)* 9(12), p. 2598. doi: 10.3390/cells9122598

Bennett, J. M., Catovsky, D., Daniel, M. T., Flandrin, G., Galton, D. A. G., Gralnick, H. R. and Sultan, C. 1976. Proposals for the Classification of the Acute Leukaemias French-American-British (FAB) Co-operative Group. *British journal of haematology* 33(4), pp. 451-458. doi: 10.1111/j.1365-2141.1976.tb03563.x

Bessy, T., Itkin, T. and Passaro, D. 2021. Bioengineering the Bone Marrow Vascular Niche. *Frontiers in cell and developmental biology* 9, pp. 645496-645496. doi: 10.3389/fcell.2021.645496

Beyer, W. F. and Fridovich, I. 1987. Assaying for superoxide dismutase activity: Some large consequences of minor changes in conditions. *Analytical biochemistry* 161(2), pp. 559-566. doi: 10.1016/0003-2697(87)90489-1

Bienert, G. P., Schjoerring, J. K. and Jahn, T. P. 2006. Membrane transport of hydrogen peroxide. *Biochimica et biophysica acta. Biomembranes* 1758(8), pp. 994-1003. doi: 10.1016/j.bbamem.2006.02.015

Bolaños, J. P. 2013. Adapting glycolysis to cancer cell proliferation: the MAPK pathway focuses on PFKFB3. *Biochemical journal* 452(3), pp. e7-e9. doi: 10.1042/bj20130560

Bonanomi, M. et al. 2021. Transcriptomics and Metabolomics Integration Reveals Redox-Dependent Metabolic Rewiring in Breast Cancer Cells. *Cancers* 13(20), p. 5058. doi: 10.3390/cancers13205058

Bonello, S. et al. 2007. Reactive Oxygen Species Activate the HIF-1 α Promoter Via a Functional NF κ B Site. *Arteriosclerosis, thrombosis, and vascular biology* 27(4), pp. 755-761. doi: 10.1161/01.ATV.0000258979.92828.bc

Bosgra, S., Mennes, W. and Seinen, W. 2005. Proceedings in uncovering the mechanism behind peroxisome proliferator-induced hepatocarcinogenesis. *Toxicology (Amsterdam)* 206(3), pp. 309-323. doi: 10.1016/j.tox.2004.07.015

Boyd, S. et al. 2015. Structure-based design of potent and selective inhibitors of the metabolic kinase PFKFB3. *Journal of medicinal chemistry* 58(8), pp. 3611-3625. doi: 10.1021/acs.jmedchem.5b00352

Brandes, R. P. 2014. Endothelial dysfunction and hypertension. *Hypertension (Dallas, Tex. 1979)* 64(5), pp. 924-928. doi: 10.1161/hypertensionaha.114.03575

Brigelius-Flohe, R. and Flohe, L. 2017. Selenium and redox signaling. *Archives of biochemistry and biophysics* 617, pp. 48-59. doi: 10.1016/j.abb.2016.08.003

Brown, D. I. and Griendling, K. K. 2009. Nox proteins in signal transduction. *Free Radical Biology and Medicine* 47(9), pp. 1239-1253. doi: <https://doi.org/10.1016/j.freeradbiomed.2009.07.023>

Burch, P. M. and Heintz, N. H. Redox regulation of cell-cycle re-entry: cyclin D1 as a primary target for the mitogenic effects of reactive oxygen and nitrogen species. (1523-0864 (Print)),

Burhans, W. C. and Heintz, N. H. 2009. The cell cycle is a redox cycle: Linking phase-specific targets to cell fate. *Free radical biology & medicine* 47(9), pp. 1282-1293. doi: 10.1016/j.freeradbiomed.2009.05.026

Burnett, A. K. et al. 2009. The impact of dose escalation and resistance modulation in older patients with acute myeloid leukaemia and high risk myelodysplastic syndrome: the results of the LRF AML14 trial. *British journal of haematology* 145(3), pp. 318-332. doi: 10.1111/j.1365-2141.2009.07604.x

Cai, L. et al. 2020. Identification and validation of a six-gene signature associated with glycolysis to predict the prognosis of patients with cervical cancer. *BMC cancer* 20(1), pp. 1133-1133. doi: 10.1186/s12885-020-07598-3

Cao, S., Li, J., Yang, K. and Li, H. 2021. Major ceRNA regulation and key metabolic signature analysis of intervertebral disc degeneration. *BMC musculoskeletal disorders* 22(1), pp. 249-249. doi: 10.1186/s12891-021-04109-8

Cerami, E. et al. 2012. The cBio cancer genomics portal: an open platform for exploring multidimensional cancer genomics data. *Cancer discovery* 2(5), pp. 401-404. doi: 10.1158/2159-8290.Cd-12-0095

Chandel, V., Sharma, P. P., Nayar, S. A., Jha, N. K., Jha, S. K., Rathi, B. and Kumar, D. 2021. In silico identification of potential inhibitor for TP53-induced glycolysis and apoptosis regulator in head and neck squamous cell carcinoma. *3 Biotech* 11(3), pp. 117-117. doi: 10.1007/s13205-021-02665-3

Chaneton, B. et al. 2012. Serine is a natural ligand and allosteric activator of pyruvate kinase M2. *Nature (London)* 491(7424), pp. 458-462.e452. doi: 10.1038/nature11540

Chen, C., Liu, Y., Liu, R., Ikenoue, T., Guan, K.-L., Liu, Y. and Zheng, P. 2008. TSC-mTOR maintains quiescence and function of hematopoietic stem cells by repressing mitochondrial biogenesis and reactive oxygen species. *The Journal of experimental medicine* 205(10), pp. 2397-2408. doi: 10.1084/jem.20081297

Chen, L. et al. 2016. PFKFB3 Control of Cancer Growth by Responding to Circadian Clock Outputs. *Scientific reports* 6(1), p. 24324. doi: 10.1038/srep24324

Chen, Y. et al. 2013. Prognostic significance of 11q23 aberrations in adult acute myeloid leukemia and the role of allogeneic stem cell transplantation. *Leukemia* 27(4), pp. 836-842. doi: 10.1038/leu.2012.319

Cheng, T., Sudderth, J., Yang, C., Mullen, A. R., Jin, E. S., MatÃ©s, J. M. and DeBerardinis, R. J. 2011. Pyruvate carboxylase is required for glutamine-independent growth of tumor cells. *Proceedings of the National Academy of Sciences - PNAS* 108(21), pp. 8674-8679. doi: 10.1073/pnas.1016627108

Chesney, J., Clark, J., Klarer, A. C., Imbert-Fernandez, Y., Lane, A. N. and Telang, S. 2014. Fructose-2,6-bisphosphate synthesis by 6-phosphofructo-2-kinase/fructose-2,6-bisphosphatase 4 (PFKFB4) is required for the glycolytic response to hypoxia and tumor growth. *Oncotarget* 5(16), pp. 6670-6686. doi: 10.18632/oncotarget.2213

Cheung, E. C. and Vousden, K. H. 2022. The role of ROS in tumour development and progression. *Nature reviews. Cancer* 22(5), pp. 280-297. doi: 10.1038/s41568-021-00435-0

Ciccarese, F. and Ciminale, V. 2017. Escaping Death: Mitochondrial Redox Homeostasis in Cancer Cells. *Frontiers in oncology* 7, pp. 117-117. doi: 10.3389/fonc.2017.00117

Cieślak-Pobuda, A., Jain, M. V., Kratz, G., Rzeszowska-Wolny, J., Ghavami, S. and Wiechec, E. 2015. The expression pattern of PFKFB3 enzyme distinguishes between induced-pluripotent stem cells and cancer stem cells. *Oncotarget* 6(30), pp. 29753-29770. doi: 10.18632/oncotarget.4995

Cohen, A. A. et al. 2009. Protein dynamics in individual human cells: Experiment and theory. *PloS one* 4(4), pp. e4901-e4901. doi: 10.1371/journal.pone.0004901

Cohen, J. 1988. *Statistical power analysis for the behavioral sciences*. 2nd ed. Hillsdale, N.J. ;: L. Erlbaum Associates.

Čolović, N., Denčić-Fekete, M., Peruničić, M. and Jurišić, V. 2019. Clinical Characteristics and Treatment Outcome of Hypocellular Acute Myeloid Leukemia Based on WHO Classification. *Indian journal of hematology & blood transfusion* 36(1), pp. 59-63. doi: 10.1007/s12288-019-01161-2

Conway O'Brien, E., Prideaux, S. and Chevassut, T. 2014. The Epigenetic Landscape of Acute Myeloid Leukemia. *Advances in hematology* 2014, pp. 1-15. doi: 10.1155/2014/103175

Corces, M. R. et al. 2016. Lineage-specific and single-cell chromatin accessibility charts human hematopoiesis and leukemia evolution. *Nature genetics* 48(10), pp. 1193-1203. doi: 10.1038/ng.3646

Cordero-Espinoza, L. and Hagen, T. 2013. Increased Concentrations of Fructose 2,6-Bisphosphate Contribute to the Warburg Effect in Phosphatase and Tensin Homolog (PTEN)-deficient Cells. *The Journal of biological chemistry* 288(50), pp. 36020-36028. doi: 10.1074/jbc.M113.510289

Costa Leite, T., Da Silva, D., Guimarães Coelho, R., Zancan, P. and Sola-Penna, M. 2007. Lactate favours the dissociation of skeletal muscle 6-phosphofructo-1-kinase tetramers down-regulating the enzyme and muscle glycolysis. *Biochemical journal* 408(1), pp. 123-130. doi: 10.1042/bj20070687

Curcio, C., Brugiapaglia, S., Bulfamante, S., Follia, L., Cappello, P. and Novelli, F. 2021. The Glycolytic Pathway as a Target for Novel Onco-Immunology Therapies in Pancreatic Cancer. *Molecules (Basel, Switzerland)* 26(6), p. 1642. doi: 10.3390/molecules26061642

Dakik, H. et al. 2021. Characterization of NADPH Oxidase Expression and Activity in Acute Myeloid Leukemia Cell Lines: A Correlation with the Differentiation Status. *Antioxidants* 10(3), p. 498. doi: 10.3390/antiox10030498

Dasgupta, S. et al. 2018. Metabolic enzyme PFKFB4 activates transcriptional coactivator SRC-3 to drive breast cancer. *Nature (London)* 556(7700), pp. 249-254. doi: 10.1038/s41586-018-0018-1

De Kouchkovsky, I. and Abdul-Hay, M. 2016. Acute myeloid leukemia: a comprehensive review and 2016 update. *Blood cancer journal (New York)* 6(7), pp. e441-e441. doi: 10.1038/bcj.2016.50

de Lecea, L., Ruiz-Lozano, P., Danielson, P. E., Peelle-Kirley, J., Foye, P. E., Frankel, W. N. and Sutcliffe, J. G. 1997. Cloning, mRNA Expression, and Chromosomal Mapping of Mouse and Human Preprocortistatin. *Genomics (San Diego, Calif.)* 42(3), pp. 499-506. doi: 10.1006/geno.1997.4763

de Sousa Abreu, R., Penalva, L. O., Marcotte, E. M. and Vogel, C. 2009. Global signatures of protein and mRNA expression levels. *Molecular BioSystems* 5(12), pp. 1512-1526. doi: 10.1039/b908315d

Deschler, B. and Lübbert, M. 2006. Acute myeloid leukemia: Epidemiology and etiology. *Cancer* 107(9), pp. 2099-2107. doi: 10.1002/cncr.22233

Dick, J. E., Jin, L., Hope, K. J., Zhai, Q. and Smadja-Joffe, F. 2006. Targeting of CD44 eradicates human acute myeloid leukemic stem cells. *Nature medicine* 12(10), pp. 1167-1174. doi: 10.1038/nm1483

DiNardo, C. D. et al. 2019. Venetoclax combined with decitabine or azacitidine in treatment-naive, elderly patients with acute myeloid leukemia. *Blood* 133(1), pp. 7-17. doi: 10.1182/blood-2018-08-868752

Ding, D.-C., Chang, Y.-H., Shyu, W.-C. and Lin, S.-Z. 2015. Human Umbilical Cord Mesenchymal Stem Cells: A New Era for Stem Cell Therapy. *Cell transplantation* 24(3), pp. 339-347. doi: 10.3727/096368915x686841

Döhner, H. et al. 2017. Diagnosis and management of AML in adults: 2017 ELN recommendations from an international expert panel. *Blood* 129(4), pp. 424-447. doi: 10.1182/blood-2016-08-733196

Döhner, H. A.-O. et al. Diagnosis and management of AML in adults: 2022 recommendations from an international expert panel on behalf of the ELN. (1528-0020 (Electronic)),

Doménech, E. et al. 2015. AMPK and PFKFB3 mediate glycolysis and survival in response to mitophagy during mitotic arrest. *Nature cell biology* 17(10), pp. 1304-1316. doi: 10.1038/ncb3231

Doroshov, J. H. 2019. Mechanisms of Anthracycline-Enhanced Reactive Oxygen Metabolism in Tumor Cells. *Oxidative medicine and cellular longevity* 2019, pp. 9474823-9474814. doi: 10.1155/2019/9474823

Dustin, C. M., Heppner, D. E., Lin, M.-C. J. and van der Vliet, A. 2020. Redox regulation of tyrosine kinase signalling: more than meets the eye. *Journal of biochemistry (Tokyo)* 167(2), pp. 151-163. doi: 10.1093/jb/mvz085

Edmonson, M. N. et al. 2019. Pediatric Cancer Variant Pathogenicity Information Exchange (PeCanPIE): a cloud-based platform for curating and classifying germline variants. *Genome research* 29(9), pp. 1555-1565. doi: 10.1101/gr.250357.119

El Hassouni, B. et al. 2020. The dichotomous role of the glycolytic metabolism pathway in cancer metastasis: Interplay with the complex tumor microenvironment and novel therapeutic strategies. *Seminars in cancer biology* 60, pp. 238-248. doi: 10.1016/j.semcan.2019.08.025

Eltzschig, H. K. et al. 2006. ATP Release From Activated Neutrophils Occurs via Connexin 43 and Modulates Adenosine-Dependent Endothelial Cell Function. *Circulation research* 99(10), pp. 1100-1108. doi: 10.1161/01.Res.0000250174.31269.70

Emini Veseli, B. et al. 2020. Small molecule 3PO inhibits glycolysis but does not bind to 6-phosphofructo-2-kinase/fructose-2,6-bisphosphatase-3 (PFKFB3). *FEBS letters* 594(18), pp. 3067-3075. doi: 10.1002/1873-3468.13878

Epsztejn, S., Kakhlon, O., Glickstein, H., Breuer, W. and Cabantchik, Z. I. 1997. Fluorescence Analysis of the Labile Iron Pool of Mammalian Cells. *Analytical biochemistry* 248(1), pp. 31-40. doi: 10.1006/abio.1997.2126

Feizabadi, M., Soleymanpour, A., Faridnouri, H. and Ajloo, D. 2019. Improving stability of biosensor based on covalent immobilization of horseradish peroxidase by γ -aminobutyric acid and application in detection of H₂O₂. *International journal of biological macromolecules* 136, pp. 597-606. doi: 10.1016/j.ijbiomac.2019.06.103

Feng, Y. and Wu, L. 2017. mTOR up-regulation of PFKFB3 is essential for acute myeloid leukemia cell survival. *Biochemical and biophysical research communications* 483(2), pp. 897-903. doi: 10.1016/j.bbrc.2017.01.031

Ferrara, F. D. and Schiffer, C. A. M. D. 2013. Acute myeloid leukaemia in adults. *The Lancet (British edition)* 381(9865), pp. 484-495. doi: 10.1016/s0140-6736(12)61727-9

Filippi, M.-D. and Ghaffari, S. 2019. Mitochondria in the maintenance of hematopoietic stem cells: new perspectives and opportunities. *Blood* 133(18), pp. 1943-1952. doi: 10.1182/blood-2018-10-808873

Finkel, T. 2001. Reactive Oxygen Species and Signal Transduction. *IUBMB life* 52(1), pp. 3-6. doi: 10.1080/15216540252774694

Florian, Maria C. et al. 2012. Cdc42 Activity Regulates Hematopoietic Stem Cell Aging and Rejuvenation. *Cell stem cell* 10(5), pp. 520-530. doi: 10.1016/j.stem.2012.04.007

Forrester, S. J., Kikuchi, D. S., Hernandez, M. S., Xu, Q. and Griending, K. K. 2018. Reactive Oxygen Species in Metabolic and Inflammatory Signaling. *Circulation research* 122(6), pp. 877-902. doi: 10.1161/circresaha.117.311401

Frigolet, M. E., Thomas, G., Beard, K., Lu, H., Liu, L. and Fantus, I. G. 2017. The bradykinin-cGMP-PKG pathway augments insulin sensitivity via upregulation of MAPK phosphatase-5 and inhibition of JNK. *American journal of physiology: endocrinology and metabolism* 313(3), pp. E321-E334. doi: 10.1152/ajpendo.00298.2016

Fruman, D. A. and Rommel, C. 2014. PI3K and cancer: lessons, challenges and opportunities. *Nature reviews. Drug discovery* 13(2), pp. 140-156. doi: 10.1038/nrd4204

Fu, W., Shi, D., Westaway, D. and Jhamandas, J. H. 2015. Bioenergetic Mechanisms in Astrocytes May Contribute to Amyloid Plaque Deposition and Toxicity. *The Journal of biological chemistry* 290(20), pp. 12504-12513. doi: 10.1074/jbc.M114.618157

Gaidzik, V. I. et al. 2016. RUNX1 mutations in acute myeloid leukemia are associated with distinct clinico-pathologic and genetic features. *Leukemia* 30(11), pp. 2160-2168. doi: 10.1038/leu.2016.126

Gao, J. et al. 2013. Integrative analysis of complex cancer genomics and clinical profiles using the cBioPortal. *Science signaling* 6(269), pp. pl1-pl1. doi: 10.1126/scisignal.2004088

Gao, R. et al. 2018. PFKFB4 Promotes Breast Cancer Metastasis via Induction of Hyaluronan Production in a p38-Dependent Manner. *Cellular physiology and biochemistry* 50(6), pp. 2108-2123. doi: 10.1159/000495055

Gao, Y., Liu, C., Xu, X., Wang, Y. and Jiang, Y. 2022. Circular RNA sterile alpha motif domain containing 4A contributes to cell 5-fluorouracil resistance in colorectal cancer by regulating the miR-545-3p/6-phosphofructo-2-kinase/fructose-2,6-bisphosphataseisotype 3 axis. *Anti-cancer drugs* 33(6), pp. 553-563. doi: 10.1097/cad.0000000000001285

Gardner, R. V., Oliver, P. and Astle, C. M. 1998. Stem Cell Factor Improves the Repopulating Ability of Primitive Hematopoietic Stem Cells after Sublethal Irradiation (and, to a Lesser Extent) after Bone Marrow Transplantation in Mice. *Stem cells (Dayton, Ohio)* 16(2), pp. 112-119. doi: 10.1002/stem.160112

Gentric, G., Mieulet, V. and Mechta-Grigoriou, F. 2017. Heterogeneity in Cancer Metabolism: New Concepts in an Old Field. *Antioxidants & Redox Signaling* 26(9), pp. 462-485. doi: 10.1089/ars.2016.6750

Giatromanolaki, A., Balaska, K., Kalamida, D., Kakouratos, C., Sivridis, E. and Koukourakis, M. I. 2017. Thermogenic protein UCP1 and UCP3 expression in non-small cell lung cancer: relation with glycolysis and anaerobic metabolism. *Cancer biology & medicine* 14(4), pp. 396-404. doi: 10.20892/j.issn.2095-3941.2017.0089

Gopalakrishna, R. and Jaken, S. 2000. Protein kinase C signaling and oxidative stress. *Free radical biology & medicine* 28(9), pp. 1349-1361. doi: 10.1016/s0891-5849(00)00221-5

Gu, M. et al. 2017. PFKFB3 promotes proliferation, migration and angiogenesis in nasopharyngeal carcinoma. *Journal of Cancer* 8(18), pp. 3887-3896. doi: 10.7150/jca.19112

Gustafsson, N. M. S. et al. 2018. Targeting PFKFB3 radiosensitizes cancer cells and suppresses homologous recombination. *Nature communications* 9(1), pp. 3872-3816. doi: 10.1038/s41467-018-06287-x

Hamidi, M. and Tajerzadeh, H. 2003. Carrier Erythrocytes: An Overview. *Drug delivery* 10(1), pp. 9-20. doi: 10.1080/713840329

Hamilton, J. A., Callaghan, M. J., Sutherland, R. L. and Watts, C. K. W. 1997. Identification of PRG1, A Novel Progesterone-Responsive Gene with Sequence Homology to 6-Phosphofructo-2-Kinase/Fructose- 2,6-Bisphosphatase. *Molecular endocrinology (Baltimore, Md.)* 11(4), pp. 490-502. doi: 10.1210/mend.11.4.9909

Hanahan, D. and Weinberg, Robert A. 2011. Hallmarks of Cancer: The Next Generation. *Cell* 144(5), pp. 646-674. doi: 10.1016/j.cell.2011.02.013

Hanaoka, S., Lin, J.-M. and Yamada, M. 2001. Chemiluminescent flow sensor for H₂O₂ based on the decomposition of H₂O₂ catalyzed by cobalt(II)-ethanolamine complex immobilized on resin. *Analytica chimica acta* 426(1), pp. 57-64. doi: 10.1016/s0003-2670(00)01181-8

Hatting, M., Tavares, C. D. J., Sharabi, K., Rines, A. K. and Puigserver, P. 2018. Insulin regulation of gluconeogenesis. *Annals of the New York Academy of Sciences* 1411(1), pp. 21-35. doi: 10.1111/nyas.13435

Hernansanz-Agustín, P. et al. 2017. Mitochondrial complex I deactivation is related to superoxide production in acute hypoxia. *Redox biology* 12, pp. 1040-1051. doi: 10.1016/j.redox.2017.04.025

Hers, H. G. and Van Schaftingen, E. 1982. Fructose 2,6-bisphosphate 2 years after its discovery. *Biochemical journal* 206(1), pp. 1-12. doi: 10.1042/bj2060001

Hitchler, M. J. and Domann, F. E. 2012. Redox regulation of the epigenetic landscape in Cancer: A role for metabolic reprogramming in remodeling the epigenome. *Free*

radical biology & medicine 53(11), pp. 2178-2187. doi: 10.1016/j.freeradbiomed.2012.09.028

Ho, T. T. et al. 2017. Autophagy maintains the metabolism and function of young and old stem cells. *Nature (London)* 543(7644), pp. 205-210. doi: 10.1038/nature21388

Hole, P. S., Darley, R. L. and Tonks, A. 2011. Do reactive oxygen species play a role in myeloid leukemias? *Blood* 117(22), pp. 5816-5826. doi: 10.1182/blood-2011-01-326025

Hole, P. S., Pearn, L., Tonks, A. J., James, P. E., Burnett, A. K., Darley, R. L. and Tonks, A. 2010. Ras-induced reactive oxygen species promote growth factor-independent proliferation in human CD34+ hematopoietic progenitor cells. *Blood* 115(6), pp. 1238-1246. doi: 10.1182/blood-2009-06-222869

Hole, P. S. et al. 2013. Overproduction of NOX-derived ROS in AML promotes proliferation and is associated with defective oxidative stress signaling. *Blood* 122(19), pp. 3322-3330. doi: 10.1182/blood-2013-04-491944

Hopkins, G. L., Robinson, A. J., Hole, P. S., Darley, R. L. and Tonks, A. 2014. Analysis of ROS-Responsive Genes in Mutant RAS Expressing Hematopoietic Progenitors Identifies the Glycolytic Pathway As a Major Target Promoting Both Proliferation and Survival. *Blood* 124(21), pp. 2210-2210. doi: 10.1182/blood.V124.21.2210.2210

Hua, Z., White, J. and Zhou, J. 2022. Cancer stem cells in TNBC. *Seminars in cancer biology* 82, pp. 26-34. doi: 10.1016/j.semcancer.2021.06.015

Hughes, A. J., Spelke, D. P., Xu, Z., Kang, C.-C., Schaffer, D. V. and Herr, A. E. 2014. Single-cell western blotting. *Nature methods* 11(7), pp. 749-755. doi: 10.1038/nmeth.2992

Huntly, B. J. P. and Gilliland, D. G. 2005. Leukaemia stem cells and the evolution of cancer-stem-cell research. *Nature reviews. Cancer* 5(4), pp. 311-321. doi: 10.1038/nrc1592

Icard, P., Fournel, L., Wu, Z., Alifano, M. and Lincet, H. 2019. Interconnection between Metabolism and Cell Cycle in Cancer. *Trends in biochemical sciences (Amsterdam. Regular ed.)* 44(6), pp. 490-501. doi: 10.1016/j.tibs.2018.12.007

Imbert-Fernandez, Y. et al. 2014. Estradiol Stimulates Glucose Metabolism via 6-Phosphofructo-2-kinase (PFKFB3). *The Journal of biological chemistry* 289(13), pp. 9440-9448. doi: 10.1074/jbc.M113.529990

Ito, K. and Ito, K. 2018. Hematopoietic stem cell fate through metabolic control. *Experimental hematology* 64, pp. 1-11. doi: 10.1016/j.exphem.2018.05.005

Ito, K. and Suda, T. 2014. Metabolic requirements for the maintenance of self-renewing stem cells. *Nature reviews. Molecular cell biology* 15(4), pp. 243-256. doi: 10.1038/nrm3772

Ivanova, J. S., Pugovkina, N. A., Neganova, I. E., Kozhukharova, I. V., Nikolsky, N. N. and Lyublinskaya, O. G. 2021. Cell cycle-coupled changes in the level of reactive oxygen species support the proliferation of human pluripotent stem cells. *Stem cells (Dayton, Ohio)* 39(12), pp. 1671-1687. doi: 10.1002/stem.3450

Jackson, S. P. and Bartek, J. 2009. The DNA-damage response in human biology and disease. *Nature (London)* 461(7267), pp. 1071-1078. doi: 10.1038/nature08467

Jaiswal, S. et al. 2009. CD47 Is Upregulated on Circulating Hematopoietic Stem Cells and Leukemia Cells to Avoid Phagocytosis. *Cell* 138(2), pp. 271-285. doi: 10.1016/j.cell.2009.05.046

Jeong, A. Y., Lee, M. Y., Lee, S. H., Hong Park, J. and Han, H. J. 2009. PPAR δ agonist-mediated ROS stimulates mouse embryonic stem cell proliferation through cooperation of p38 MAPK and Wnt/ β -catenin. *Cell cycle (Georgetown, Tex.)* 8(4), pp. 611-619. doi: 10.4161/cc.8.4.7752

Jin, L. et al. 2009. Monoclonal Antibody-Mediated Targeting of CD123, IL-3 Receptor α Chain, Eliminates Human Acute Myeloid Leukemic Stem Cells. *Cell stem cell* 5(1), pp. 31-42. doi: 10.1016/j.stem.2009.04.018

Jones, B. C., Pohlmann, P. R., Clarke, R. and Sengupta, S. 2022. Treatment against glucose-dependent cancers through metabolic PFKFB3 targeting of glycolytic flux. *Cancer and metastasis reviews*, doi: 10.1007/s10555-022-10027-5

Jóźwiak, P., Forma, E., Bryś, M. and Krześlak, A. 2014. O-GlcNAcylation and metabolic reprogramming in cancer. *Frontiers in endocrinology (Lausanne)* 5, pp. 145-145. doi: 10.3389/fendo.2014.00145

Ju, H.-Q., Lin, J.-F., Tian, T., Xie, D. and Xu, R.-H. 2020. NADPH homeostasis in cancer: functions, mechanisms and therapeutic implications. *Signal transduction and targeted therapy* 5(1), pp. 231-231. doi: 10.1038/s41392-020-00326-0

Ju, H. Q. et al. 2017. ITD mutation in FLT3 tyrosine kinase promotes Warburg effect and renders therapeutic sensitivity to glycolytic inhibition. *Leukemia* 31(10), pp. 2143-2150. doi: 10.1038/leu.2017.45

Juan, C. A., Pérez de la Lastra, J. M., Plou, F. J. and Pérez-Lebeña, E. 2021. The Chemistry of Reactive Oxygen Species (ROS) Revisited: Outlining Their Role in Biological Macromolecules (DNA, Lipids and Proteins) and Induced Pathologies. *International journal of molecular sciences* 22(9), p. 4642. doi: 10.3390/ijms22094642

Juntilla, M. M., Patil, V. D., Calamito, M., Joshi, R. P., Birnbaum, M. J. and Koretzky, G. A. 2010. AKT1 and AKT2 maintain hematopoietic stem cell function by regulating reactive oxygen species. *Blood* 115(20), pp. 4030-4038. doi: 10.1182/blood-2009-09-241000

Kaelin, W. G. and Ratcliffe, P. J. 2008. Oxygen Sensing by Metazoans: The Central Role of the HIF Hydroxylase Pathway. *Molecular cell* 30(4), pp. 393-402. doi: 10.1016/j.molcel.2008.04.009

Kamata, H., Honda, S.-I., Maeda, S., Chang, L., Hirata, H. and Karin, M. 2005. Reactive oxygen species promote TNF α -induced death and sustained JNK activation by inhibiting MAP kinase phosphatases. *Cell* 120(5), p. 649.

Kamminga, L. M. et al. 2006. The Polycomb group gene Ezh2 prevents hematopoietic stem cell exhaustion. *Blood* 107(5), pp. 2170-2179. doi: 10.1182/blood-2005-09-3585

Kang, X., Wei, X., Jiang, L., Niu, C., Zhang, J., Chen, S. and Meng, D. 2016. Nox2 and Nox4 regulate self-renewal of murine induced-pluripotent stem cells: NOX2 and NOX4 in Stem Cell Self-Renewal. *IUBMB life* 68(12), pp. 963-970. doi: 10.1002/iub.1574

Kaya, A., Lee, B. C. and Gladyshev, V. N. 2015. Regulation of Protein Function by Reversible Methionine Oxidation and the Role of Selenoprotein MsrB1. *Antioxidants & Redox Signaling* 23(10), pp. 814-822. doi: 10.1089/ars.2015.6385

KB, U. 2020. *P16118* . *F261_HUMAN*.
<https://www.uniprot.org/uniprotkb/P16118/entry>: UniProt. Available at: [Accessed: 20th March].

Keidar, M. 2015. Plasma for cancer treatment. *Plasma sources science & technology* 24(3), pp. 33001-33020. doi: 10.1088/0963-0252/24/3/033001

Kessler, R., Fleischer, M., Springsguth, C., Bigl, M., Warnke, J.-P. and Eschrich, K. 2019. Prognostic Value of PFKFB3 to PFKFB4 mRNA Ratio in Patients With Primary Glioblastoma (IDH-Wildtype). *Journal of neuropathology and experimental neurology* 78(9), pp. 865-870. doi: 10.1093/jnen/nlz067

Kihara, R. et al. 2014. Comprehensive analysis of genetic alterations and their prognostic impacts in adult acute myeloid leukemia patients. *Leukemia* 28(8), pp. 1586-1595. doi: 10.1038/leu.2014.55

Kinder, M., Wei, C., Shelat, S. G., Kundu, M., Zhao, L., Blair, I. A. and Puré, E. 2010. Hematopoietic stem cell function requires 12/15-lipoxygenase–dependent fatty acid metabolism. *Blood* 115(24), pp. 5012-5022. doi: 10.1182/blood-2009-09-243139

Klauke, K. et al. 2013. Polycomb Cbx family members mediate the balance between haematopoietic stem cell self-renewal and differentiation. *Nature cell biology* 15(4), pp. 353-+. doi: 10.1038/ncb2701

Koczula, K. M. et al. 2016. Metabolic plasticity in CLL: adaptation to the hypoxic niche. *Leukemia* 30(1), pp. 65-73. doi: 10.1038/leu.2015.187

Koglin, N. et al. 2011. Specific PET Imaging of xC— Transporter Activity Using a 18F-Labeled Glutamate Derivative Reveals a Dominant Pathway in Tumor Metabolism. *Clinical cancer research* 17(18), pp. 6000-6011. doi: 10.1158/1078-0432.Ccr-11-0687

Kohlmann, A. et al. 2010. Gene expression profiling in AML with normal karyotype can predict mutations for molecular markers and allows novel insights into perturbed biological pathways. *Leukemia* 24(6), pp. 1216-1220. doi: 10.1038/leu.2010.73

Kohlmann, A. et al. 2008. An international standardization programme towards the application of gene expression profiling in routine leukaemia diagnostics: the Microarray Innovations in LEukemia study prephase. *British journal of haematology* 142(5), pp. 802-807. doi: 10.1111/j.1365-2141.2008.07261.x

Konieczny, J. and Arranz, L. 2018. Updates on old and weary haematopoiesis. *International journal of molecular sciences* 19(9), p. 2567. doi: 10.3390/ijms19092567

Kotowski, K. et al. 2021. Role of pfkfb3 and pfkfb4 in cancer: Genetic basis, impact on disease development/progression, and potential as therapeutic targets. *Cancers* 13(4), pp. 1-29. doi: 10.3390/cancers13040909

Koussounadis, A., Langdon, S. P., Um, I. H., Harrison, D. J. and Smith, V. A. 2015. Relationship between differentially expressed mRNA and mRNA-protein correlations in a xenograft model system. *Scientific reports* 5(1), pp. 10775-10775. doi: 10.1038/srep10775

Kramer, P. A., Ravi, S., Chacko, B., Johnson, M. S. and Darley-Usmar, V. M. 2014. A review of the mitochondrial and glycolytic metabolism in human platelets and leukocytes: Implications for their use as bioenergetic biomarkers. *Redox biology* 2(1), pp. 206-210. doi: 10.1016/j.redox.2013.12.026

Kunisaki, Y. et al. 2013. Arteriolar niches maintain haematopoietic stem cell quiescence. *Nature (London)* 502(7473), pp. 637-643. doi: 10.1038/nature12612

Lee, S.-R., Yang, K.-S., Kwon, J., Lee, C., Jeong, W. and Rhee, S. G. 2002. Reversible Inactivation of the Tumor Suppressor PTEN by H₂O₂. *The Journal of biological chemistry* 277(23), pp. 20336-20342. doi: 10.1074/jbc.M111899200

Lewandowski, J. P., Sheehan, K. B., Bennett, P. E. and Boswell, R. E. 2010. Mago Nashi, Tsunagi/Y14, and Ranshi form a complex that influences oocyte differentiation in *Drosophila melanogaster*. *Developmental biology* 339(2), pp. 307-319. doi: 10.1016/j.ydbio.2009.12.035

Ley, T. J. 2013. Genomic and Epigenomic Landscapes of Adult De Novo Acute Myeloid Leukemia. *The New England journal of medicine* 369(1), pp. 98-98. doi: 10.1056/NEJMx130028

Li, F.-L. et al. 2018a. Acetylation accumulates PFKFB3 in cytoplasm to promote glycolysis and protects cells from cisplatin-induced apoptosis. *Nature communications* 9(1), pp. 508-517. doi: 10.1038/s41467-018-02950-5

Li, J., Zhang, Y., Yang, C. and Rong, R. 2020a. Discrepant mRNA and Protein Expression in Immune Cells. *Current genomics* 21(8), pp. 560-563. doi: 10.2174/1389202921999200716103758

Li, L. et al. 2003. Identification of the haematopoietic stem cell niche and control of the niche size. *Nature* 425(6960), pp. 836-841. doi: 10.1038/nature02041

Li, X. et al. 2020b. The metabolic role of PFKFB4 in androgen-independent growth in vitro and PFKFB4 expression in human prostate cancer tissue. *BMC urology* 20(1), pp. 61-61. doi: 10.1186/s12894-020-00635-0

Li, X. et al. 2018b. Expression of PFKFB3 and Ki67 in lung adenocarcinomas and targeting PFKFB3 as a therapeutic strategy. *Molecular and cellular biochemistry* 445(1-2), pp. 123-134. doi: 10.1007/s11010-017-3258-8

Li, X. et al. 2020c. Prognostic model of invasive ductal carcinoma of the breast based on differentially expressed glycolysis-related genes. *PeerJ (San Francisco, CA)* 8, pp. e10249-e10249. doi: 10.7717/peerj.10249

Li, Y., Rivera, D., Ru, W., Gunasekera, D. and Kemp, R. G. 1999. Identification of Allosteric Sites in Rabbit Phosphofructo-1-kinase. *Biochemistry (Easton)* 38(49), pp. 16407-16412. doi: 10.1021/bi991761l

Li, Z. et al. 2017. Exploring the antitumor mechanism of high-dose cytarabine through the metabolic perturbations of ribonucleotide and deoxyribonucleotide in human promyelocytic Leukemia HL-60 Cells. *Molecules (Basel, Switzerland)* 22(3), p. 499. doi: 10.3390/molecules22030499

Lima, C. D. and Mondragón, A. 1994. Mechanism of type II DNA topoisomerases: a tale of two gates. *Structure (London)* 2(6), pp. 559-560. doi: 10.1016/s0969-2126(00)00055-1

Liu, D. et al. 2021. Long noncoding RNA GSEC promotes neutrophil inflammatory activation by supporting PFKFB3-involved glycolytic metabolism in sepsis. *Cell death & disease* 12(12), pp. 1157-1157. doi: 10.1038/s41419-021-04428-7

Liu, F., Li, L., Zhang, B., Fan, W., Zhang, R., Liu, G. and Liu, X. 2019. A novel electrochemical sensor based on microporous polymeric nanospheres for measuring peroxy nitrite anion released by living cells and studying the synergistic effect of antioxidants. *Analyst (London)* 144(23), pp. 695-6913. doi: 10.1039/c9an01693g

Liu, H., Nishitoh, H., Ichijo, H. and Kyriakis, J. M. 2000. Activation of Apoptosis Signal-Regulating Kinase 1 (ASK1) by Tumor Necrosis Factor Receptor-Associated Factor 2 Requires Prior Dissociation of the ASK1 Inhibitor Thioredoxin. *Molecular and Cellular Biology* 20(6), pp. 2198-2208. doi: 10.1128/mcb.20.6.2198-2208.2000

Liu, S. et al. 2022. MiR-652-5p elevated glycolysis level by targeting TIGAR in T-cell acute lymphoblastic leukemia. *Cell death & disease* 13(2), pp. 148-148. doi: 10.1038/s41419-022-04600-7

Locasale, J. W. 2012. Metabolic rewiring drives resistance to targeted cancer therapy. *Molecular systems biology* 8(1), pp. 597-n/a. doi: 10.1038/msb.2012.30

Lu, H., Chen, S., You, Z., Xie, C., Huang, S. and Hu, X. 2020. PFKFB4 negatively regulated the expression of histone acetyltransferase GCN5 to mediate the tumorigenesis of thyroid cancer. *Development, growth & differentiation* 62(2), pp. 129-138. doi: 10.1111/dgd.12645

Lu, L., Chen, Y. and Zhu, Y. 2017. The molecular basis of targeting PFKFB3 as a therapeutic strategy against cancer. *Oncotarget* 8(37), pp. 62793-62802. doi: 10.18632/oncotarget.19513

Luther, M. A., Cai, G. Z. and Lee, J. C. 1986. Thermodynamics of dimer and tetramer formations in rabbit muscle phosphofructokinase. *Biochemistry (Easton)* 25(24), pp. 7931-7937. doi: 10.1021/bi00372a022

Lyu, Q. et al. 2019. Real-Time and In-Situ Monitoring of H₂O₂ Release from Living Cells by a Stretchable Electrochemical Biosensor Based on Vertically Aligned Gold Nanowires. *Analytical chemistry (Washington)* 91(21), pp. 13521-13527. doi: 10.1021/acs.analchem.9b02610

Macut, H. et al. 2019. Tuning PFKFB3 Bisphosphatase Activity Through Allosteric Interference. *Scientific reports* 9(1), pp. 20333-20310. doi: 10.1038/s41598-019-56708-0

Madaci, L., Colle, J., Venton, G., Farnault, L., Loriod, B. and Costello, R. 2021. The contribution of single-cell analysis of acute leukemia in the therapeutic strategy. *Biomarker research* 9(1), pp. 1-50. doi: 10.1186/s40364-021-00300-0

Maier, T., Güell, M. and Serrano, L. 2009. Correlation of mRNA and protein in complex biological samples. *FEBS letters* 583(24), pp. 3966-3973. doi: 10.1016/j.febslet.2009.10.036

Mailloux, R. J. and Harper, M.-E. 2011. Uncoupling proteins and the control of mitochondrial reactive oxygen species production. *Free radical biology & medicine* 51(6), pp. 1106-1115. doi: 10.1016/j.freeradbiomed.2011.06.022

Mair, F. et al. 2020. A Targeted Multi-omic Analysis Approach Measures Protein Expression and Low-Abundance Transcripts on the Single-Cell Level. *Cell reports (Cambridge)* 31(1), pp. 107499-107499. doi: 10.1016/j.celrep.2020.03.063

Marinho, H. S., Real, C., Cyrne, L., Soares, H. and Antunes, F. 2014. Hydrogen peroxide sensing, signaling and regulation of transcription factors. *Redox biology* 2(1), pp. 535-562. doi: 10.1016/j.redox.2014.02.006

Marsin, A.-S., Bouzin, C., Bertrand, L. and Hue, L. 2002. The Stimulation of Glycolysis by Hypoxia in Activated Monocytes Is Mediated by AMP-activated Protein Kinase and Inducible 6-Phosphofructo-2-kinase. *The Journal of biological chemistry* 277(34), pp. 30778-30783. doi: 10.1074/jbc.M205213200

McEver, R. P. 2015. Selectins: Initiators of leucocyte adhesion and signalling at the vascular wall. *Cardiovascular research* 107(3), pp. 331-339. doi: 10.1093/cvr/cvv154

Medinger, M. and Passweg, J. R. 2017. Acute myeloid leukaemia genomics. *British journal of haematology* 179(4), pp. 530-542. doi: 10.1111/bjh.14823

Minchenko, O., Opentanova, I. and Caro, J. 2003. Hypoxic regulation of the 6-phosphofructo-2-kinase/fructose-2,6-bisphosphatase gene family (PFKFB-1–4) expression in vivo. *FEBS letters* 554(3), pp. 264-270. doi: 10.1016/s0014-5793(03)01179-7

Minchenko, O. H., Ogura, T., Opentanova, I. L., Minchenko, D. O. and Esumi, H. 2005. Splice isoform of 6-phosphofructo-2-kinase/ fructose-2,6-bisphosphatase-4: Expression and hypoxic regulation. *Molecular and cellular biochemistry* 280(1-2), pp. 227-234. doi: 10.1007/s11010-005-8009-6

Mohrin, M. et al. 2015. Stem cell aging. A mitochondrial UPR-mediated metabolic checkpoint regulates hematopoietic stem cell aging. *Science (American Association for the Advancement of Science)* 347(6228), pp. 1374-1377. doi: 10.1126/science.aaa2361

Mondal, S. et al. 2019. Therapeutic targeting of PFKFB3 with a novel glycolytic inhibitor PFK158 promotes lipophagy and chemosensitivity in gynecologic cancers: Therapeutic targeting of PFKFB3. *International journal of cancer* 144(1), pp. 178-189. doi: 10.1002/ijc.31868

Morikawa, J. et al. 2003. Identification of signature genes by microarray for acute myeloid leukemia without maturation and acute promyelocytic leukemia with t(15;17)(q22;q12)(PML/RAR alpha). *INTERNATIONAL JOURNAL OF ONCOLOGY* 23(3), pp. 617-625.

Mucanj, V., Shay, J. E. S. and Simon, M. C. 2012. Effects of hypoxia and HIFs on cancer metabolism. *International journal of hematology* 95(5), pp. 464-470. doi: 10.1007/s12185-012-1070-5

Naoe, T. and Kiyoi, H. 2013. Gene mutations of acute myeloid leukemia in the genome era. *International journal of hematology* 97(2), pp. 165-174. doi: 10.1007/s12185-013-1257-4

Navarro-Sabaté, A., Manzano, A., Riera, L. s., Rosa, J. L., Ventura, F. and Bartrons, R. 2001. The human ubiquitous 6-phosphofructo-2-kinase/fructose-2,6-bisphosphatase gene (PFKFB3): promoter characterization and genomic structure. *Gene* 264(1), pp. 131-138. doi: 10.1016/s0378-1119(00)00591-6

Nguyen, S. et al. 2002. A white blood cell index as the main prognostic factor in t(8;21) acute myeloid leukemia (AML): a survey of 161 cases from the French AML Intergroup. *Blood* 99(10), pp. 3517-3523. doi: 10.1182/blood.V99.10.3517

Nolfi-Donagan, D., Braganza, A. and Shiva, S. 2020. Mitochondrial electron transport chain: Oxidative phosphorylation, oxidant production, and methods of measurement. *Redox biology* 37, pp. 101674-101674. doi: 10.1016/j.redox.2020.101674

Novellademunt, L. et al. 2012. Progestins activate 6-phosphofructo-2-kinase/fructose-2,6-bisphosphatase 3 (PFKFB3) in breast cancer cells. *Biochemical journal* 442(2), pp. 345-356. doi: 10.1042/bj20111418

O'Neal, J. et al. 2016. Inhibition of 6-phosphofructo-2-kinase (PFKFB3) suppresses glucose metabolism and the growth of HER2+ breast cancer. *Breast cancer research and treatment* 160(1), pp. 29-40. doi: 10.1007/s10549-016-3968-8

Ozcan, S. C. et al. 2021. Simultaneous inhibition of PFKFB3 and GLS1 selectively kills KRAS-transformed pancreatic cells. *Biochemical and biophysical research communications* 571, pp. 118-124. doi: 10.1016/j.bbrc.2021.07.070

Ozcan, S. C. et al. 2020. PFKFB2 regulates glycolysis and proliferation in pancreatic cancer cells. *Molecular and cellular biochemistry* 470(1-2), pp. 115-129. doi: 10.1007/s11010-020-03751-5

Pacini, N. and Borziani, F. 2014. Cancer stem cell theory and the warburg effect, two sides of the same coin? *International journal of molecular sciences* 15(5), pp. 8893-8930. doi: 10.3390/ijms15058893

Palmieri, F. 2004. The mitochondrial transporter family (SLC25): physiological and pathological implications. *Pflügers Archiv* 447(5), pp. 689-709. doi: 10.1007/s00424-003-1099-7

Pan, X., Li, H., Tan, J., Weng, X., Zhou, L., Weng, Y. and Cao, X. 2020. Mir-1297 suppresses osteosarcoma proliferation and aerobic glycolysis by regulating pfkfb2. *OncoTargets and therapy* 13, pp. 11265-11275. doi: 10.2147/ott.S274744

Pandor, A. et al. 2018. Ponatinib for Treating Chronic Myeloid Leukaemia: An Evidence Review Group Perspective of a NICE Single Technology Appraisal. *Pharmacoeconomics* 36(8), pp. 903-915. doi: 10.1007/s40273-018-0627-4

Papaemmanuil, E. et al. 2016. Genomic Classification and Prognosis in Acute Myeloid Leukemia. *The New England journal of medicine* 374(23), pp. 2209-2221. doi: 10.1056/NEJMoa1516192

Parra, V. et al. 2017. Inhibition of mitochondrial fission prevents hypoxia-induced metabolic shift and cellular proliferation of pulmonary arterial smooth muscle cells.

Biochimica et biophysica acta. Molecular basis of disease 1863(11), pp. 2891-2903.
doi: 10.1016/j.bbadis.2017.07.018

Parvez, S., Long, M. J. C., Poganik, J. R. and Aye, Y. 2018. Redox Signaling by Reactive Electrophiles and Oxidants. *Chemical reviews* 118(18), pp. 8798-8888. doi: 10.1021/acs.chemrev.7b00698

Paschka, P. et al. 2018. Adding dasatinib to intensive treatment in core-binding factor acute myeloid leukemia-results of the AMLSG 11-08 trial. *Leukemia* 32(7), pp. 1621-1630. doi: 10.1038/s41375-018-0129-6

Pegoraro, C., Maczkowiak, F. and Monsoro-Burq, A. H. 2013. Pfkfb (6-phosphofructo-2-kinase/fructose-2,6-bisphosphatase) isoforms display a tissue-specific and dynamic expression during *Xenopus laevis* development. *Gene Expression Patterns* 13(7), pp. 203-211. doi: 10.1016/j.gep.2013.04.002

Pilkis, S. J., El-Maghrabi, M. R., Pilkis, J., Claus, T. H. and Cumming, D. A. 1981. Fructose 2,6-bisphosphate. A new activator of phosphofructokinase. *The Journal of biological chemistry* 256(7), pp. 3171-3174. doi: 10.1016/s0021-9258(19)69584-0

Poli, G., Leonarduzzi, G., Biasi, F. and Chiarotto, E. 2004. Oxidative Stress and Cell Signalling. *Current medicinal chemistry* 11(9), pp. 1163-1182. doi: 10.2174/0929867043365323

Ponka, P. 1999. Cellular iron metabolism. *Kidney international* 55(S69), pp. S2-S11. doi: 10.1046/j.1523-1755.1999.055Suppl.69002.x

Potter, N. et al. 2019. Single cell analysis of clonal architecture in acute myeloid leukaemia. *Leukemia* 33(5), pp. 1113-1123. doi: 10.1038/s41375-018-0319-2

Pouyssegur, J. and Mechta-Grigoriou, F. 2006. Redox regulation of the hypoxia-inducible factor. *Biological chemistry* 387(10/11), pp. 1337-1346. doi: 10.1515/bc.2006.167

Qian, S. et al. 2016. TIGAR cooperated with glycolysis to inhibit the apoptosis of leukemia cells and associated with poor prognosis in patients with cytogenetically normal acute myeloid leukemia. *Journal of hematology and oncology* 9(1), pp. 128-128. doi: 10.1186/s13045-016-0360-4

Rabe, P., Gehmlich, M., Peters, A., Krumbholz, P., Nordström, A. and Stäubert, C. 2022. Combining metabolic phenotype determination with metabolomics and transcriptional analyses to reveal pathways regulated by hydroxycarboxylic acid receptor 2. *Discover. Oncology* 13(1), pp. 47-47. doi: 10.1007/s12672-022-00503-3

Rae, T. D., Schmidt, P. J., Pufahl, R. A., Culotta, V. C. and O'Halloran, T. V. 1999. Undetectable Intracellular Free Copper: The Requirement of a Copper Chaperone for Superoxide Dismutase. *Science (American Association for the Advancement of Science)* 284(5415), pp. 805-808. doi: 10.1126/science.284.5415.805

Ran, X., Luo, J., Zuo, C., Huang, Y., Sui, Y., Cen, J. and Tang, S. 2022. Developing metabolic gene signatures to predict intrahepatic cholangiocarcinoma prognosis and mining a miRNA regulatory network. *Journal of clinical laboratory analysis* 36(1), pp. e24107-n/a. doi: 10.1002/jcla.24107

Rapin, N. et al. 2014. Comparing cancer vs normal gene expression profiles identifies new disease entities and common transcriptional programs in AML patients. *Blood* 123(6), pp. 894-904. doi: 10.1182/blood-2013-02-485771

Reczek, C. R. and Chandel, N. S. 2014. ROS-dependent signal transduction. *Current opinion in cell biology* 33, pp. 8-13. doi: 10.1016/j.ceb.2014.09.010

Reikvam, H., Hatfield, K. J., Kittang, A. O., Hovland, R. and Bruserud, Ø. 2011. Acute Myeloid Leukemia with the t(8;21) Translocation: Clinical Consequences and Biological Implications. *Journal of biomedicine & biotechnology* 2011, pp. 104631-104623. doi: 10.1155/2011/104631

Renders, S. et al. 2021. Niche derived netrin-1 regulates hematopoietic stem cell dormancy via its receptor neogenin-1. *Nature communications* 12(1), pp. 608-615. doi: 10.1038/s41467-020-20801-0

Richert, L. et al. 2003. Effects of clofibric acid on mRNA expression profiles in primary cultures of rat, mouse and human hepatocytes. *Toxicology and applied pharmacology* 191(2), pp. 130-146. doi: 10.1016/s0041-008x(03)00231-x

Ristow, M. and Schmeisser, K. 2014. Mitohormesis: Promoting Health and Lifespan by Increased Levels of Reactive Oxygen Species (ROS). *Dose-response* 12(2), pp. 288-341. doi: 10.2203/dose-response.13-035.Ristow

Robinson, A. J. et al. 2020. Reactive oxygen species drive proliferation in acute myeloid leukemia via the glycolytic regulator PFKFB3. *Cancer research (Chicago, Ill.)* 80(5), pp. 937-949. doi: 10.1158/0008-5472.Can-19-1920

Rodriguez, S., Wang, L., Mumaw, C., Srour, E. F., Lo Celso, C., Nakayama, K.-i. and Carlesso, N. 2011. The SKP2 E3 ligase regulates basal homeostasis and stress-induced regeneration of HSCs. *Blood* 117(24), pp. 6509-6519. doi: 10.1182/blood-2010-11-321521

Ros, S. et al. 2012. Functional metabolic screen identifies 6-phosphofructo-2-kinase/fructose-2, 6-biphosphatase 4 as an important regulator of prostate cancer cell survival. *Cancer discovery* 2(4), pp. 328-343. doi: 10.1158/2159-8290.Cd-11-0234

Rossi, D. J., Bryder, D., Zahn, J. M., Ahlenius, H., Sonu, R., Wagers, A. J. and Weissman, I. L. 2005. Cell Intrinsic Alterations Underlie Hematopoietic Stem Cell Aging. *Proceedings of the National Academy of Sciences - PNAS* 102(26), pp. 9194-9199. doi: 10.1073/pnas.0503280102

Sachdev, S., Ansari, S. A., Ansari, M. I., Fujita, M. and Hasanuzzaman, M. 2021. Abiotic Stress and Reactive Oxygen Species: Generation, Signaling, and Defense Mechanisms. *Antioxidants* 10(2), p. 277. doi: 10.3390/antiox10020277

Saeki, N. and Imai, Y. 2020. Reprogramming of synovial macrophage metabolism by synovial fibroblasts under inflammatory conditions. *Cell communication and signaling* 18(1), pp. 188-188. doi: 10.1186/s12964-020-00678-8

Saha, T. and Lukong, K. E. 2022. Breast Cancer Stem-Like Cells in Drug Resistance: A Review of Mechanisms and Novel Therapeutic Strategies to Overcome Drug Resistance. *Frontiers in oncology* 12, pp. 856974-856974. doi: 10.3389/fonc.2022.856974

Sancho, P., Barneda, D. and Heeschen, C. 2016. Hallmarks of cancer stem cell metabolism. *British journal of cancer* 114(12), pp. 1305-1312. doi: 10.1038/bjc.2016.152

Sanz, M. A. et al. 2019. Management of acute promyelocytic leukemia: updated recommendations from an expert panel of the European LeukemiaNet. *Blood* 133(15), pp. 1630-1643. doi: 10.1182/blood-2019-01-894980

Satooka, H. and Hara-Chikuma, M. 2016. Aquaporin-3 Controls Breast Cancer Cell Migration by Regulating Hydrogen Peroxide Transport and Its Downstream Cell Signaling. *Molecular and Cellular Biology* 36(7), pp. 1206-1218. doi: 10.1128/mcb.00971-15

10.1128/mcb.00971-15.

Scadden, D. T. et al. 2003. Osteoblastic cells regulate the haematopoietic stem cell niche. *Nature* 425(6960), pp. 841-846. doi: 10.1038/nature02040

Scalise, M., Console, L., Rovella, F., Galluccio, M., Pochini, L. and Indiveri, C. 2020. Membrane Transporters for Amino Acids as Players of Cancer Metabolic Rewiring. *Cells (Basel, Switzerland)* 9(9), p. 2028. doi: 10.3390/cells9092028

Schnittger, S. et al. 2011. RUNX1 mutations are frequent in de novo AML with noncomplex karyotype and confer an unfavorable prognosis. *Blood* 117(8), pp. 2348-2357. doi: 10.1182/blood-2009-11-255976

Sengsuk, C., Tangvarasittichai, O., Chantanaskulwong, P., Pimanprom, A., Wantaneeeyawong, S., Choowet, A. and Tangvarasittichai, S. 2014. Association of Iron Overload with Oxidative Stress, Hepatic Damage and Dyslipidemia in Transfusion-Dependent [beta]-Thalassemia/HbE Patients. *Indian journal of clinical biochemistry* 29(3), p. 298. doi: 10.1007/s12291-013-0376-2

Sha, L. Y., Lv, Z. Q., Liu, Y. J., Zhang, Y., Sui, X., Wang, T. and Zhang, H. 2021. Shikonin inhibits the Warburg effect, cell proliferation, invasion and migration by downregulating PFKFB2 expression in lung cancer. *MOLECULAR MEDICINE REPORTS* 24(2), doi: 10.3892/mmr.2021.12199

Shao, L. et al. 2022. Identification of genomic determinants contributing to cytokine release in immunotherapies and human diseases. *Journal of translational medicine* 20(1), pp. 1-12. doi: 10.1186/s12967-022-03531-3

Shen, C., Ding, L., Mo, H., Liu, R., Xu, Q. and Tu, K. 2021. Long noncoding RNA FIRRE contributes to the proliferation and glycolysis of hepatocellular carcinoma cells

by enhancing PFKFB4 expression. *Journal of Cancer* 12(13), pp. 4099-4108. doi: 10.7150/jca.58097

Shi, L., Pan, H., Liu, Z., Xie, J. and Han, W. 2017. Roles of PFKFB3 in cancer. *Signal transduction and targeted therapy* 2(1), p. 17044. doi: 10.1038/sigtrans.2017.44

Shi, W.-K. et al. 2018. PFKFB3 blockade inhibits hepatocellular carcinoma growth by impairing DNA repair through AKT. *Cell death & disease* 9(4), pp. 428-412. doi: 10.1038/s41419-018-0435-y

Shlush, L. I. et al. 2014a. Identification of pre-leukaemic haematopoietic stem cells in acute leukaemia. *Nature (London)* 506(7488), pp. 328-333. doi: 10.1038/nature13038

Shlush, L. I. et al. 2014b. Identification of pre-leukaemic haematopoietic stem cells in acute leukaemia. *Nature (London)* 506(7488), pp. 328-333. doi: 10.1038/nature13038

Short, N. J., Konopleva, M., Kadia, T. M., Borthakur, G., Ravandi, F., DiNardo, C. D. and Daver, N. 2020. Advances in the treatment of acute myeloid leukemia: New drugs and new challenges. *Cancer discovery* 10(4), pp. 506-525. doi: 10.1158/2159-8290.Cd-19-1011

Shysh, A. C., Nguyen, L. T., Guo, M., Vaska, M., Naugler, C. and Rashid-Kolvear, F. 2017. The incidence of acute myeloid leukemia in Calgary, Alberta, Canada: A retrospective cohort study. *BMC public health* 18(1), pp. 94-94. doi: 10.1186/s12889-017-4644-6

Sies, H. 1986. Biochemistry of Oxidative Stress. *Angewandte Chemie (International ed.)* 25(12), pp. 1058-1071. doi: 10.1002/anie.198610581

Sies, H. 1993. Strategies of antioxidant defense. *European journal of biochemistry* 215(2), pp. 213-219. doi: 10.1111/j.1432-1033.1993.tb18025.x

Simsek, T. et al. 2010. The Distinct Metabolic Profile of Hematopoietic Stem Cells Reflects Their Location in a Hypoxic Niche. *Cell stem cell* 7(3), pp. 380-390. doi: 10.1016/j.stem.2010.07.011

Sinisa, M. 2018. Analysis of Survival and of Time Until Recurrence of Disease of Patients With Papillary Thyroid Carcinoma—Multivariant Analysis. *Medicinski arhiv* 72(4), p. 280. doi: 10.5455/medarh.2018.72.280-284

Sirover, M. A. 2018. Pleiotropic effects of moonlighting glyceraldehyde-3-phosphate dehydrogenase (GAPDH) in cancer progression, invasiveness, and metastases. *Cancer and metastasis reviews* 37(4), pp. 665-676. doi: 10.1007/s10555-018-9764-7

Sobotta, M. C. et al. 2015. Peroxiredoxin-2 and STAT3 form a redox relay for H₂O₂ signaling. *Nature chemical biology* 11(1), pp. 64-70. doi: 10.1038/nchembio.1695

Sola-Penna, M., Da Silva, D., Coelho, W. S., Marinho-Carvalho, M. M. and Zancan, P. 2010. Regulation of mammalian muscle type 6-phosphofructo-1-kinase and its implication for the control of the metabolism. *IUBMB life* 62(11), pp. 791-796. doi: 10.1002/iub.393

Song, W.-P. et al. 2020. Different transcriptome profiles between human retinoblastoma Y79 cells and an etoposide-resistant subline reveal a chemoresistance mechanism. *BMC ophthalmology* 20(1), pp. 92-92. doi: 10.1186/s12886-020-01348-6

Sreedhar, A., Petruska, P., Miriyala, S., Panchatcharam, M. and Zhao, Y. 2017. UCP2 overexpression enhanced glycolysis via activation of PFKFB2 during skin cell transformation. *Oncotarget* 8(56), pp. 95504-95515. doi: 10.18632/oncotarget.20762

Steensma, D. P., Bejar, R., Jaiswal, S., Lindsley, R. C., Sekeres, M. A., Hasserjian, R. P. and Ebert, B. L. 2015. Clonal hematopoiesis of indeterminate potential and its distinction from myelodysplastic syndromes. *Blood* 126(1), pp. 9-16. doi: 10.1182/blood-2015-03-631747

Steinbichler, T. B., Dudás, J., Skvortsov, S., Ganswindt, U., Riechelmann, H. and Skvortsova, I.-I. 2018. Therapy resistance mediated by cancer stem cells. *Seminars in cancer biology* 53, pp. 156-167. doi: 10.1016/j.semcancer.2018.11.006

Stengel, A., Kern, W., Meggendorfer, M., Nadarajah, N., Perglerová, K., Haferlach, T. and Haferlach, C. 2018. Number of RUNX1 mutations, wild-type allele loss and additional mutations impact on prognosis in adult RUNX1-mutated AML. *Leukemia* 32(2), pp. 295-302. doi: 10.1038/leu.2017.239

Sun, Y., Chen, B.-R. and Deshpande, A. 2018. Epigenetic regulators in the development, maintenance, and therapeutic targeting of acute myeloid leukemia. *Frontiers in oncology* 8, pp. 41-41. doi: 10.3389/fonc.2018.00041

Takehima, H. et al. 2014. Frequent involvement of chromatin remodeler alterations in gastric field cancerization. *Cancer letters* 357(1), pp. 328-338. doi: 10.1016/j.canlet.2014.11.038

Takubo, K. et al. 2013. Regulation of Glycolysis by Pdk Functions as a Metabolic Checkpoint for Cell Cycle Quiescence in Hematopoietic Stem Cells. *Cell stem cell* 12(1), pp. 49-61. doi: 10.1016/j.stem.2012.10.011

Thomas, D. and Majeti, R. 2017. Biology and relevance of human acute myeloid leukemia stem cells. *Blood* 129(12), pp. 1577-1585. doi: 10.1182/blood-2016-10-696054

Tian, T., Li, X. and Zhang, J. 2019. mTOR Signaling in Cancer and mTOR Inhibitors in Solid Tumor Targeting Therapy. *International journal of molecular sciences* 20(3), p. 755. doi: 10.3390/ijms20030755

Trenti, A., Tedesco, S., Boscaro, C., Ferri, N., Cignarella, A., Trevisi, L. and Bolego, C. 2017. The Glycolytic Enzyme PFKFB3 Is Involved in Estrogen-Mediated Angiogenesis via GPER1. *The Journal of pharmacology and experimental therapeutics* 361(3), pp. 398-407. doi: 10.1124/jpet.116.238212

Truong, T. H. and Carroll, K. S. 2013. Redox regulation of protein kinases. *Critical reviews in biochemistry and molecular biology* 48(4), pp. 332-356. doi: 10.3109/10409238.2013.790873

Valko, M., Leibfritz, D., Moncol, J., Cronin, M. T. D., Mazur, M. and Telser, J. 2007. Free radicals and antioxidants in normal physiological functions and human disease. *The international journal of biochemistry & cell biology* 39(1), pp. 44-84. doi: 10.1016/j.biocel.2006.07.001

Van Schaftingen, E., Hue, L. and Hers, H. G. 1980. Fructose 2,6-bisphosphate, the probably structure of the glucose- and glucagon-sensitive stimulator of phosphofructokinase. *Biochemical journal* 192(3), pp. 897-901. doi: 10.1042/bj1920897

Van Zant, G., Holland, B. P., Eldridge, P. W. and Chen, J.-J. 1990. Genotype-restricted growth and aging patterns in hematopoietic stem cell populations of allophenic mice. *The Journal of experimental medicine* 171(5), pp. 1547-1565. doi: 10.1084/jem.171.5.1547

Visnjic, D., Kalajic, Z., Rowe, D. W., Katavic, V., Lorenzo, J. and Aguila, H. L. 2004. Hematopoiesis is severely altered in mice with an induced osteoblast deficiency. *Blood* 103(9), pp. 3258-3264. doi: 10.1182/blood-2003-11-4011

Wang, Y., Qu, C., Liu, T. and Wang, C. 2020. PFKFB3 inhibitors as potential anticancer agents: Mechanisms of action, current developments, and structure-activity relationships. *European journal of medicinal chemistry* 203, pp. 112612-112612. doi: 10.1016/j.ejmech.2020.112612

Wang, Y., Xiong, X., Hua, X. and Liu, W. 2021. Expression and Gene Regulation Network of Metabolic Enzyme Phosphoglycerate Mutase Enzyme 1 in Breast Cancer Based on Data Mining. *BioMed research international* 2021, pp. 1-39. doi: 10.1155/2021/6670384

Waypa, G. B., Smith, K. A. and Schumacker, P. T. 2016. O₂ sensing, mitochondria and ROS signaling: The fog is lifting. *Molecular aspects of medicine* 47-48, pp. 76-89. doi: 10.1016/j.mam.2016.01.002

Wei, A. et al. 2018. Venetoclax with Low-Dose Cytarabine Induces Rapid, Deep, and Durable Responses in Previously Untreated Older Adults with AML Ineligible for Intensive Chemotherapy. *Blood* 132(Supplement 1), pp. 284-284. doi: 10.1182/blood-2018-99-118729

Weltmann, K. D. and von Woedtke, T. 2016. Plasma medicine-current state of research and medical application. *Plasma physics and controlled fusion* 59(1), p. 14031. doi: 10.1088/0741-3335/59/1/014031

Wojcicki, A. V., Kasowski, M. M., Sakamoto, K. M. and Lacayo, N. 2020. Metabolomics in acute myeloid leukemia. *Molecular genetics and metabolism* 130(4), pp. 230-238. doi: 10.1016/j.ymgme.2020.05.005

Wolpaw, A. J. and Dang, C. V. 2018. Exploiting Metabolic Vulnerabilities of Cancer with Precision and Accuracy. *Trends in cell biology* 28(3), pp. 201-212. doi: 10.1016/j.tcb.2017.11.006

Won, E. J. et al. 2015. Direct confirmation of quiescence of CD34+CD38- leukemia stem cell populations using single cell culture, their molecular signature and clinicopathological implications. *BMC cancer* 15(1), pp. 217-217. doi: 10.1186/s12885-015-1233-x

Xia, Y., Hong, H., Ye, L., Wang, Y., Chen, H. and Liu, J. 2013. Corrigendum to “Label-free quantitative proteomic analysis of right ventricular remodeling in infant Tetralogy of Fallot patients” *Journal of Proteomics* 84: 78–91, 2013. *Journal of proteomics* 91, pp. 620-620. doi: 10.1016/j.jprot.2013.10.001

Xiao, Y. et al. 2021. Inhibition of PFKFB3 induces cell death and synergistically enhances chemosensitivity in endometrial cancer. *Oncogene* 40(8), pp. 1409-1424. doi: 10.1038/s41388-020-01621-4

Xin, Y. et al. 2017. A pericentric inversion of chromosome X disrupting F8 and resulting in haemophilia A. *Journal of clinical pathology* 70(8), pp. 656-661. doi: 10.1136/jclinpath-2016-204050

Yalcin, A. et al. 2009. Nuclear Targeting of 6-Phosphofructo-2-kinase (PFKFB3) Increases Proliferation via Cyclin-dependent Kinases. *The Journal of biological chemistry* 284(36), pp. 24223-24232. doi: 10.1074/jbc.M109.016816

Yamamoto, T. et al. 2014. Reduced methylation of PFKFB3 in cancer cells shunts glucose towards the pentose phosphate pathway. *Nature communications* 5(1), pp. 3480-3480. doi: 10.1038/ncomms4480

Yang, J. et al. 2021. Glycolysis reprogramming in cancer-associated fibroblasts promotes the growth of oral cancer through the lncRNA H19/miR-675-5p/PFKFB3 signaling pathway. *International journal of oral science* 13(1), pp. 12-12. doi: 10.1038/s41368-021-00115-7

Yi, M., Ban, Y., Tan, Y., Xiong, W., Li, G. and Xiang, B. 2019. 6-Phosphofructo-2-kinase/fructose-2,6-biphosphatase 3 and 4: A pair of valves for fine-tuning of glucose metabolism in human cancer. *Molecular metabolism (Germany)* 20, pp. 1-13. doi: 10.1016/j.molmet.2018.11.013

Yilmaz, Ö. H., Valdez, R., Theisen, B. K., Guo, W., Ferguson, D. O., Wu, H. and Morrison, S. J. 2006. Pten dependence distinguishes haematopoietic stem cells from leukaemia-initiating cells. *Nature* 441(7092), pp. 475-482. doi: 10.1038/nature04703

Zawacka-Pankau, J. et al. 2011. Inhibition of glycolytic enzymes mediated by pharmacologically activated p53: targeting Warburg effect to fight cancer. *The Journal of biological chemistry* 286(48), pp. 41600-41615. doi: 10.1074/jbc.M111.240812

Zeida, A., Trujillo, M., Ferrer-Sueta, G., Denicola, A., Estrin, D. A. and Radi, R. 2019. Catalysis of Peroxide Reduction by Fast Reacting Protein Thiols. *Chemical reviews* 119(19), pp. 10829-10855. doi: 10.1021/acs.chemrev.9b00371

Zhang, C., Gou, X., He, W., Yang, H. and Yin, H. 2020a. A glycolysis-based 4-mRNA signature correlates with the prognosis and cell cycle process in patients with bladder cancer. *Cancer cell international* 20(1), pp. 177-177. doi: 10.1186/s12935-020-01255-2

Zhang, Y. et al. 2020b. Coral-like hierarchical structured carbon nanoscaffold with improved sensitivity for biomolecular detection in cancer tissue. *Biosensors & bioelectronics* 150, pp. 111924-111924. doi: 10.1016/j.bios.2019.111924

Zhao, J. 2016. Cancer stem cells and chemoresistance: The smartest survives the raid. *Pharmacology & therapeutics (Oxford)* 160, pp. 145-158. doi: 10.1016/j.pharmthera.2016.02.008

Zhao, L. et al. 2017. Long noncoding RNA LINC00092 acts in cancer-associated fibroblasts to drive glycolysis and progression of ovarian cancer. *Cancer research (Chicago, Ill.)* 77(6), pp. 1369-1382. doi: 10.1158/0008-5472.Can-16-1615

Zhao, X., Zhao, H., Yan, L., Li, N., Shi, J. and Jiang, C. 2020. Recent Developments in Detection Using Noble Metal Nanoparticles. *Critical reviews in analytical chemistry* 50(2), pp. 97-110. doi: 10.1080/10408347.2019.1576496

Zhu, H. et al. 2018. T-ALL leukemia stem cell 'stemness' is epigenetically controlled by the master regulator SPI1. *eLife* 7, doi: 10.7554/eLife.38314